

Report

Shallow Reservoirs in the Barents Sea

Norwegian Petroleum Safety Authority

21 DECEMBER, 2017

 **add energy**
Well Control & Blowout Support

Shallow Reservoirs in the Barents Sea

DATE: December 21, 2017	REVISION / REFERENCE ID: 0	PAGES: 132
CLIENT: Norwegian Petroleum Safety Authority		
CONTACT: Eivind Hovland		
DISTRIBUTION: Petroleumstilsynet, Add Energy		

ROLE:	NAME:	SIGNATURE:
Author	Terje Løkke-Sørensen, Ray Tommy Oskarsen, Amir Paknejad	
Author	Bernt Aadnøy, Sigbjørn Sangesland, Ståle Emil Johansen	
Reviewer	Morten Haug Emilsen	
Approved		

ABSTRACT:

Some reservoirs in the Barents Sea are shallow and pose challenges related to robust well design especially for horizontal injection and production wells. This report addresses these challenges and potential mitigating options including well integrity, fracturing and rock stability, relief well drilling and methods for monitoring of the overburden.

KEY WORDS:

Shallow reservoir, Barents Sea, Drilling

REPRODUCTION:

This report is created by **add energy as**. The report may not be altered or edited in any way or otherwise copied for public or private use without written permission from the author.



add energy

Offices

Stavanger (HQ)
Oslo
Aberdeen
Houston
Muscat
Chennai
Yangon
Singapore
Perth
Brisbane
Melbourne
Wellington

addenergy.no

Table of Contents

SAMMENDRAG	IX
SUMMARY	XI
1. INTRODUCTION	13
1.1 Overview of wells drilled through shallow reservoirs	14
1.2 Data sources and references	15
1.3 Appendices	15
1.4 Authors.....	15
2. GEOLOGICAL DEVELOPMENT, STRATIGRAPHY AND UPLIFT HISTORY OF THE BARENTS SEA.....	17
2.1 General	17
2.2 Uplift and erosion	19
2.3 Implications of net erosion on rock properties	20
2.4 Net erosion and petroleum prospectivity	21
2.4.1 Effects caused by net erosion that could affect leakage from the trap	22
2.5 Methodology for quantifying net erosion.....	23
2.6 Net erosion estimates	24
2.7 Shallow reservoirs net erosion estimates	25
3. MODEL PRODUCTION WELL AND INJECTION WELL	27
3.1 Well objectives	27
3.2 Formation & reservoir characteristics	27
3.3 Well design	28
3.4 Well profile	29
3.5 Model production well	30
3.6 Model injection well – with 9 5/8" set into the reservoir	31
3.7 Model injection well – with 9 5/8" set above the reservoir	32
4. WELL INTEGRITY ASSESSMENT.....	33
4.1 General	33
4.2 Challenges	33
4.3 NORSOK D-010 Standard.....	34
4.4 Well barriers in the model injection well	35
4.4.1 Alternative 1 - production casing set above reservoir.....	35
4.4.2 Alternative 2 – production casing set into the reservoir.....	46
4.5 Well barriers in the model production well.....	52
4.5.1 Assessment of loads on WBE	52
5. GEOMECHANICAL ASSESSMENT.....	54
5.1 Challenges	54
5.2 Shallow Fracture Pressure – Regional Comparison	55
5.3 Fracture model for the Barents Sea	57
5.4 Upward fracture growth	62
5.5 Does the Barents Sea have reverse fault stresses?	62
5.5.1 The North Sea is a relaxed depositional basin	62
5.5.2 Characteristics of reverse fault stress states	63
5.6 Flow capacity in natural faults	64
5.7 Subsidence and reservoir compaction	65
6. METHODS FOR DETECTION OF FLUID MIGRATION FROM RESERVOIR TO SEABED	66
6.1 Challenges	66
6.2 Introduction	67
6.3 3D and 4D seismic data acquisition	68
6.4 Status and future development of geophysical monitoring.....	68

6.5	Continuous active marine seismic monitoring	69
6.6	Complex geophysical processing of time lapse data	70
6.7	Broadband seismic techniques for enhanced 4D seismic analysis.....	70
6.8	Quantitative analysis and uncertainty assessment of time lapse data	70
6.9	Combining various geophysical monitoring techniques	71
6.10	Geomechanics and stress monitoring	71
6.11	Passive seismic monitoring	72
6.12	Technologies deployed in wells	72
7.	METHODS FOR DETECTION OF LEAKS FROM THE RESERVOIR AT SEABED	74
7.1	Challenges	74
7.2	Introduction	75
7.3	Examples of leakage from injection wells.....	77
7.4	Overview of technologies for detection of leaks from seabed	78
7.5	Characterization of injection water and fluids leaking to sea.....	79
7.6	Technologies for leakage detection at the seabed and/or in the sea water column	79
7.6.1	Active acoustic, multibeam technologies	80
7.6.2	Multibeam seabed survey using surface vessel	80
7.6.3	Autonomous Underwater Vehicle (AUV)	81
8.	RELIEF WELL DESIGN	83
8.1	Challenges	83
8.2	Model Well	84
8.3	Downhole Ranging Techniques.....	85
8.3.1	Active Electromagnetic Ranging	86
8.3.2	Passive Magnetostatic Ranging	88
8.3.3	Ranging techniques in development.....	89
8.3.4	Cross-by and triangulation	89
8.3.5	Direct relief-well approach	90
8.4	Relief Well Trajectories.....	91
8.5	Surface Site Selection	92
8.5.1	Relief Well Intersect Target	93
8.6	Relief Well Design	95
8.6.1	Relief well 1 – Parallel heel-to-hoe approach	95
8.6.2	Relief well 2 – Direct approach	98
8.6.3	Relief well 3 – Parallel toe-to-heel approach	100
8.7	Ranging and Positional Uncertainty Analysis	102
8.8	Dynamic Kill Method.....	105
8.8.1	Challenges with Multiple Relief Wells	106
8.9	Relief Well Injection Spool.....	106
	REFERENCE LIST	108
	FURTHER READING	110
A.	BLOWOUT AND KILL SIMULATIONS.....	114
A.1	Background information and input data – reservoir fluid	114
A.2	Background information and input data - reservoir data	114
A.3	Scenarios	114
A.4	Blowout Results	116
A.5	Dynamic kill requirements.....	117
A.5.1	Relief well casing design	117
A.5.2	Kill requirements	117
A.5.3	Kill requirements discussion	118
A.6	Software	119
B.	OVERBURDEN LEAKAGE RESISTANCE	121
B.1	Introduction	121
B.1.1	The effects of fluid type.....	121
B.1.2	Drilling with mud.....	121

B.1.3	Well stimulation with solid free fluids	122
B.1.4	Comparing solutions	122
B.1.5	Summary.....	123
B.2	Rock Mechanics	123
B.2.1	Injection scenario	123
B.2.2	Prognosis for the model wells.....	124
B.3	Potential for leaks to surface	124
B.3.1	Simple analysis.....	126
B.3.2	Complex analysis.....	126
C.	CLEAN SEA PAYLOADS	130
D.	AUV MOUNTED SYSTEMS.....	131

List of Tables

Table 1.1:	Wells with shallow reservoirs (Source: PSA)	14
Table 1.2:	Chapter authors	15
Table 3.1:	Parameters used in assessments	27
Table 3.2:	Design elements used in assessments.....	28
Table 3.3:	Well profile	29
Table 4.1:	Colors/Abbreviations	34
Table 4.2:	Primary well barrier elements	38
Table 4.3:	Well barrier elements – In-situ formation	39
Table 4.4:	Well barrier elements – Injection wells/disposal wells	40
Table 4.5:	Well barrier element – Casing cement.....	41
Table 4.6:	Secondary well barrier elements – Alternative 1	44
Table 4.7:	Secondary well barrier elements – In-situ formation.....	45
Table 4.8:	Secondary well barrier elements – Casing cement	45
Table 4.9:	Well barriers	48
Table 4.10:	Primary well barriers – Alternative 2	49
Table 4.11:	Primary well barrier elements – Casing cement	50
Table 4.12:	Secondary well barriers – Alternative 2	50
Table 4.13:	Loads on formation	51
Table 4.14:	Primary WBE load comparison	52
Table 4.15:	Secondary WBE load comparison	53
Table 5.1:	Shallow fracture data from the North Sea (Aadnøy, 2010).....	55
Table 5.2:	Fracture data from Peon normalized to seabed (PSA 2017).....	56
Table 5.3:	Fracture data from Barents Sea normalized to seabed (PSA 2017)	56
Table 5.4:	Fracture data from the Barents Sea (PSA 2017)	57
Table 5.5:	Fracture data from the Barents Sea is normalized to a water depth of 450 mRKB.....	59
Table 5.6:	Stress states versus fracture directions	63
Table 6.1:	Possible methods used for monitoring of overburden	67
Table 7.1:	Incidents relating to injection on the NCS from 1997 to 2013 (Øfjord, G.D., 2013).....	77
Table 7.2:	Overview of technologies for detection of leaks from seabed	78
Table 8.1:	Shallow horizontal well directional plan	84
Table 8.2:	Proposed relief-well surface locations	93
Table 8.3:	Intersection point used for relief well design	94
Table 8.4:	Relief well 1 – parallel heel-to-toe approach.....	96
Table 8.5:	Relief well 2 – direct approach.....	98
Table 8.6:	Relief well 3 – parallel toe-to-heel approach.....	100
Table A.1:	Key fluid data after characterization.....	114
Table A.2:	Key reservoir data	114
Table A.3:	Blowout results	116
Table A.4:	Kill requirements	117

List of Figures

Figure 1.1:	Well 7324/7-3 S (SPE/IADC – 184654-MS, p. 2)	13
Figure 1.2:	Overview of well locations in Barents Sea (Source: PSA).....	14
Figure 2.1:	Geological history of western Barents Sea. Modified from Faleide et.al.(2010).....	17
Figure 2.2:	Lithostratigraphic units in the Barents Sea	19
Figure 2.3:	Mechanical and chemical processes in sandstones and shales during burial and compaction. Modified from Marion (1990).	20
Figure 2.4:	Conceptual illustration of cementation rate as a function of time and burial	21
Figure 2.5:	Effects of uplift and erosion on the processes affecting petroleum prospectivity. Modified from Henriksen et al. (2011)	22
Figure 2.6:	Quantification of net erosion from compaction techniques using P-wave velocity vs. depth trend for shales.	23
Figure 2.7:	Location of net erosion estimates from Barents Sea wells. Modified from Faleide et al. (2010).	24

Figure 2.8:	Net erosion map created from seismic interval velocities for the top BCU Horizon	25
Figure 2.9:	Regional east-west geological cross section number combined with net erosion estimates from seismic velocities and velocity depth trends in wells.	26
Figure 3.1:	Well profile – vertical section	29
Figure 3.2:	Model production well	30
Figure 3.3:	Model injection well – 9 5/8" casing set into the reservoir	31
Figure 3.4:	Model injection well – 9 5/8" casing set above the reservoir	32
Figure 4.1:	Model injection well	35
Figure 4.2:	Model injection well - 9 5/8" production casing set above reservoir	36
Figure 4.3:	NORSOK D-010 WBS – Cemented production casing set above reservoir.....	37
Figure 4.4:	In-situ formation	38
Figure 4.5:	Comparison of BHP development.....	39
Figure 4.6:	Production liner cement	41
Figure 4.7:	Casing cement dual well barrier.....	43
Figure 4.8:	Model injection well – 9 5/8" production casing set above reservoir	46
Figure 4.9:	Platform production/injection/observation well.....	47
Figure 4.10:	Casing cement	49
Figure 4.11:	In-situ formation	51
Figure 4.12:	Production well.....	52
Figure 5.1:	Fracture data normalized to seabed	57
Figure 5.2:	Depth references used when data is normalized to various water depths	58
Figure 5.3:	Fracture data from the Barents Sea normalized to a seabed depth of 450 mRKB.	60
Figure 5.4:	Fracture curve and horizontal stress curves for the model production and injection wells at water depth of 450 mRKB.....	61
Figure 5.5:	Stress ratio	63
Figure 5.6:	Reported stress ration from Scandinavia.....	64
Figure 6.1:	Nomenclature	67
Figure 6.2:	4D Seismic	68
Figure 6.3:	Seismic monitoring at a CO ₂ storage site.....	69
Figure 6.4:	Repeatability of seismic air guns	70
Figure 6.5:	The major link in quantitative geophysical monitoring	71
Figure 6.6:	4D seismic before and after the Tohoku earthquake	72
Figure 6.7:	A micro-seismic event recorded on DAS/2/	73
Figure 7.1:	Seabed bathymetry	74
Figure 7.2:	AUV	75
Figure 7.3:	Potential leak paths to sea floor (Øfjord, G.D.,2013) (Source: Statoil)	76
Figure 7.4:	Illustration of seabed crater near Tordis - scale meters (Edvin, Tor & Øverland, Jon Arne) (Source: Statoil)	77
Figure 7.5:	Hydrographic Survey (ORG Geophysical AS)	80
Figure 7.6:	Hugin – AUV	82
Figure 7.7:	HUGIN bathymetry from the Ormen Lange field – year 2002 (NUI AS)	82
Figure 8.1:	Model production/injection well profile	85
Figure 8.2:	Wellbore positional uncertainty ellipse at the 9 5/8" casing shoe	86
Figure 8.3:	Principle of electromagnetic ranging with downhole injection in openhole.....	87
Figure 8.4:	Triangulation after cross-by reduces the positional uncertainty box.....	90
Figure 8.5:	Example ranging strategy for a by-pass and plug-back intersect.....	91
Figure 8.6:	Relief well trajectories for kill points at different depths	92
Figure 8.7:	Proposed relief well sites with possible wind and current exclusion zones	94
Figure 8.8:	Relief well 1 vertical section view.....	96
Figure 8.9:	Relief well 1 horizontal plan view	97
Figure 8.10:	Relief well 1 ladder view.....	97
Figure 8.11:	Relief well 2 section view	99
Figure 8.12:	Relief well 2 plan view	99
Figure 8.13:	Relief well 3 section view	101
Figure 8.14:	Relief well 3 plan view.....	101
Figure 8.15:	Relief well 3 ladder view.....	102
Figure 8.16:	Maximum separation at cross-by depth for relief well 1.....	103
Figure 8.17:	Maximum separation at cross-by depth for relief well 2.....	104
Figure 8.18:	Maximum separation at cross-by depth for relief well 3.....	104

Figure 8.19: Minimum required kill rate for the defined scenarios	105
Figure 8.20: Relief well injection spool hardware configuration	107
Figure A.1: Schematic of blowout scenario	115
Figure A.2: Flowing pressure profiles	116
Figure A.3: Pump curves for the worst case kill scenario.....	118
Figure B.1: a) penetrating fluid b) non-penetrating fluid (Aadnøy 2010)	121
Figure B.2: Possible fracture patterns	123
Figure B.3: Fracture curve and horizontal stress curve for the production and injection wells cases for a water depth of 450 mRKB.....	124
Figure B.4: Deformation caused by injection into several wells (Zhang, 2012)	126
Figure B.5: Typical Pressure-Time curve for extended Leak-Off-Tests. From Ybray et.al. (2011).	127
Figure B.6: Repetitive 5-spot pattern (a) and (b) Finite Element model with loading (Zhang et.al.2012)	128

Sammendrag

Denne rapporten beskriver brønndesign og driftsutfordringer med undersjøiske injeksjons- og produksjonsbrønner i grunne reservoarer som ligger 200-700 m under havbunnen i Barentshavet. Disse Jura og Trias reservoarene ble løftet opp og 2000 m overliggende lag ble erodert vekk. Det finnes flere grunne olje- og gassfunn, av disse er Wisting-funnet mest utforsket.

Hypotetiske brønndesignmodeller for horisontale produksjons- og injeksjonsbrønner i denne rapporten ble laget for analyse og diskusjonsformål knyttet til brønnintegritet, hvordan oppdage lekkasjer fra reservoaret og videre migrasjon gjennom overliggende lag til havbunnen.

Lekkasje fra reservoaret til havbunnen skyldes enten svikt i menneskeskapte brønnskomponeanter eller ved oppsprekking av formasjonen. Injeksjonsbrønner gir det høyeste trykkbelastningen på brønnbarrierer og formasjonen.

Kravet om to brønnbarrierer som beskrevet i NORSOK-D010 Well Integrity-standarden kan oppfylles. Det svakeste brønnbarriereelementet er formasjonen rundt brønnen. Trykkbelastninger på denne kan styres ved regulering av ringromstrykk mellom foringsrørene som er i kommunikasjon med åpen formasjon, samt holde nedi-hulls injeksjonstrykket trygt under bruddstyrken til formasjonen.

Analyse av oppsprekkingstester fra brønner i Barentshavet viser at oppsprekkingstrykket er høyere enn brønner i Nordsjøen, noe som muligens indikerer at horisontale spenninger er høyere enn de vertikale. Konsekvensen av dette er at sprekker fortrinnsvis vil forplante seg horisontalt i stedet for vertikalt. Naturlige sprekker har variabel hydraulisk ledningsevne og må unngås gjennom nøye tolkning av seismiske data før boring av brønnen.

Overvåking av reservoarer er gjort for mange offshore-felt, men direkte overvåking av den overliggende formasjonen er ikke vanlig. Det er sannsynlig at lekkasje fra reservoaret kan oppdages ved hjelp av geofysiske målinger og integrerte inversjons- og tolkningsteknikker. Det vil være vanskelig å kvantifisere mengden gass eller væske som lekker gjennom undergrunnen.

Multibeam og sidesøkende sonaroppmåling er nyttige teknikker for å oppdage lekkasje av gassbobler i vannsøylen på grunn av sterke akustiske tilbakespredningsegenskaper. Endringer i sjøbunnens topografi (krater) forårsaket av betydelig utstrømning gjennom sprekker vil sannsynligvis bli oppdaget.

Overflatefartøy og autonome undervannsfarkoster (AUV) utstyrt med sensorer og sensorsystemer kan hjelpe til å oppdage og overvåke lekkasjer til havbunn fra injeksjonsbrønner. Det vil imidlertid være vanskelig å oppdage injeksjonsvann som ikke inneholder olje eller gass i sjøvannssøylen.

En AUV kan skanne et område på 50 km² på 20 timer. Behandling og tolkning av data krever vanligvis 50% av undersøkelsestiden. Derfor bør undersøkelsen utføres ukentlig for å ha tid til databehandling og tolkning.

I tilfelle det utenkelige skjer og en utblåsning oppstår, kan utblåsningen stoppes med en avlastningsbrønn og pumping av boreslam – såkalt dynamisk dreping. Modellering av tre mulige avlastningsbrønner ble utført i studiet. Konklusjonen er at den vertikale avlastningsbrønnen er å foretrekke, da dette gir kortest varighet på utblåsningen. For modellbrønnen kan treffpunktet (intersection) være skoen på 9 5/8" eller 7" produksjonsforingsrør. Dette krever et direkte treff med høy innfallsvinkel. Det forventes flere tilbakeplugginger og forbiboringer (sidesteg) for å øke nøyaktigheten av relativ posisjonering gjennom magnetisk avstandsmåling før man borer inn i den blåsende brønn. Magnetisering av foringsrøret før det installeres i modellbrønnen vil redusere antall sidesteg.

For et grunt reservoar kan det være vanskelig å oppnå tilstrekkelig hydrostatisk- og friksjonstrykk under en dynamisk drepeoperasjon. Simuleringer viser at utblåsning i modell brønnen kan drepes med en avlastningsbrønn ved å pumpe 8000 - 9500 liter per minutt av 1,25 SG drepeslam. Ekstra pumpekapasitet kan oppnås ved bruk av dedikert injeksjonsventil (kill spool) som settes på avlastningsbrønnen.

Det anbefales å:

- Utføre en omfattende formasjonsfrakturstudie basert på rådata brønndata for å øke nøyaktigheten.
- Gjennomføre mulighetsstudier vedrørende bruk av geofysiske metoder for kontinuerlig overvåking av lekkasje i overliggende formasjon for å kunne forstå de lokale forholdene for det aktuelle feltet.

Summary

This report describes the well design and operational challenges with subsea injection and production wells in shallow reservoirs between 200 – 700 m underneath seabed in the Barents Sea. These Jurassic and Triassic reservoirs were uplifted by significant glacial erosion/uplift cycles which removed up to 2000 m of strata. There are several shallow oil and gas discoveries, with the Wisting discovery being the most appraised.

Hypothetical well design models for horizontal production and injection wells were established for analysis and discussion of challenges relating to well integrity and how to detect leaks from the reservoir, migration through the overburden and to the seabed.

The leak path from the reservoir to seabed is either caused by the breakdown of manmade well components or through fracturing of the overburden formation. By their nature, injection wells give the highest pressure loads on the well barriers and the formation.

The requirement of having two well barriers as described in NORSOK-D010 Well Integrity standard can be fulfilled. The weakest well barrier element is the in-situ formation which must be protected from excessive loads through pressure bleed-off in casing annuli open to formation and by keeping the downhole injection pressure safely below the fracture pressure.

Analysis of leak-off data from Barents Sea wells shows that the fracture pressures are higher than wells in the North Sea, possibly indicating that horizontal stresses are higher than the vertical stress. The consequence of this is that a fracture will preferentially propagate in a horizontal plane rather than upwards. There are a considerable number of natural fractures with variable hydraulic conductivity which need to be avoided through careful interpretation of seismic data before drilling the well.

Monitoring of producing reservoirs is done for many offshore fields, but direct monitoring of the overburden is not common. It is likely that leakage from the reservoir can be detected by using geophysical measurements, integrated inversion and interpretation techniques. It will be difficult to quantify the amount of gas or fluid leaking through the subsurface.

Multibeam and side scan sonar surveying are useful techniques for detecting seepage of gas bubbles in water columns which give strong acoustic backscatter properties. Changes in seabed bathymetry (plume/crater) caused by significant amount of leakage through conduits (fractures) are likely to be detected.

Surface vessels and autonomous underwater vehicles (AUVs) equipped with sensors and sensor systems can assist in detection and monitoring leakage to seabed from injection wells. However, it will be difficult to detect whether injection water containing no oil or gas is in the sea water column.

An AUV may be able to scan an area of 50 km² in 20 hours. Processing and interpretation of data typically requires 50% of the survey time. Therefore, performing the surveys once a week allows time for data processing and interpretation of data.

In the event the unthinkable happens and a blow-out occurs, can it be stopped? Modelling of three possible relief well trajectories was carried out. The conclusion is that the vertical relief well is preferable as this may give the shortest time duration of the blowout. For the model well, the intersection point can be the shoe of the 9 5/8" or the 7" production liner. This requires a direct intersect with high incident angle. Several plug backs and re-drills (sidetrack) to increase the accuracy of relative positioning through magnetic ranging before the final intersect must be expected. Pre-magnetization of the casing in the model well will reduce the number of sidetracks.

For a shallow reservoir, achieving the hydrostatic and frictional pressure during a dynamic kill is challenging. Simulations show that the model well can be killed with a single relief well by pumping 50 – 60 BPM of 1,25 SG kill mud. Additional pumping capacity can be achieved through a kill spool.

It is recommended to:

- Perform a comprehensive formation fracture study based on raw-data well data to increase accuracy.
- Conduct feasibility studies relating to the use of geophysical methods for continuous leak monitoring of leak overburden to understand the local conditions for the actual field.

1. Introduction

This report is a result of a study assignment awarded to Add Energy by the Petroleum Safety Authority (PSA or PTil) in Norway pertaining to describing the challenges in achieving a robust well design for shallow injection and production wells in the Barents Sea. Shallow reservoirs covered by this report are reservoirs located between 200 – 700 m below seabed.

There are several exploration wells already drilled through shallow potential reservoirs, with the Wisting (OMV) discovery being the most significant. By drilling a 2354 m MD long horizontal appraisal well approx. 280 m below the seabed and 1400 m MD horizontal section, completed with cemented liners and production tested, the operator has de-risked important factors which could accelerate a potential field development.

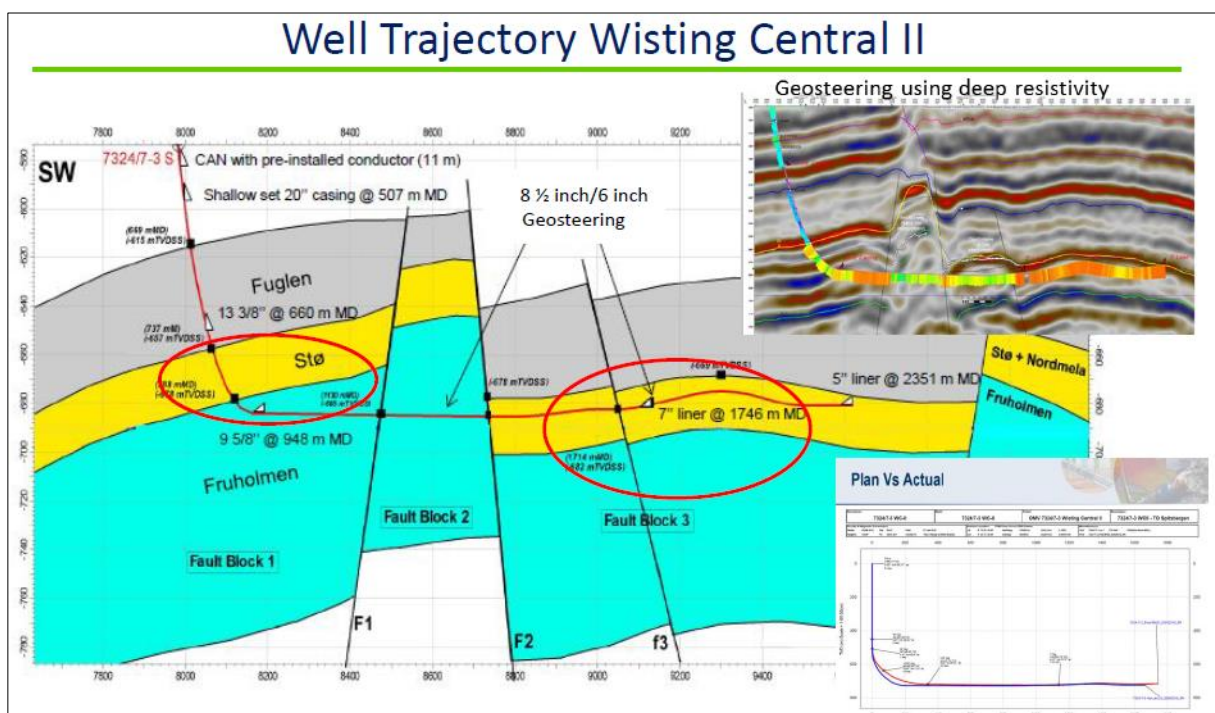


Figure 1.1: Well 7324/7-3 S (SPE/IADC – 184654-MS, p. 2)

The industry realizes that these types of wells are different than deeper and normal wells. The most central challenges are:

- Can the wells be constructed with two well barriers in accordance with the regulations / NORSOK D-010 Well Integrity standard?
- Can the formation strength of the overlying formation be predicted?
- Can failures in man-made well barrier elements or formation break-down due to production or injection loads be detected before reservoir fluids escape to seabed?
- Can escaping reservoir fluids or injection water into the sea column be detected?
- Can a blowout from a shallow reservoir be killed with a relief well?

1.1 Overview of wells drilled through shallow reservoirs

The figure below shows an overview of wells drilled in the Barents Sea.

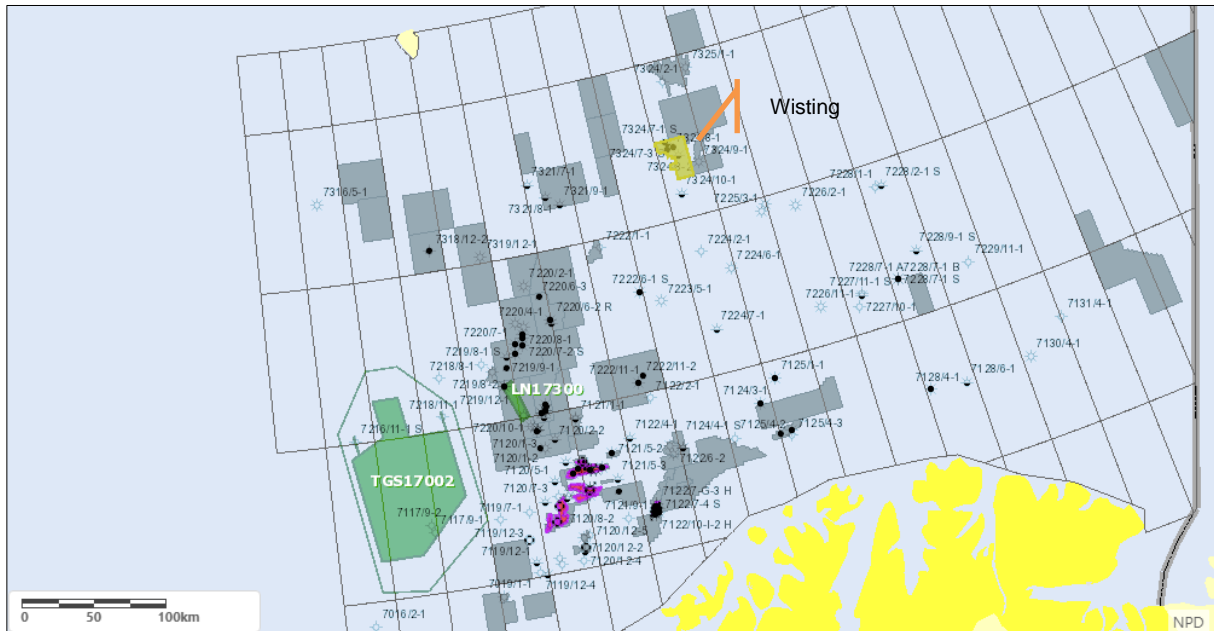


Figure 1.2: Overview of well locations in Barents Sea (Source: PSA)

The table below provides a summary of wells drilled into shallow reservoirs in the Barents Sea and North Sea from 2005 to 2016.

Table 1.1: Wells with shallow reservoirs (Source: PSA)

Well no.	Well name	Operator	Year	Casing program	Total depth (m)	Water depth (m)	Overburden thickness (mTVD)
7324/7-1 S	Wisting Central II	OMV	2016	36"x30", 13 3/8", 9 5/8", 7" liner, 5" liner	2354 mMD, 1402 m MD horizontal	402	250
7324/8-1	Wisting Central	OMV	2013	36"x30", 9 5/8"	930 m TVD RKB	398	246
7324/7-1 S	Wisting Alternative	OMV	2013	36"x30", 13 3/8", 9 5/8"	2477 m TVD RKB, 2535 m MD RKB	413	351
7324/7-2	Wisting Main/Hanssen	OMV	2014	36"X30' cond, 20" surface, 9 5/8", 7" liner	1719 m TVD RKB	417,5	262
7324/8-2	Bjaaland	OMV	2015	36"X30" cond, 20"x13 3/8" casing, 9 5/8" liner, 7" liner	840 m TVD RKB	394	238
35/2-2	PEON	Statoil	2009	30", 13 3/8", 9 5/8"	640 m TVD RKB	372	208

Well no.	Well name	Operator	Year	Casing program	Total depth (m)	Water depth (m)	Overburden thickness (mTVD)
35/2-1	PEON	Statoil	2005	30", 20"X13 3/8", 9 5/8"	713 m TVD RKB	384	167
7220/2-1	Isfjell	Statoil	2014	30", 13 3/8", 9 5/8"	1690 m TVD RKB	429	360
7222/11-1	Caurus Carn A0	Statoil	2008	30", 13 3/8", 9 5/8"	2625 m TVD RKB	356	264
7225/3-1	Norvarg	Total E&P	2011	36"X30", 20", 13 3/8", 9 5/8", 7"	4147 m TVD RKB	377	307
7226/2-1	Ververis	Statoil	2008	30", 20", 13 3/8", 9 5/8"	3023 m TVD RKB	347	522
7324/9-1	Mercury Main Realgrunnen	Statoil	2014	30", 20"x9 5/8"	1100 m TVD RKB	414	225
7319/12-1	Pingvin	Statoil	2014	30", 20"x13 3/8"	1540 m TVD RKB	422	537
7324/2-1	Apollo	Statoil	2014	30", 20"X13 3/8", 9 5/8"	1090 m TVD RKB	444	347
					Average->	398	306

1.2 Data sources and references

The sources used in this study were primarily obtained through literature searches on internet, supported by literature published by the authors of this study. Reproduced source material is referenced.

References are listed at the end of each chapter.

1.3 Appendices

Appendices are located at the end of the document.

1.4 Authors

The authors of this report are listed in the table below.

Table 1.2: Chapter authors

Chapter title	Author	Title/company
1. Introduction	Terje Løkke-Sørensen	Add Energy
2. Description of geology and formations	Ståle Emil Johansen	NTNU
3. Model production and injection wells	Terje Løkke-Sørensen	Add Energy
4. Well integrity assessment	Terje Løkke-Sørensen	Add Energy

Chapter title	Author	Title/company
5. Geomechanical assessment	Bernt Sigve Aadnøy	NTNU
6. Monitoring of overburden	Ståle Emil Johansen	NTNU
7. Monitoring of seabed	Sigbjørn Sangesland	NTNU
8. Relief well	Ray Tommy Oskarsen and Amir Paknejad	Add Energy

2. Geological development, stratigraphy and uplift history of the Barents Sea

2.1 General

The western Barents Sea is bounded by passive margins to the west and north. Caledonian rocks are the basement of the southwestern Barents Sea, and the geological history is dominated by rift phases in Carboniferous-, middle Jurassic-early Cretaceous-, and early Tertiary times. These rift systems have gradually shifted westward through time (see Figure 2.1). The rift phases of different geological ages are illustrated by colours in the figure below. This study is focusing on the southwestern part of the Barents Sea.

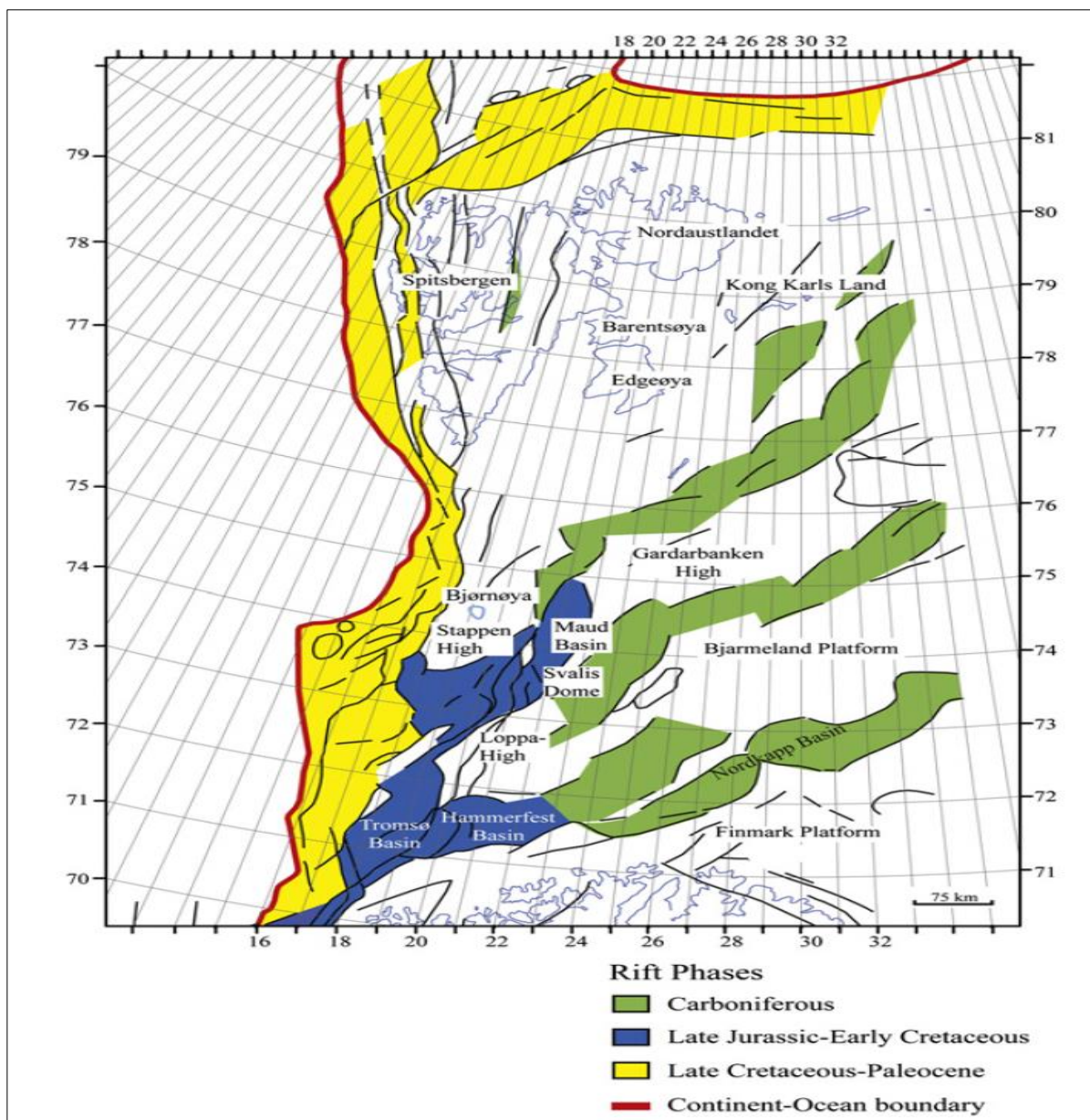


Figure 2.1: Geological history of western Barents Sea. Modified from Faleide et.al.(2010)

In the first rift phase in middle Carboniferous time, a large rift zone existed in the entire area and extended several hundred kilometres towards the north east. It consisted of many smaller basins and graben systems that later were filled in, and in late Carboniferous- and Permian times the Barents Sea was a large platform area.

In the west and the north-west some of the fault systems were active again in late Permian- and early Triassic times. The Triassic period continued with large scale and rapid subsidence. Thick layers of sediments were deposited. The sediments came from the east and south east, with the Uralian Mountains as the main source.

Lower to Middle Jurassic sandstones (Stø Formation) represent one of the main reservoir intervals in the Barents Sea (Figure 2.2). These rocks most likely covered the entire area, also the Loppa High and other areas that were later eroded due to uplift and tectonic activity.

The next important period of rifting in the Barents Sea occurred in late Jurassic- and early Cretaceous time. The Upper Jurassic Hekkingen source rock was deposited during this period. In the phase after the rifting very deep Cretaceous basins developed and thick sedimentary layers were deposited. In the western areas subsidence continued in upper Cretaceous time, but in the rest of the area the Upper Cretaceous unit is thin or absent (Figure 2.2).

The Norwegian-Greenland Sea opened in Cenozoic time, and the development of the western area is strongly influenced by this event. In the westernmost areas volcanism was common in the Eocene period. Later in Cenozoic time the basins were subsiding, and the entire margin was covered by thick sediment wedges derived from the uplifted Barents Sea area further east. Late Cenozoic uplift and erosion removed most of the Cenozoic sediments, and partly also older strata. In the south-western Barents Sea between 1000 and 1500 meters of strata were removed, in some places even more. During the latest development in the area a huge sedimentary wedge of Upper Pliocene to Holocene sediments were deposited along the entire margin.

The causes for uplift in the Barents Sea are debated. Fjeldskaar and Amantov (2016) summarize this debate and propose a sequence of events that can explain the observed Cenozoic uplift and erosion. In their model uplift started in the west and was caused by lateral plate movements before opening of the Norwegian-Greenland Sea. When the uplifted areas in the west were eroded this triggered isostatic movements and continued erosion that gradually influenced larger areas of the Barents Sea. If this uplift is added to the isostatic response to the glacial erosion in the last three million years, most of the uplift and erosion can be explained.

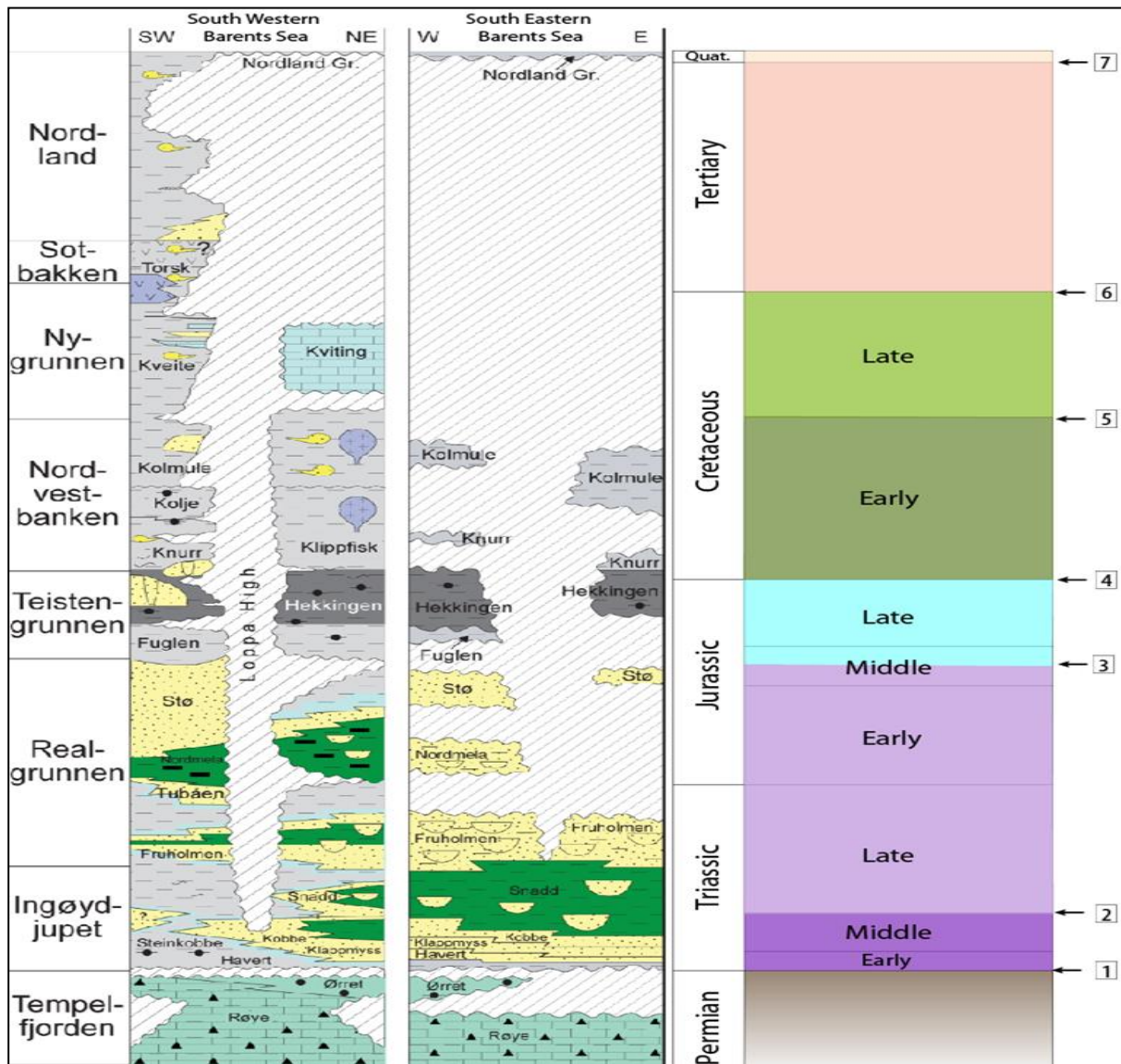


Figure 2.2: Lithostratigraphic units in the Barents Sea

Approximate ages of the key seismic horizons are shown by numbers 1-7. Modified from Gradstein et al. (2012) and NPD (2016).

2.2 Uplift and erosion

Uplift and erosion are the most significant elements in the late geological development of the Barents Sea. They are also the elements that have had greatest influence on the hydrocarbon system. Although the processes often are linked to each other, removal of overburden must be distinguished from uplift of the earth surface (England and Molnar, 1990, Japsen and Chalmers, 2000). Overburden can be eroded by water or ice without any uplift occurring, and it is therefore important to differentiate between the two. In this study the term “net erosion” describes the difference between current day burial and the maximum burial depth with reference to a surface horizon.

2.3 Implications of net erosion on rock properties

Rocks are influenced by burial and sediments will generally compact with increased burial depths and loading. The physical properties will change in the rocks as they undergo both mechanical and chemical compaction with increased burial depth (Bjørlykke and Jahren, 2015). Figure 2.3 explains depositional trends of each of them for shales and sandstones.

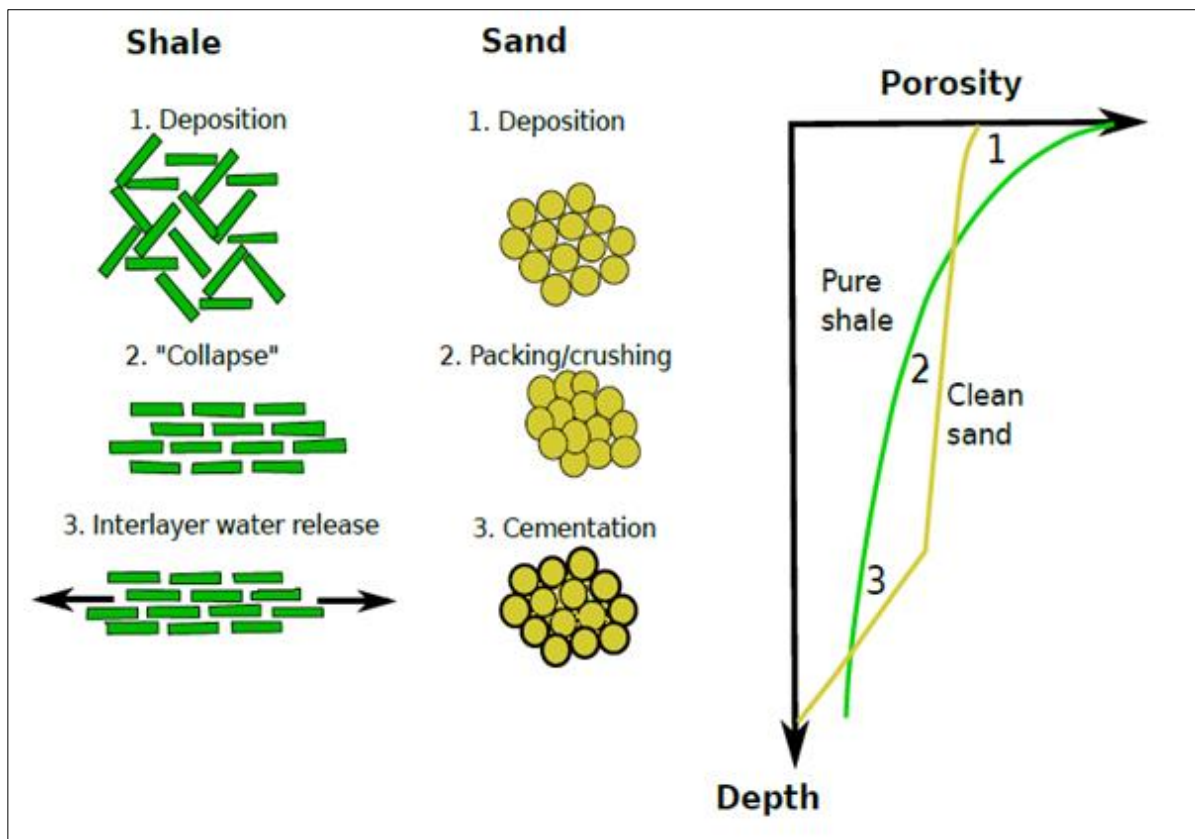


Figure 2.3: Mechanical and chemical processes in sandstones and shales during burial and compaction. Modified from Marion (1990).

The shales have higher initial porosities than coarser sediments like silt and sandstones, and the mechanical compaction will affect clay rich sediments more than sandstones (Mondol et al., 2007). Sandstones are mechanically compacted through grain crushing and the compaction is generally controlled by grain shape, size and sorting. Chemical compaction is controlled by time, temperature and mineralogy (Bjørlykke and Jahren, 2015, Lander and Walderhaug, 1999, Storvoll et al., 2005). For sandstones chemical compaction starts at approximately 60-70°C (Bjørlykke and Jahren, 2015). At these temperatures quartz will start to precipitate and will further reduce the porosity and increase the stiffness of the rock. Cementation will also continue during uplift, but at a lower rate, if the temperatures are high enough (Figure 2.4).

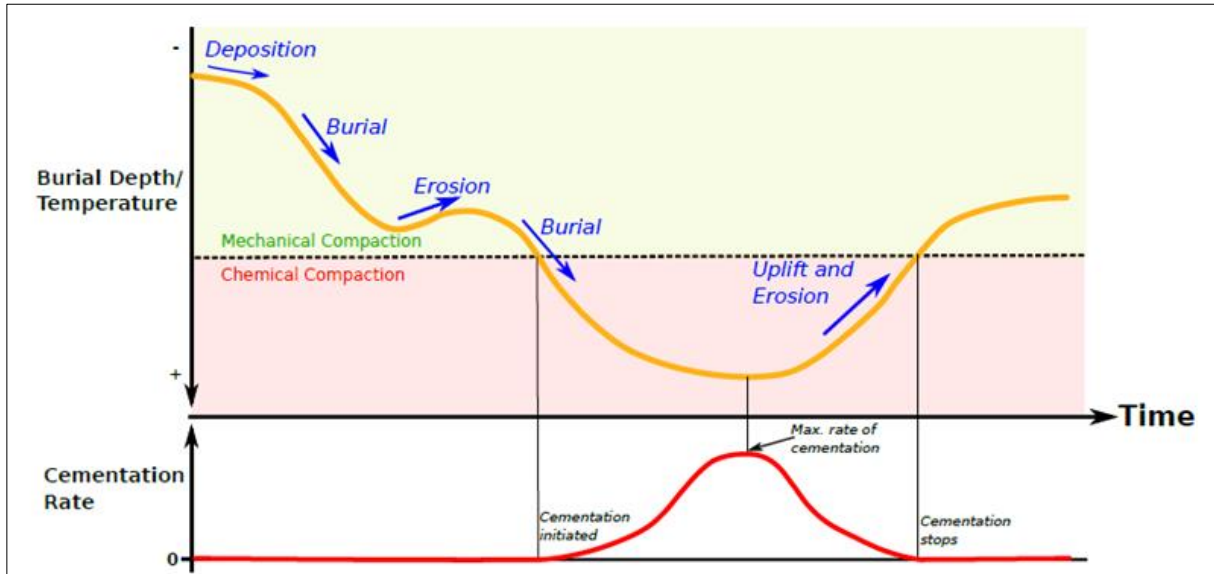


Figure 2.4: Conceptual illustration of cementation rate as a function of time and burial

The top graph in Figure 2.4 is showing changing temperature related to mechanical and chemical compaction.

Chemical compaction in shales involves mineral transformation in addition to porosity loss due to compaction. The most common alterations of clay minerals is the transformation of smectite to illite starting at around 70-80 °C (Bjørlykke and Jahren, 2015).

Changes in the rock properties with depth are the basis for methods for estimation of net erosion.

2.4 Net erosion and petroleum prospectivity

Net erosion is the most critical factor for understanding the distribution of shallow reservoirs in the Barents Sea and for evaluation of areas with potential leakage from reservoirs. This includes both natural leakage and leakage potentially caused by injection during the production phase.

To understand and quantify net erosion is important for understanding the geological development of an area. This is again fundamental for understanding the potential for leakage from the reservoir. Figure 2.5 summarizes typical effects on a petroleum system.

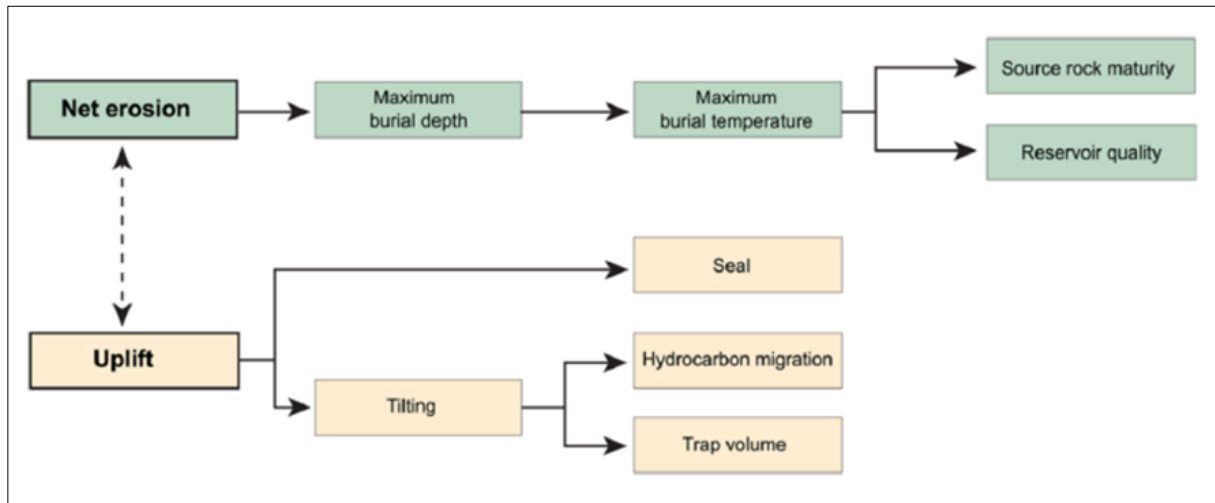


Figure 2.5: Effects of uplift and erosion on the processes affecting petroleum prospectivity. Modified from Henriksen et al. (2011)

2.4.1 Effects caused by net erosion that could affect leakage from the trap

Seal capacity: When a sealing rock experiences uplift and erosion, failure of the cap rock can occur. This can cause fracturing of the shale and leakage of hydrocarbons through the cap rock. Hydraulic fracturing and seal failure can also happen when there is overpressure although it has also been observed that cap rocks have kept their sealing capacity during uplift. Ductile seals like evaporites and hot shales can have this capacity.

Structural changes: When reservoirs are uplifted a pre-existing hydrocarbon accumulation can be tilted. This will lead to spillage of oil and gas. Structural changes can also create closures that were not present in the past. The result of this could be underfilled structures if no further hydrocarbons were generated after uplift.

Gas expansion and gas release from oil: Removal of overburden and decrease in pressure will cause gas to expand. If the structure was filled to spill point before overburden was removed, this could lead to expulsion from the closure. In a case where the seal is not leaking, it will result in oil spill out of the trap, and the gas will be trapped above the oil. In contrast, if gas is leaking from the top of the trap, this could also lead to an underfilled oil trap.

Fracture enhancement of reservoirs: The amount of strain reservoir rocks are able to withstand before fracturing is often significantly less than cap rocks can withstand. Thus, fracturing can also enhance porosity and permeability. A detailed explanation of the origin and consequence of rock fracturing is given by Sorkhabi (2015).

Remigration: When hydrocarbons are lost due to failure of seals, overpressure and hydrofracturing or spillage the hydrocarbons could extend all the way to the surface. However, the possibility of remigration is still present. This means that hydrocarbons from a deeper horizon can migrate to a new location and possibly get trapped in shallower or adjacent structures.

Reservoir quality: A rock that has been buried and uplifted will have a compaction and diagenetic state that reflects its maximum burial depth. Diagenetic processes are irreversible and will reduce both porosity and permeability, thus this gives poorer reservoir quality than normally expected at the new depth.

2.5 Methodology for quantifying net erosion

Several different techniques can be used to quantify uplift and erosion:

- Maximum burial studies estimating removed overburden using sonic velocity, density or vitrinite reflectance.
- Fission-track studies use apatite fission track data to constrain the erosional and cooling history of a basin.
- Geomorphological studies of present topography for estimation of uplift and subsidence, by correlation of offshore geology and onshore morphological elements.
- Sediment supply studies for estimating increased erosion rates and possible related uplift.
- Structural studies on seismic data for estimation of relative uplift and removal of overburden.
- Studies of seismic velocities for detailed lateral variations of net erosion.

The technique that uses shale velocities measured in wells is illustrated below (Figure 2.6).

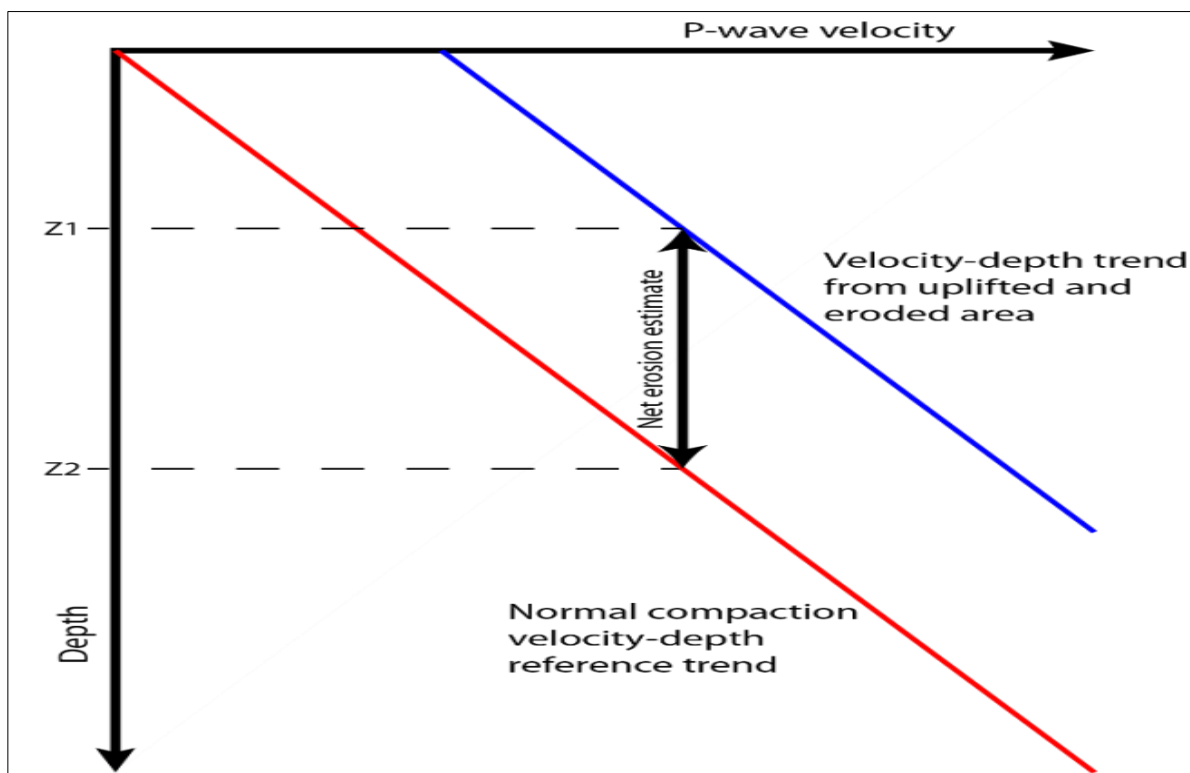


Figure 2.6: Quantification of net erosion from compaction techniques using P-wave velocity vs. depth trend for shales.

The difference between the reference trend (red) and the blue trend line which has undergone uplift and erosion will give the net erosion estimate. The net erosion is the difference between present day burial depth for the formation (Z1) and maximum burial depth (Z2).

2.6 Net erosion estimates

Net erosion estimates from different methods are summarized below. The shallow reservoirs in the Barents Sea are situated in areas with high net erosion. Figure 2.7 shows the estimates calculated from velocities in wells. The figure shows an increasing trend towards the north and north east and partial correlation with individual structural elements.

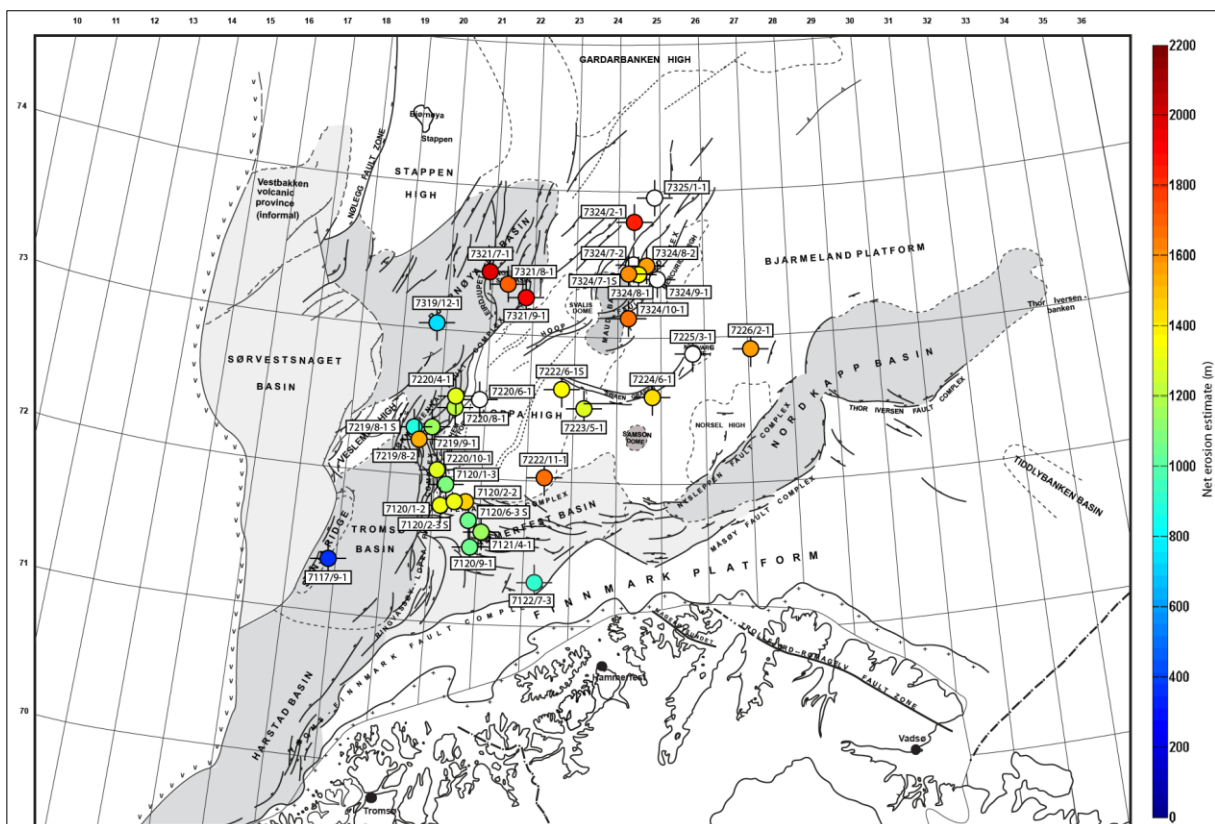


Figure 2.7: Location of net erosion estimates from Barents Sea wells. Modified from Faleide et al. (2010).

Compared to using wells, the spatial resolution using seismic interval velocities for the estimation is significantly improved (Figure 2.8). The net erosion map created from seismic interval velocities for the top BCU Horizon shows increasing net erosion from south to north and from west to east. Due to the dense velocity grid compared to the well database this map is much more detailed. Net erosion results from velocity trends in wells are included for comparison. In the blue area at the Loppa High net erosion is not estimated.

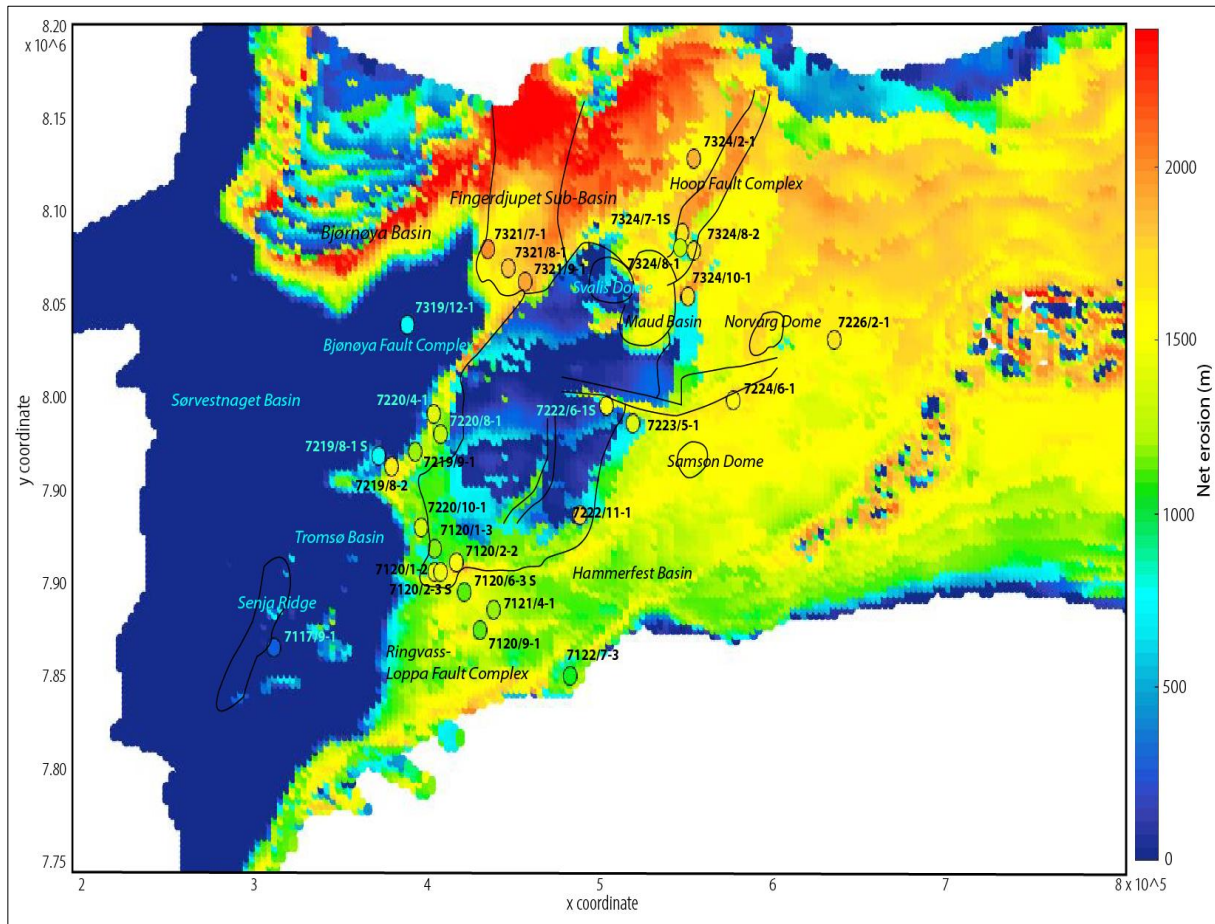


Figure 2.8: Net erosion map created from seismic interval velocities for the top BCU Horizon

2.7 Shallow reservoirs net erosion estimates

The most important shallow reservoirs in Barents Sea are probably of Late Triassic and Jurassic age. The Jurassic sedimentary unit is thin compared to the Triassic package (Figure 2.9). The Jurassic units are also characterized by many faults, and the high fault activity continued from late Jurassic- into early Cretaceous time. After the period with high faulting activity a period with large scale Cretaceous subsidence occurred. The present-day thickness of the Cretaceous overburden formation varies in the study area, thickest in the west and thinner towards the east.

The entire region continued to subside into the Early Tertiary period. In places formations reached a maximum burial depth close to 2000 meters deeper than it is buried today before it was uplifted.

Based on erosion estimates and quantification of sediment volumes, it has been estimated that the glacial erosion can account for 40-60% of the total estimated net erosion (Baig et al., 2016, Laberg et al., 2012). Isostatic response to the glacial erosion can explain a significant part of this uplift and erosion, but glaciers can also erode without any simultaneous uplift. Most authors date maximum burial and the subsequent

onset of uplift to have occurred in middle Eocene time, approximately 40 million years ago.

This erosion did not affect the westernmost areas, but the rest of the study area was strongly affected by the event (Figure 2.9). It is the northern and north-eastern areas that have been eroded the most. In the Fingerdjuvet sub-basin almost 2000 meters of strata was removed and in the Hoop area more than 1600 meters was eroded (Figure 2.7 and Figure 2.8). This is the explanation for the shallow Jurassic and Triassic reservoirs in these areas.

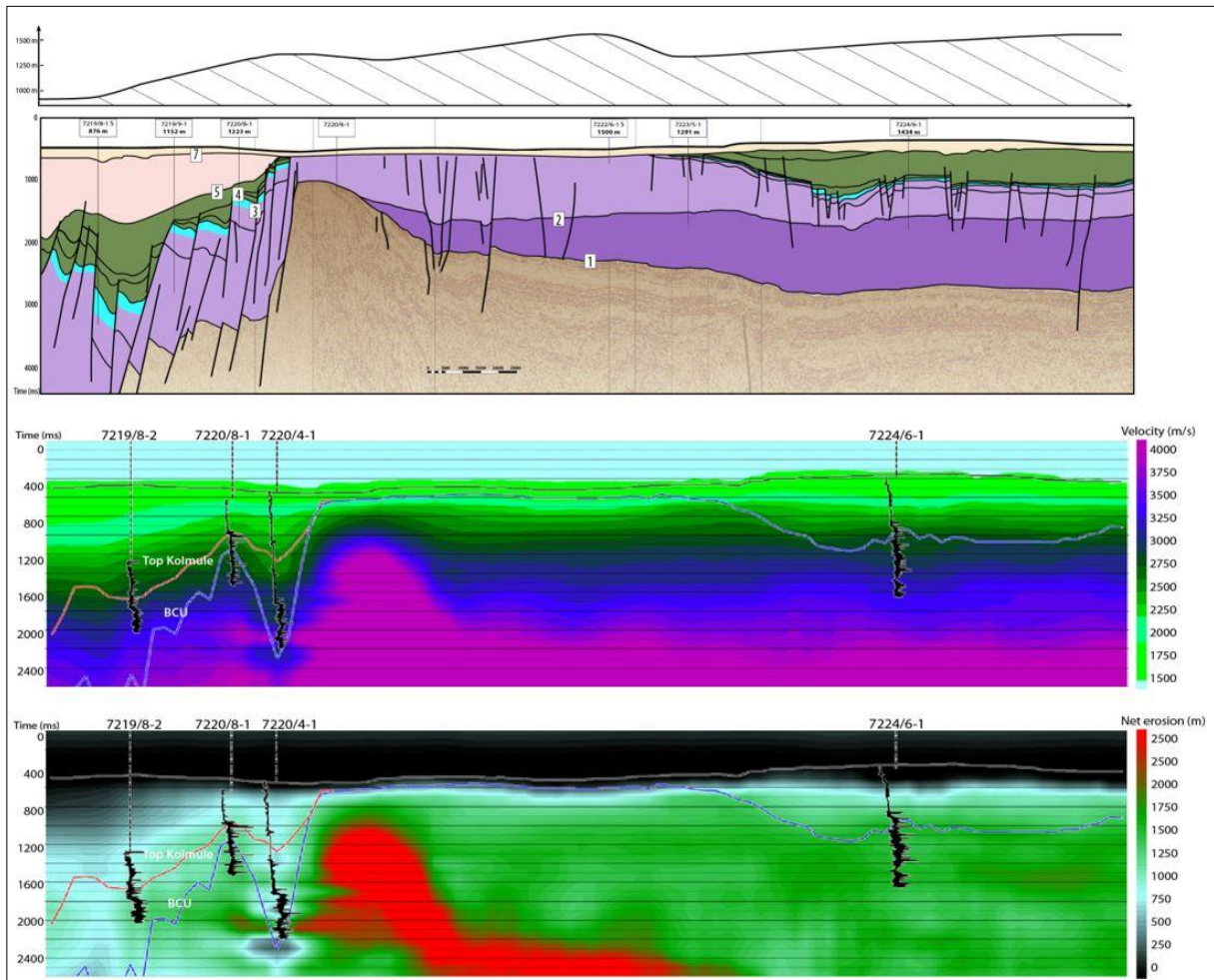


Figure 2.9: Regional east-west geological cross section number combined with net erosion estimates from seismic velocities and velocity depth trends in wells.

Net erosion estimates are included in the well position on top of the geological model (upper figure). The amount of net erosion is illustrated by the shaded area below the smoothed line on top of the model. Scale for net erosion is shown in the upper left corner of the figure. The seismic interval velocities used to estimate net erosion are included below the geological model (middle figure). The actual net erosion from seismic velocities is shown in the lower figure.

3. Model Production Well and Injection Well

A (hypothetical/model) production well and injection well design has been established to assist with focusing the assessments. The Wisting Central II well (7324/7-3S) with its long 1403 m horizontal section is used as a reference to define well design criteria.

3.1 Well objectives

The well objectives are:

- Production well: Produce oil and associated gas from one or multiple zones/compartments by use of horizontal well. Ability to access well with WL/CT to log and isolate water producing zones at a later stage by setting of straddle packers / cementing.
- Injection well: Inject water / gas to improve recovery. Ability to access well with WL/CT to log.

3.2 Formation & reservoir characteristics

The table below shows the parameters that are used in assessments:

Table 3.1: Parameters used in assessments

Parameter	Value	Justification
Seabed	450 mRKB	50% of the Barents Sea is between 200 – 500 m.
Top reservoir	450 mRKB + 300 m = 710 mTVDRKB	The depth of shallow reservoirs varies between 225 m to 537 m. The selected 300 m overburden thickness is used to highlight potential issues with formation integrity.
Reservoir thickness	30 m gross	This is not a critical parameter
P, reservoir	1,03 sg	Normally pressured
T, reservoir	17 °C	
LOT vs depth	See chapter 5.	This is a critical parameter.

3.3 Well design

The table below shows the basis of design elements that are used in assessments.

Table 3.2: Design elements used in assessments

Element	Description	Justification
Max. horizontal displacement	1310 m	Wells to be drilled from a well cluster – a long range is beneficial for optimizing number of clusters. Horizontal displacement will be restricted by ability to slide to correct azimuth/hole angle during directional drilling. (Wisting Central II ca. 1750 m)
Horizontal section range	1170 mMD	Allow for penetrating faults and draining several reservoir compartments. (Wisting Central II: 1450 mMD)
Kick-off point	450 + 50 M = 500 mTVD	
Dogleg range	8-12 deg/30 m	Wisting Central II well: 9-12 deg/30 m
30" Conductor	Setting depth: 498mTVD/498 mMD Driven or cemented	4 joints, may need a larger OD or CAN solution if soil is unconsolidated.
18 ¾" Wellhead	WP 690 bar, VX/HX	Standard size / profile / rating. Can use 345 bar rating.
20" x 13 ⅜" surface casing	Setting depth: 660 mTVD/680 mMD, cemented with TOC at seabed.	Standard size. Foundation for BOP, Formation integrity to circulate out a 8 m ³ , 1,03 sg swabbed kick in case of drilling into the reservoir (planned or accidental)
9 ⅝" production casing	Setting depth: 710 mTVD/1200 mMD, cemented with TOC at 200 mMD above shoe/or top reservoir	Standard size casing. Isolate open hole / unstable formation before drilling the horizontal section. Reduce friction – increase reach when sliding to orient BHA. Formation integrity to circulate out a 4 m ³ , 1,03 sg swabbed kick.
Production well: 7" sand screen	On 5,5" blank pipe, with swell packers. OD of screens varies, 6 1/8" – 7"	Sand screens to prevent production of particles from unconsolidated sands. Swell packers to prevent cross flow in annulus / seal of shale sections which may become destabilized.
Injection well: 7" production liner	Setting depth: 710 mTVD/2000 mMD	Standard size. Cemented liner to prevent cross flow in annulus / out of zone injection. Seal-off shale sections which may react with water? Ability to isolate / shut off water injection zones later with straddle packers / cement.
5" production tubing	SCSSV set at 50 m below seabed and production packer.	Standard size and solution.
SS VXT	Subsea vertical tree	Subsea solution
Gas lift	Not required / not effective given vertical height of 300 mTVD from reservoir to seabed.	Alternatively, a seabed pump could be used.

3.4 Well profile

Table 3.3: Well profile

MD (m)	CL (m)	Inc (°)	Azi (°)	TVD (m)	NS (m)	EW (m)	V.Sec (m)	Dogleg (°/30m)
0		0	0	0	0	0	0	0
500	500	0	0	500	0	0	0	0
830	330	90	0	710	210	0	210	8.18
2000	1170	90	0	710	1380	0	1380	0

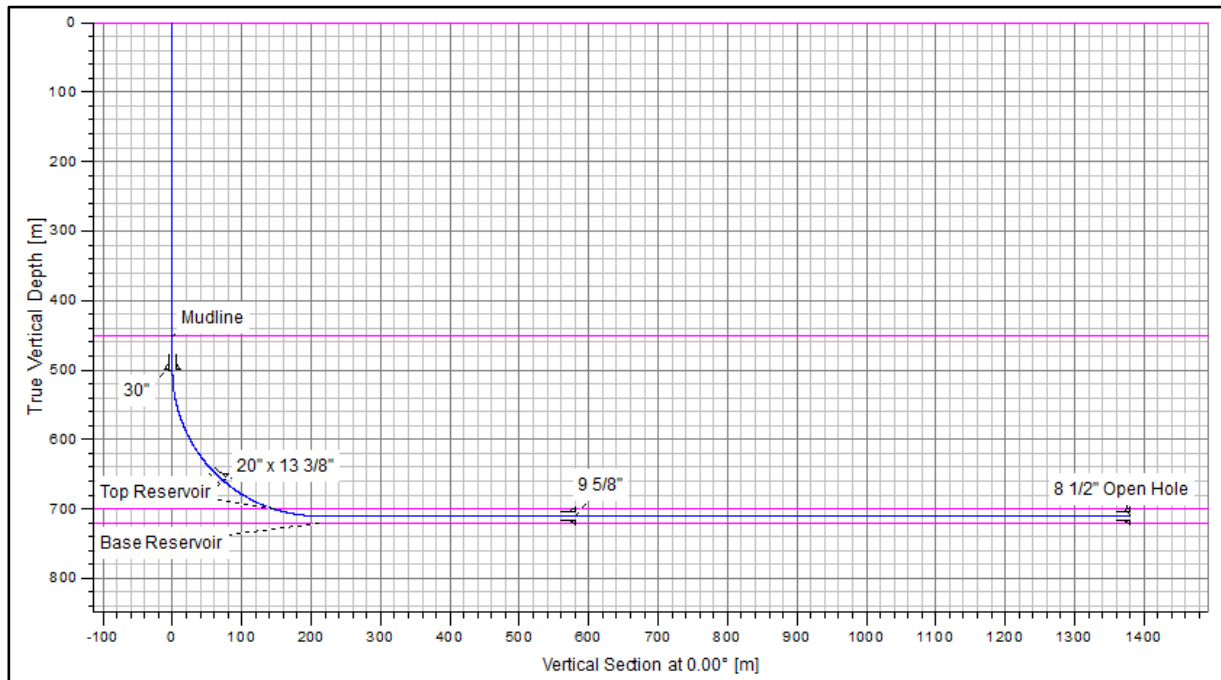


Figure 3.1: Well profile – vertical section

3.5 Model production well

The illustration below shows a hypothetical production well, with 9 5/8" production casing into the reservoir with sand screens in the productive interval.

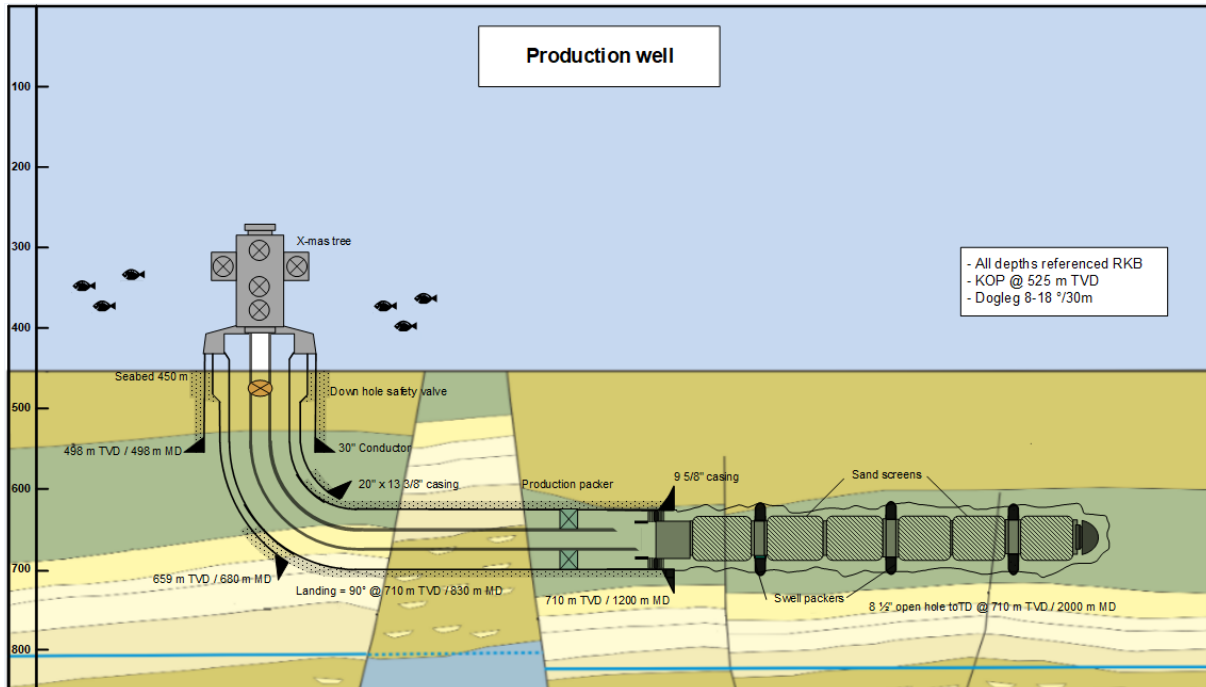


Figure 3.2: Model production well

3.6 Model injection well – with 9 5/8" set into the reservoir

The illustration below shows a hypothetical injection well, with 9 5/8" production casing into the reservoir with a cemented reservoir liner in the injection interval.

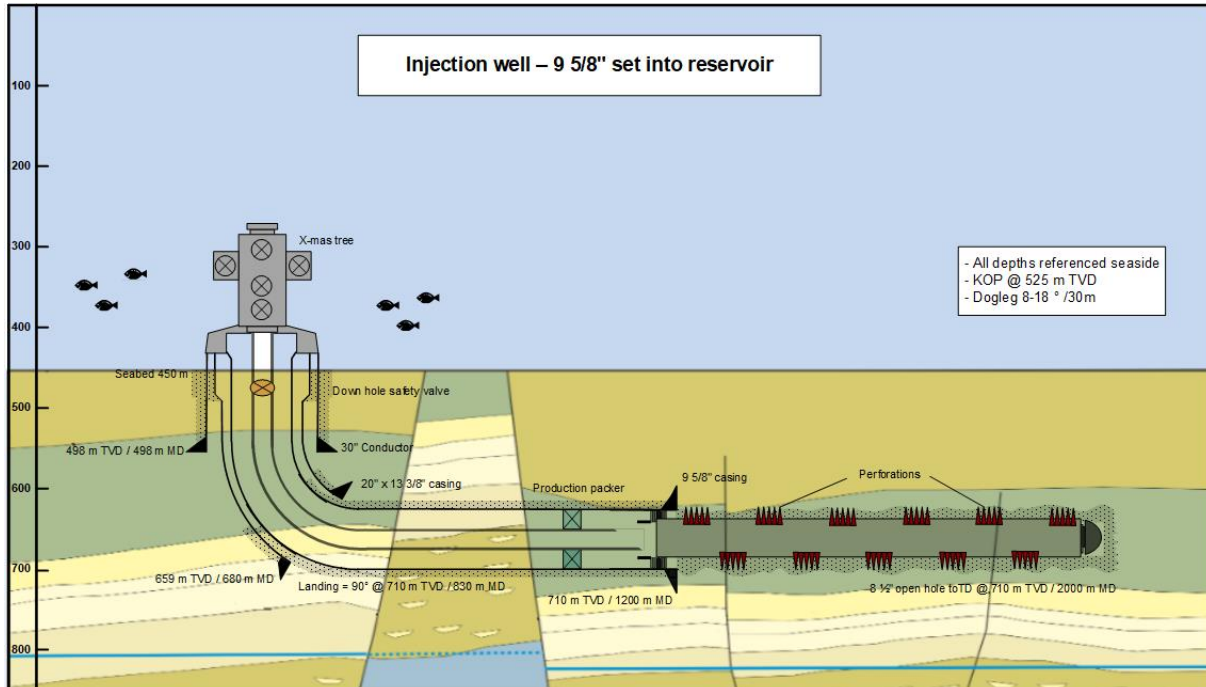


Figure 3.3: Model injection well – 9 5/8" casing set into the reservoir

3.7 Model injection well – with 9 5/8" set above the reservoir

The illustration below shows a hypothetical injection well, with 9 5/8" production casing above the reservoir with a cemented reservoir liner in the injection interval.

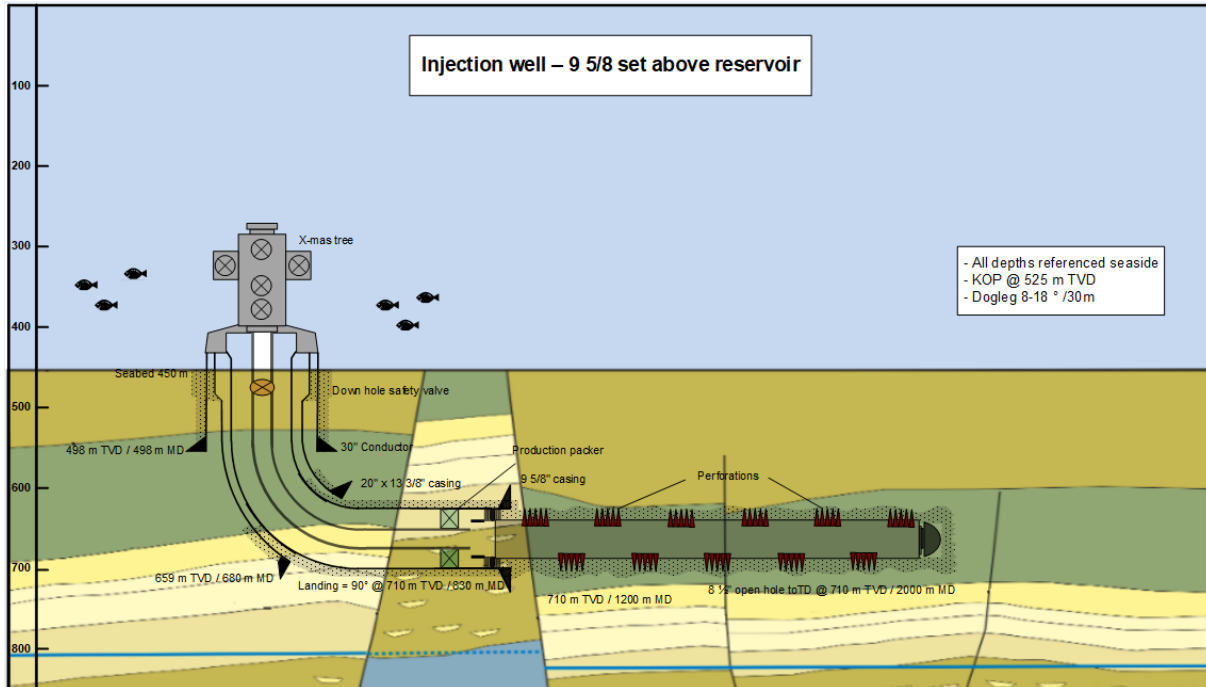


Figure 3.4: Model injection well – 9 5/8" casing set above the reservoir

4. Well Integrity Assessment

4.1 General

Well integrity during the well construction phase is about replacing the natural seal of the cap rock with lasting man-made sealing well barrier elements such as cement, casing, tubing and packers. The well design, construction techniques and well barriers are the same for shallow reservoirs as for deeper reservoirs. When producing the hydrocarbons or injecting water to improve recovery, excessive pressure increase in the reservoir could cause fracturing on the cap-rock formation of the reservoir cap rock and overlaying formations with potential for escape of formation fluids to the seabed.

The main difference comparing deep and shallow reservoirs may, is the thickness or thinness of the overburden, lower differential pressure and weaker formations.

In this chapter, we will define the well barriers for the model production and injection wells, compare these with performance requirements described in NORSOK D-010 Well Integrity standard and identify differences between shallow and deep wells.

4.2 Challenges

Challenge: How to control downhole injection pressure to prevent fracturing of the overburden?

To prevent fracturing of the reservoir cap rock and overlaying formations with potential for escape of formation fluids to the seabed, the downhole injection pressure must be monitored by use of pressure sensors and kept within defined values. Overlaying fractures must be identified from seismic imaging and LWD logs, then isolated with casing/liner cement or swell packers. A field specific rock mechanical model should be established based on XLOT data, geological modelling and regional principal stresses.

Challenge: Insufficient formation strength at the intermediate casing?

In the case where production casing is set into the reservoir, the intermediate casing, casing cement and in-situ formation at the intermediate shoe depth become well barrier elements in the secondary well barrier. All well barrier elements must be strong enough to contain any escaping reservoir fluids. The fracture pressure must be estimated based on extended leak-off test data and regional rock stress models. With open hole exposed in casing annuli, the B-annulus pressure should be continuously monitored. This requires a subsea WH with access to B-annulus with the ability to bleed off to avoid fracturing of the formation.

4.3 NORSOK D-010 Standard

In this section, the model well designs are compared with requirements and guidelines in NORSOK Standard D-010 Well Integrity in Drilling and Well Operations, rev. 4, 2013 (D-010). The work process is described below:

1. Define well barriers (have used D-010 examples to the extent possible)
2. Define/establish well barrier element (WBE) acceptance criteria (D-010 requirements only)
3. Assess the risk of not fulfilling the WBE performance criteria which can be related to:
 - a. Directional drilling (dogleg 8 deg/30 m)
 - b. Running of tools & liners (HD/TVD ratio: 1380 m /710m = 1,94)
 - c. Formation integrity

The following colors / abbreviations are used to categorize risk of non-compliance with D-010 standard:

Table 4.1: Colors/Abbreviations

NC-Risk	Description
Low	Likely to comply with D-010. No particular issues compared to normal wells
Medium	Can happen and may have serious consequences
High	Unlikely to comply with D-010 requirements with high potential for significant consequences.

The tables presented below contain the requirements (R), guidelines (G) and in Well Barrier Element Acceptance tables (EAC) with any supplemental requirements/guidelines listed in 5.4, 7.4 and 8.4 Well barrier elements acceptance criteria in D-010 standard.

As the loads on WBE in an injection well are larger than in a production well, the analysis is focused on injection well.

4.4 Well barriers in the model injection well

Secondary oil recovery or reservoir pressure maintenance by matrix water injection or gas flooding could exert excessive pressure loads on well barrier elements.

The model well in Figure 4.1 shows the 9 5/8" production casing set into the reservoir. In the following sections, the WB with casing set above the reservoir is analyzed first.

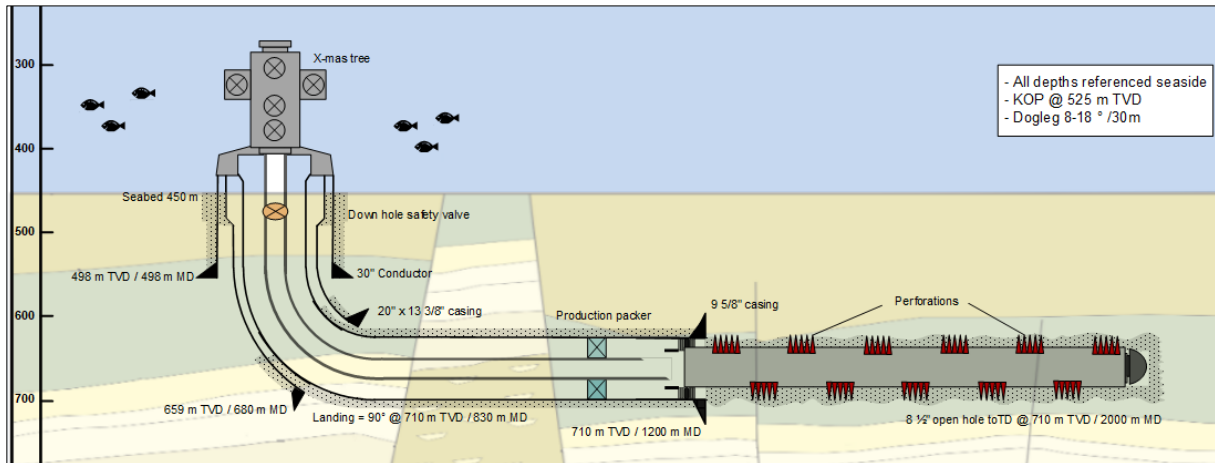


Figure 4.1: Model injection well

4.4.1 Alternative 1 - production casing set above reservoir

Reasons for setting the 9 5/8" production casing set above the reservoir can be;

- Case off unstable formation or loss zones before drilling the long horizontal section
- Use 9 5/8" casing/formation at the shoe/casing cement as WBE in the secondary well barrier.
- Facilitate deeper intersection for a relief well if blowout should occur when drilling into the reservoir
- Economic reasons; less hole volume to be removed and discharged, faster drilling (ROP) and less steel.

The model well in Figure 4.2 shows the 9 5/8" production casing set above the reservoir.

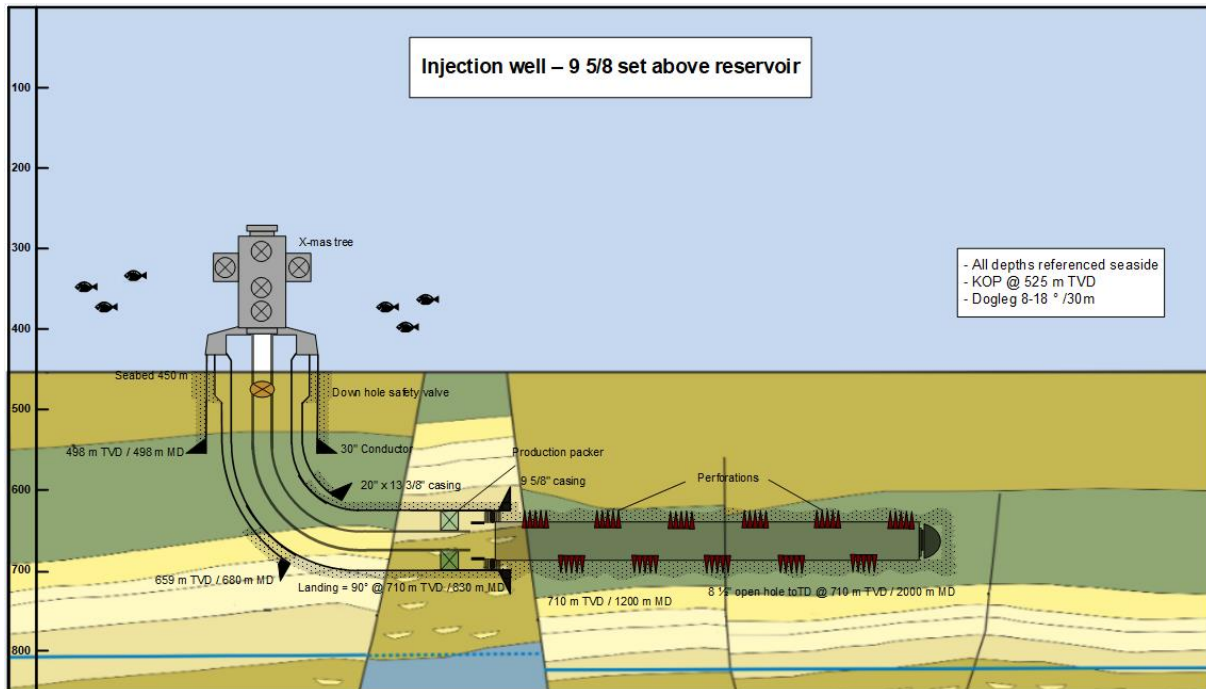


Figure 4.2: Model injection well - 9 5/8" production casing set above reservoir

The figure below shows one solution for defining the well barriers with the 9 5/8" production casing set above the reservoir.

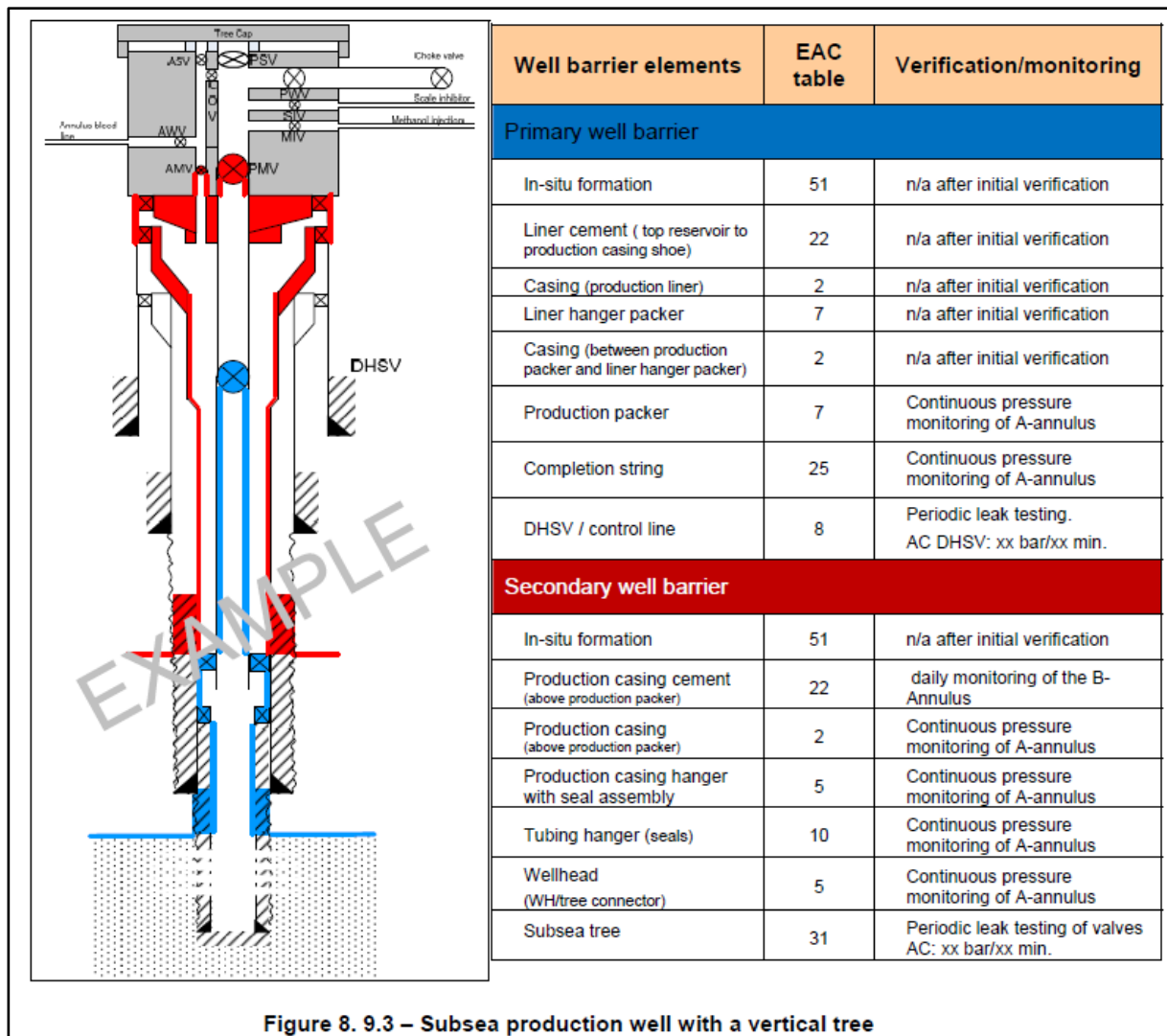


Figure 8.9.3 – Subsea production well with a vertical tree

Figure 4.3: NORSOK D-010 WBS – Cemented production casing set above reservoir

With this in mind, let us discuss the issues relating to the well barriers and the WBEs.

4.4.1.1 Primary well barrier, Alternative 1 - production casing set above reservoir

The primary well barrier elements are described in Table 4.2.

Table 4.2: Primary well barrier elements

WBE	Issues / comments	NC-risk
<i>In-situ Formation</i>	See discussion to follow.	High
<i>Liner cement</i>	Production casing set above the reservoir. See discussion to follow	High
<i>Liner</i>	Unable to run the liner to TD due to higher friction than estimated and limited gravitational push force from the drill pipe. This can be overcome by use of DC to increase push, rotating the liner, use of reamer shoe and OBM for better lubricity.	Medium
<i>Liner Lap Packer</i>	This is normally set by hydraulic pressure and should not be affected by shallow setting depth. However, excessive casing wear on the low side of the production casing may cause ovality and could affect the sealing performance of the packer rubber element.	Medium
<i>Casing</i>	This short section exposed below the production packer and is not subject to any abnormal forces compared to a normal well. Casing wear can be estimated and mitigated in design by increasing casing wall thickness. Operationally, the use drill pipe wear protectors can be an option.	Low
<i>Production Packer</i>	This is normally set by hydraulic pressure and should not be affected by shallow setting depth. However, excessive casing wear on the low side of the production casing may cause ovality and could affect the sealing performance of the packer rubber element.	Medium
<i>Tubing</i>	The stresses in the tubing caused by high dogleg 8-11 deg/30 m dogleg is assumed to be low. Temperature induced stresses from injection of seawater at ambient temperature should be less than in normal wells, given very low change in temperature.	Low
<i>DHSV</i>	Can be positioned minimum 50 blow seabed in the vertical part (coincides with KOP)	Low

In-situ Formation Acceptance Criteria

The in-situ formation surrounding the injection wellbore interval will be exposed to pressure loads arising from the pumping of water/gas into the matrix of reservoir rock through the perforations. Continuous excessive pressure loads or peaks can cause fracturing and fracture propagation to seabed.

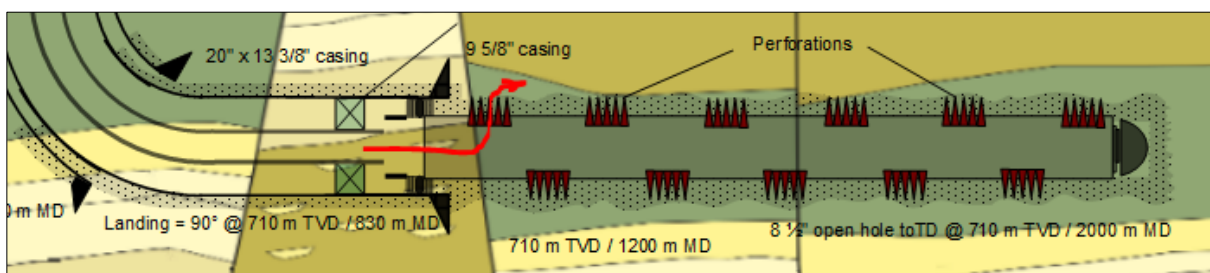


Figure 4.4: In-situ formation

Figure 4.5 shows simulated injection pressures in a vertical well and horizontal well versus number of injection days. In either case, injection pressure will reach caprock strength, at which time injection will have to cease to avoid possible fracture propagation towards seabed.

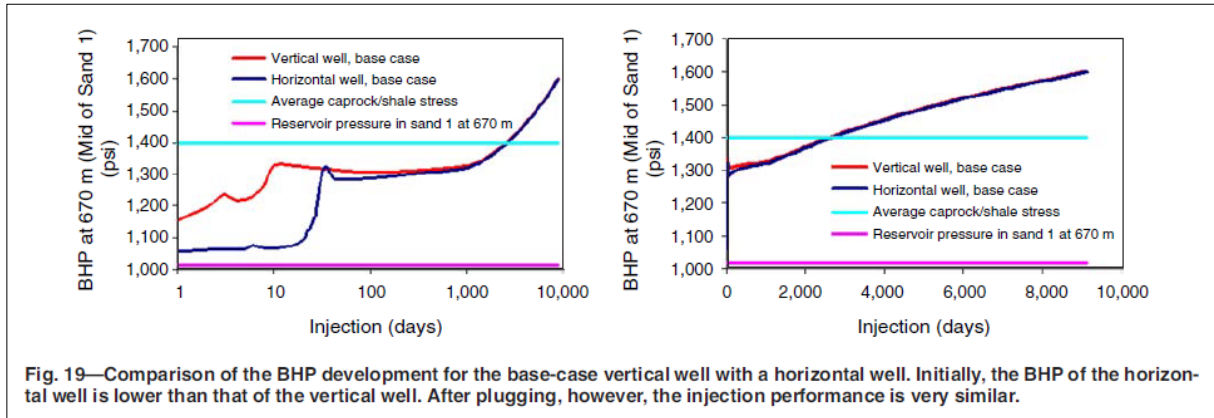


Fig. 19—Comparison of the BHP development for the base-case vertical well with a horizontal well. Initially, the BHP of the horizontal well is lower than that of the vertical well. After plugging, however, the injection performance is very similar.

This paper (SPE 180143) was accepted for presentation at the SPE Europec featured at the 78th EAGE Conference and Exhibition, Vienna, Austria, 30 May–2 June 2016, and revised

Figure 4.5: Comparison of BHP development

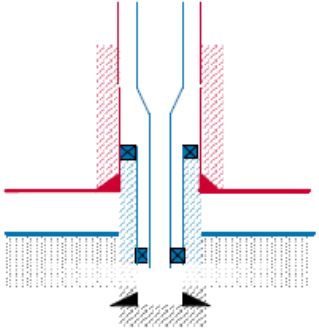
The tables presented below contain the requirements (R), guidelines (G) and in Well Barrier Element Acceptance tables (EAC) with supplemental requirements/ guidelines listed in sections 5.4, 7.4 and 8.4 Well barrier elements acceptance criteria in the D-010 standard.

Table 4.3: Well barrier elements – In-situ formation

#	NORSOK D-010 Requirements and guidelines	Type	Evaluation Comments
EAC 51 In-situ Formation	The element is the formation that has been drilled through and is located adjacent to the casing annulus isolation material or plugs set in the wellbore.		This is the formation surrounding the 9% casing cement and 7" liner cement.
1.	Is the formation impermeable with no flow potential?	G	The cap rock above / sediments above are impermeable
2.	Is the wellbore placed away from fractures and/or faults that may lead to out of zone injection or crossflow?	R	It is assumed that the well will be placed away from known fractures (from seismic interpretation) – however, there is always a risk that fractures can be penetrated during drilling, noticed or unnoticed.
3.	Will/is the formation integrity exceed(ing) the maximum wellbore pressure induced?	R	Downhole injection pressure must be controlled to be less
4.	Was the formation selected such that it will not be affected by changes in reservoir pressure over time (depletion, compaction, fracturing, re-activation of faults).	R	Compaction / subsidence likely to occur?
5.	Is the formation bonding directly to the casing/liner annulus material (e.g. casing cement) or plugs in the wellbore?	R	Yes
6.	Formation integrity pressure shall be verified by; PIT, or LOT, or XLOT or documented field model	R	All the methods can technically be applied. PIT and LOT is the most common. However, it is only the XLOT that will give the fracture opening pressure – a value that is critical to decide.

In addition;

Table 4.4: Well barrier elements – Injection wells/disposal wells

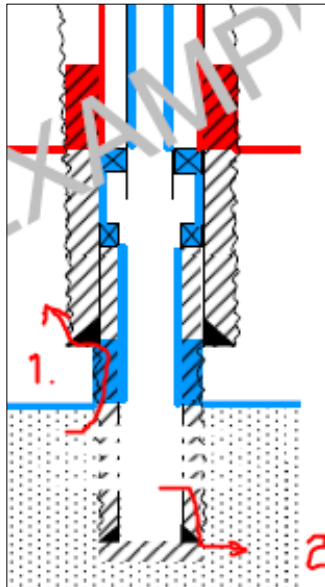
#	NORSOK D-010 Requirements and guidelines	Type	Evaluation / Comments
7.7.4	<i>Injection wells / disposal wells</i>		
1.	The well shall be constructed such that the injected media will be contained within the targeted formation zone (reservoir) without risk of out of zone injection.	R	This implies that physical characteristics of the reservoir and overburden is known, i.e. data collected during the exploration / appraisal phase: Cores, LOT/EXLOT, seismic logging and open hole logs
2.	For wells injecting at a pressure greater than the fracture closure pressure at the injection depth, the following applies:		Given the short vertical distance to the seabed, this is assumed not to be an option.
3.	a) the production packer shall be installed at a depth ensuring the injection or a casing leak below the production packer will not lead to fracturing of the cap rock or leak to shallower formation when applying maximum injection pressure (see figure 7.7.4.1);	R	Assumed N/A in the horizontal part.  Figure 7.7.4.1
4.	b) the casing/liner cement shall be logged and as a minimum have bonding from upper most injection point to 30 m MD above top reservoir;	R	N/A as the casing cement is not planned to be a part of primary and secondary well barriers.
5.	c) it shall be documented that the injection will not result in a reservoir pressure exceeding the strength of the cap rock	R	This requirement is ambiguous. It implies that one must know the formations strength of the cap-rock (see above). The reservoir pressure underneath the cap-rock will have to be estimated by reservoir simulations. The worst-case scenario will be to set pressure equal to the estimated / measured injection pressure in the perforations, given the short distance from the perforations to the cap rock. Further, the WH/surface injection pressure must be controlled which can be achieved by automatic shut-down / pressure relief valves.

Formation integrity testing - discussion

The pressure integrity of the in-situ formation is normally tested after having drilled 3-5 m of new formation below the casing shoe. The pressure in the well is increased until leak-off (LOT) is observed or stopped at a pre-determined pressure (leak-to). None of these methods gives a measurement of the formation fracture opening pressure, which is measured by conducting extended leak-off testing (ELOT). From a well construction point of view, it is not desirable to weaken the formation through ELOT “mini-fracturing” which may result in mud losses and reduction of wellbore stability. However, in an injection well it is imperative to know fracture pressure, so that the downhole injection

volumes can be maximized without fracturing the overburden. *SEE: Section 5 - Geomechanical Assessment.*

Reservoir Liner Cement Acceptance Criteria



The production liner cement is a WBE. The purpose of the liner cement in this context is to:

- a) prevent flow in the annulus between the liner and open hole and into the secondary well barrier, or
- b) prevent flow in annulus and into zones where injection is not desired, like natural fractures that could become a leak path to seabed.

From a commercial point of view:

- c) direct the flow into zones that will give the best recovery / pressure maintenance, or
- d) if zonal isolation is not required for EOR purposes, then an open hole completion without use of cement can be an option. (Not further discussed – see Production Well)

Figure 4.6: Production liner cement

The table below addresses production liner cement as a WBE.

Table 4.5: Well barrier element – Casing cement

WBE	NORSOK D-010 Requirements and guidelines	Type	Evaluation / Comments
EAC 51 Casing Cement	This element consists of cement in solid state located in the annulus between concentric casing strings, or the casing/liner and the formation.		
1.	A cement program shall be issued for each cement job, <i>minimum</i> covering the following:		
2.	casing/liner centralization and stand-off to achieve pressure and sealing integrity over the <i>entire</i> required isolation length;	R	Achievable
3.	use of fluid spacers;	R	Achievable
4.	effects of hydrostatic pressure differentials inside and outside casing and ECD during pumping and loss of hydrostatic pressure prior to cement setting up;	R	Effects can be managed by use of lighter cement / reduced displacement rates.
5.	the risk of lost returns and mitigating measures during cementing.	R	Losses should be avoided
6.	For critical cement jobs, HPHT conditions and complex/foam slurry designs the cement program shall be verified independent (internal or external), qualified personnel.	R	Achievable
7.	The cement recipe shall be lab tested with dry samples and additives from the rigsite under representative well conditions. The tests shall provide thickening time and compressive strength development.	R	Achievable

WBE	NORSOK D-010 Requirements and guidelines	Type	Evaluation / Comments
8.	The properties of the set cement shall provide lasting zonal isolation, structural support, and withstand expected temperature exposure.	R	Achievable
9.	Cement slurries used for isolating sources of inflow containing hydrocarbons shall be designed to prevent gas migration, including CO ₂ and H ₂ S, if present.	R	Achievable
10.	Casing cement length;		
11.	shall be designed to allow for future use of the well (sidetracks, recompletions, and abandonment).	R	Sidetracks can be done out of 7" liner (5 ½ hole)
12.	General: Shall be <i>minimum</i> 100 m MD above a casing shoe/window.	R	Achievable
13.	Conductor: Should be defined based on structural integrity requirements.	G	N/A
14.	Surface casing: Shall be defined based on load conditions from wellhead equipment and operations, and	R	N/A
15.	TOC should be at surface/seabed	G	N/A
16.	The cement length shall be verified by one of the following:		
17.	Bonding logs: Logging methods/tools shall be selected based on ability to provide data for verification of bonding. The measurements shall provide azimuthal / segmented data. The logs shall be verified by qualified personnel and documented	R	It is possible to log on drill pipe to find intervals with good zonal isolation to target specific injection zones.
18.	100 % displacement efficiency based on records from the cement operation (volumes pumped, returns during cementing, etc.). Actual displacement pressure/volumes should be compared with simulations using industry recognized software. In case of losses, it shall be documented that the loss zone is <i>above</i> planned TOC. Acceptable documentation is job record comparison with similar loss case(s) on a reference well that has achieved sufficient length verified by logging.	R	Not a good method for qualifying intervals with good cement.
19.	In the event of losses, it is acceptable to use the PIT/FIT or LOT as the verification method <i>only</i> if the casing cement shall be used as a WBE for drilling the next hole section. (This method shall not be used for verification of casing cement as a WBE for production or permanent abandonment.)	R	N/A
20.	Critical casing cement shall be logged and is defined by the following scenarios:		
21.	the production casing/production liner when set into/through a source of inflow with hydrocarbons;	R	Achievable – see 17.
22.	the production casing/production liner when the same casing cement is a part of the primary and secondary well barriers;	R	N/A
23.	wells with injection pressure which exceeds the formation integrity at the cap rock.	R	Given the short vertical distance to the seabed, deliberate fracturing is considered not to be an option
24.	Actual cement length for a qualified WBE shall be:		

WBE	NORSOK D-010 Requirements and guidelines	Type	Evaluation / Comments
25.	above a potential source of inflow/ reservoir;	R	This implies that the distance between the casing shoe and top reservoir should be at least 50 mMD cater for space above top reservoir. See 26. Under.
26.	50 m MD verified by displacement calculations or 30 m MD when verified by bonding logs. The formation integrity shall exceed the maximum expected pressure at the base of the interval.	R	The best method is to verify by cement bond logs. Loss of returns during cementing – see discussion overleaf
27.	2 x 30m MD verified by bonding logs when the same casing cement will be a part of the primary and secondary well barrier.	R	N/A in this case
28.	The formation integrity shall exceed the maximum expected pressure at the base of each interval.	R	Applicable, see 4.2.2
29.	For wells with injection pressure exceeding the formation integrity at the cap rock: The cement length shall extend from the upper most injection point to 30 m MD above top reservoir verified by bonding logs.	R	N/A, see 4.2.2

Loss of returns during cementing of reservoir liner – discussion

When cementing a 1300 – 1500 mMD long horizontal (rotational) liner, the main contributor to increased bottom hole pressure is friction loss in annulus (ECD). The bottom hole pressure could exceed the formation strength in the open hole and cause losses to the formation. The consequences can be that there is no cement around the top part of the liner, exposing the formation between the casing shoe and top of reservoir to injection pressure, with potential for fracturing. If not remedied by, for example, squeeze cementing, the liner cement is no longer a WBE in the primary well barrier. The primary well barrier must be redefined as shown in figure below.

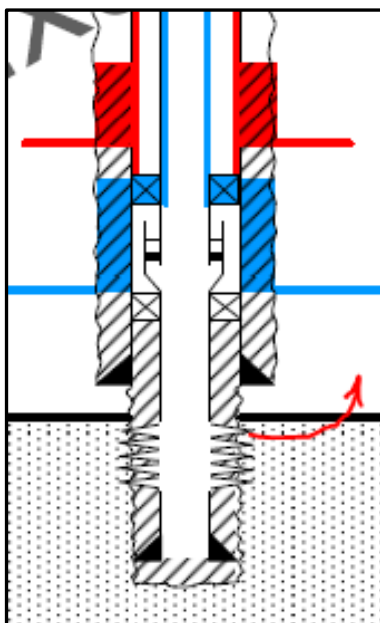


Figure 4.7: Casing cement dual well barrier

One acceptable solution is to define the 9 5/8" casing cement to be a WBE in the primary and secondary well barriers, given that two (2) intervals with accumulated 30 mMD of good cement can be measured by cement bond log. *SEE*: Section 4.5 Well barriers in production well. The reduction in formation strength needs to be assessed at the basis of the deepest sealing interval of the casing cement, which could result in reduced injection pressures.

Fracturing of the cap rock is more serious as this could instigate a weak point in the wellbore / in-situ formation. If the loss zone is near a perforated interval, the injection fluid could reopen and propagate fractures – in worst case back to the seabed.

Liner cementing jobs must be carefully planned, simulated and controlled during displacement to prevent fracturing / losses.

4.4.1.2 Secondary well barrier, Alternative 1 – production casing set above reservoir

With reference to Figure 4.3, the secondary well barrier elements are:

Table 4.6: Secondary well barrier elements – Alternative 1

WBE	Issues / comments	NC-risk	Well barrier figure
<i>In-situ Formation</i>	See discussion below.	High	
<i>Production casing cement</i>	Production casing set above the reservoir. See discussion below	High	
<i>Production casing</i>	More wear due to higher build angle /dog leg. This can be estimated and mitigated in design by increasing casing wall thickness. Operationally, the use drill pipe wear protectors can be an option.	Medium	
<i>Production casing hanger</i>	As per normal well	Low	
<i>Tubing hanger</i>	As per normal well	Low	
<i>Wellhead</i>	As per normal well	Low	
<i>Subsea production tree</i>	As per normal well	Low	

In-situ formation acceptance criteria

The table below shows only requirements that could be difficult to achieve.

Table 4.7: Secondary well barrier elements – In-situ formation

Check	NORSOK D-010 Requirements and guidelines	Type	Evaluation Comments
EAC 51 In-situ Formation	<i>The element is the formation that has been drilled through and is located adjacent to the casing annulus isolation material or plugs set in the wellbore.</i>		<i>This is the formation surrounding the 9 5/8" casing cement and 7" liner cement.</i>
1.	Is the formation impermeable with no flow potential?	G	The cap rock above / sediments above are impermeable
2.	Is the wellbore placed away from fractures and/or faults that may lead to out of zone injection or crossflow?	R	It is assumed that the well will be placed away from known fractures (from seismic interpretation) – however, there is always a risk that fractures can be penetrated without being noticed.
3.	Will/is the formation integrity exceed(ing) the maximum wellbore pressure induced?	R	Downhole injection pressure must be controlled to be less
4.	Was the formation selected such that it will not be affected by changes in reservoir pressure over time (depletion, compaction, fracturing, re-activation of faults).	R	Compaction / subsidence likely to occur?
5.	"Is the formation bonding directly to the casing/liner annulus material (e.g. casing cement) or plugs in the wellbore?"	R	Yes

Casing cement acceptance criteria

The table below shows only requirements that could be difficult to achieve.

Table 4.8: Secondary well barrier elements – Casing cement

WBE	NORSOK D-010 Requirements and guidelines	Type	Evaluation / Comments
EAC 51 Casing Cement	<i>This element consists of cement in solid state located in the annulus between concentric casing strings, or the casing/liner and the formation.</i>		<i>9 5/8" casing cement</i>
1.	The cement length shall be verified by one of the following:		
2.	a) Bonding logs: Logging methods/tools shall be selected based on ability to provide data for verification of bonding. The measurements shall provide azimuthal / segmented data. The logs shall be verified by qualified personnel and documented	R	It is possible to use acoustic LWD or WL log on drill pipe to establish the top of cement
3.	b) 100 % displacement efficiency based on records from the cement operation (volumes pumped, returns during cementing, etc.). Actual displacement pressure/volumes should be compared with simulations using industry recognized software. In case of losses, it shall be documented that the loss zone is <i>above</i> planned TOC. Acceptable documentation is job record comparison with similar loss case(s) on a reference well that has achieved sufficient length verified by logging.	R	This is the most common method. However, given the short vertical height of cement (+/-20 – 50 mTVD), it can be very difficult to observe a static pressure increase of 0,8 – 2,4 bar!

4.4.2 Alternative 2 – production casing set into the reservoir

The reasons for setting 9 5/8" production casing into the reservoir can be:

- Verify presence of HC bearing reservoir, and if none is found - have the option to conduct an open hole sidetrack to another location.
- Reduce the length of the next section.
- Isolate potential unstable formation & fault zones before entering the target zones.

The model well in Figure 4.8 shows the 9 5/8" production casing set above the reservoir.

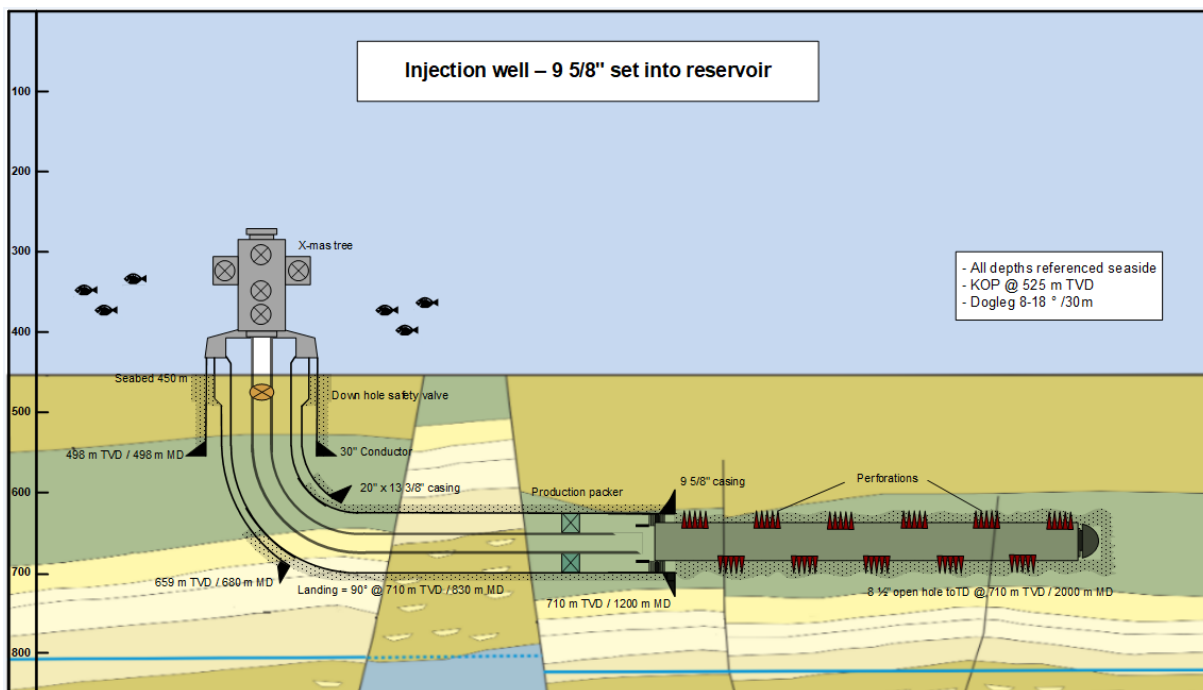


Figure 4.8: Model injection well – 9 5/8" production casing set above reservoir

Figure 4.9 shows one solution for defining the well barriers with the 9 5/8" production casing set into the reservoir. It shows a solution for a platform well, which is very similar to a subsea well disregarding the location/type of XMT, type of wellhead and sand screens in the reservoir.

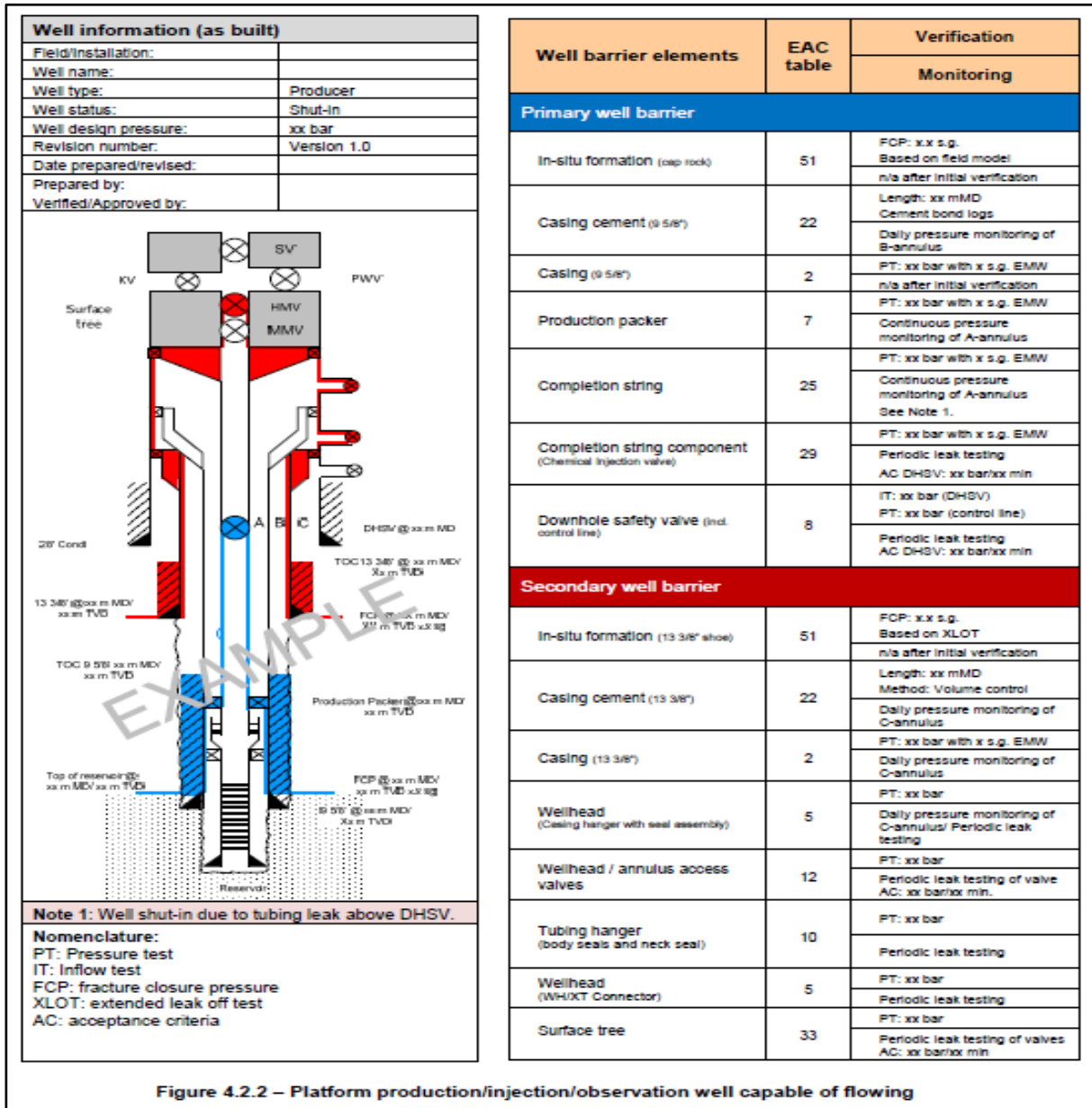
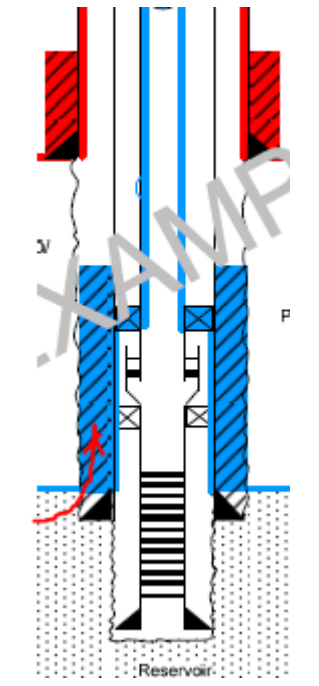
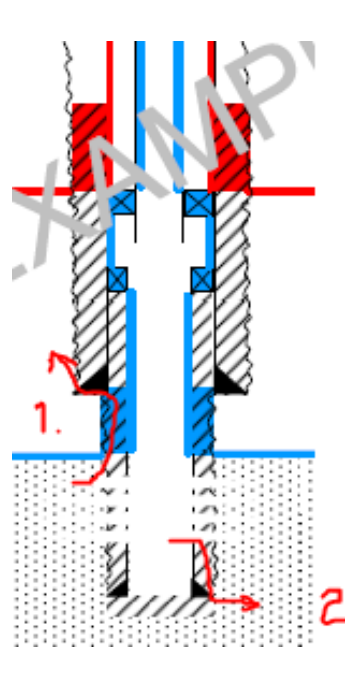
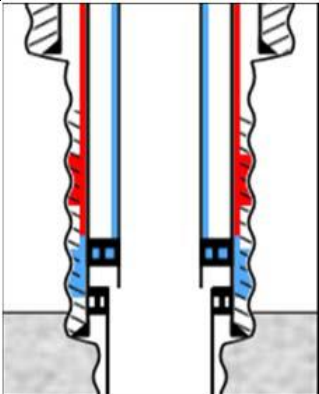
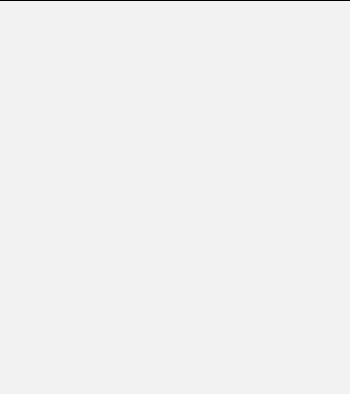


Figure 4.9: Platform production/injection/observation well

IMPORTANT: This solution alters the well barriers described in Alternative 1 as illustrated below:

Table 4.9: Well barriers

Production casing set into the reservoir	Comments	Production casing set above the reservoir
	<p><-Secondary WBE: Intermediate casing cement and formation. The production liner and liner cement are not a WBE</p> <p>Primary WBE: Production casing cement and formation - ></p> <p>Annulus: Casing / liner cement (blue) prevents flow / pressure from reservoir and into secondary (red) WB</p>	
	<p>This can be an alternative solution If the formation strength at the intermediate casing shoe is less than wellbore pressure when exposed reservoir fluids/pressure through leaks in the primary WB.</p>	

4.4.2.1 Primary well barrier – Alternative 2, production casing set into the reservoir

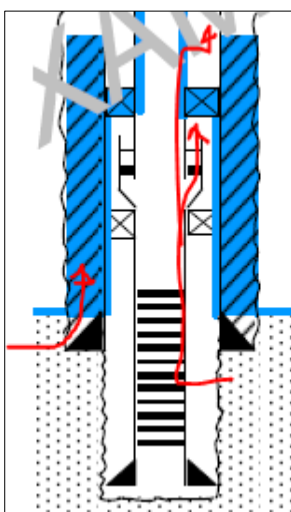
The primary WBEs are:

Table 4.10: Primary well barriers – Alternative 2

WBE	Issues / comments	NC-risk	WB Figure
<i>In-situ Formation</i>	See discussion in Alternative 1, 4.3.1.1.1	High	
<i>Production casing cement</i>	See discussion to follow	High	
<i>Production casing</i>	See discussion in Alternative 1, 4.3.1.1.3	Medium	
<i>Production packer</i>	This is normally set by hydraulic pressure and should not be affected by shallow setting depth. However, excessive casing wear on the low side of the production casing may cause ovality and could affect the sealing performance of the packer rubber element.	Medium	
<i>Production tubing</i>	The stresses in the tubing caused by high dogleg 8-11 deg/30 m dogleg is assumed to be low. Temperature induced stresses from injection of seawater at ambient temperature should be less than in normal wells, given very low change in temperature.	Low	
<i>Downhole safety valve</i>	Can be positioned minimum 50 blow seabed in the vertical part (coincide with KOP)	Low	

Casing cement acceptance criteria

The purpose of the casing cement is to:



- prevent flow in annuli (open hole / casing) between top of the reservoir and into the secondary well barrier, and
- prevent undesired flow into zones that will not give the best recovery / pressure maintenance.
- if zonal isolation is not required for EOR purposes, then an open hole completion without use of cement can be an option. (Not further discussed – see Production Well)

Figure 4.10: Casing cement

With reference to analysis of the reservoir liner cement in 4.4.1.1, the table below shows additional criteria that applies or can be difficult to achieve:

Table 4.11: Primary well barrier elements – Casing cement

WBE	NORSOK D-010 Requirements and guidelines	Type	Evaluation / Comments
EAC 51 Casing Cement	<i>This element consists of cement in solid state located in the annulus between concentric casing strings, or the casing/liner and the formation.</i>		
1.	Critical casing cement shall be logged and is defined by the following scenarios:		
2.	the production casing/production liner when set into/through a source of inflow with hydrocarbons;	R	Applies. Pipe conveyed logging is required.
3.	Actual cement length for a qualified WBE shall be:		
4.	50 m MD verified by displacement calculations or 30 m MD when verified by bonding logs. The formation integrity shall exceed the maximum expected pressure at the base of the interval.	R	Cement bond log is required. If no zones with good cement can be found, a LOT/XLOT can be an alternative verification method.

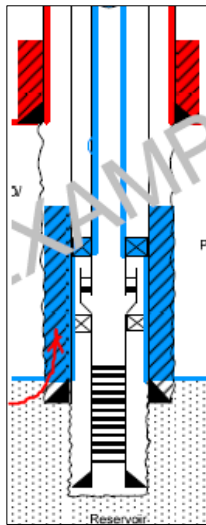
4.4.2.2 Secondary well barrier – Alternative 2, production casing set into reservoir

The secondary WBEs are:

Table 4.12: Secondary well barriers – Alternative 2

WBE	Issues / comments	NC-risk	WB Figure
<i>In-situ formation</i>	The formation strength, see below	High	
<i>Casing cement</i>	As per normal well	Low	
<i>Intermediate / surface casing cement (20" x 13 3/8")</i>	As per normal well	Low	
<i>Production casing hanger</i>	N/A in this case – no hanger	Low	
<i>Wellhead</i>	As per normal well	Low	
<i>Tubing hanger</i>	As per normal well	Low	
<i>Subsea XMT</i>	As per normal well	Low	

In-situ formation at the intermediate casing shoe - discussion



In the event of failure of the primary well barrier, the secondary well barrier shall be able to contain the escaping reservoir fluids and injection media (water or gas). The weakest WBE is the in-situ formation around the 13 3/8" intermediate casing shoe. This is shale with a fracture pressure of +/-97 bar@659 m.

A breakdown of the 9 5/8" casing cement or corroded holes in the 9 5/8" casing underneath the production packer could lead to pressure build-up in the B-annulus.

If the event occurs without being registered, continuous injection may lead to fracturing of the formation with propagation of fractures to seabed, with the risk of creating a permanent leak path to seabed.

Figure 4.11: In-situ formation

To reduce the probability of fracturing of the formation at the 13 3/8" shoe, one will to regulate the downhole injection. The consequence is that these injection rates/volumes may not give profitable production.

The table below shows that a given (arbitrarily) downhole injection pressure of 95 bar (23 bar above virgin reservoir pressure), the 9 5/8" by 13 3/8" annulus pressure is 90 bar at the 13 3/8" which is 7 bar less than the fracture pressure.

Table 4.13: Loads on formation

Loads on formation @ 13 3/8" csg shoe set at 659 mTVDSS					
	Fluid type	Depth mTVDSS	Pressure		Pfrac - Pw Bar
			SG	Bar	
Fracture pressure @ 13 3/8"		659	1,50	97	
Reservoir pressure- virgin	Oil	710	1,03	72	
Annulus pressure - static	Gas	659	0,00	72	25
	Oil	659	0,70	68	29
Reservoir inj. pressure	Water	710		95	
Annulus pressure - injection	Water	659	1,00	90	7

Another option is to have continuous pressure recording of the B-annulus pressure and downhole injection pressure to stop/reduce injection when pressure exceeds allowable set points.

4.5 Well barriers in the model production well

The model well for production well is almost identical to the injection well, with exception of the reservoir section which is completed with sand screens instead of a cemented liner.

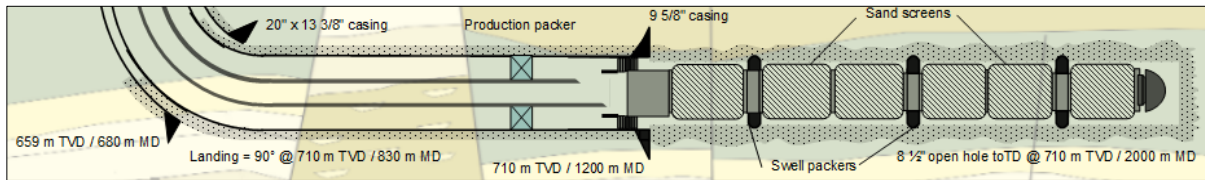


Figure 4.12: Production well

4.5.1 Assessment of loads on WBE

The following tables show overviews of NC risks for a production well compared with an injection well.

Table 4.14: Primary WBE load comparison

WBE in primary well barrier	NC Risk - Injection well	Comments ->	NC risk Prod well
<i>In-situ Formation @ above top reservoir</i>	High	Flowing well pressure is less. Shut-in well pressure is equal or less than original reservoir pressure (unless injection has increased the pressure)	Low
<i>Production casing cement</i>	High	As above. However, gas has substantially less viscosity / less density and can migrate through micro-annuli. This can be mitigated by use of gas-tight cement	Medium
<i>Production casing</i>	Medium	Same. With end of tubing inserted into the receptacle on top of the sand screen hanger, marginal corrosion is expected	Medium
<i>Production packer</i>	Medium	Same.	Medium
<i>Production tubing</i>	Low	Same. Can be subject to corrosion from water component, and erosion in event that sand screens are damaged. Monitoring of sand content in well flow is assumed.	Low
<i>Downhole safety valve</i>	Low	Shut-in pressures are expected to be higher due to gas / oil in well.	Low

Table 4.15: Secondary WBE load comparison

WBE in secondary well barrier	NC risk – Injection well	Comments ->	NC risk – production well
<i>In-situ Formation @13 3/8" shoe</i>	High	Migration of gas from the reservoir through failed cement around the 9 5/8" casing can 72 bar pressure, gas filled B-annulus (weightless gas), which is 9 bar less the fracture pressure.	Low
<i>Intermediate casing cement</i>	Low	As above.	Low
<i>Intermediate casing</i>	Low	As above. Gas tight connections are assumed. See discussion below.	Low
<i>Casing hanger</i>	Low	As above.	Low
<i>Wellhead</i>	Low	As above.	Low
<i>Tubing hanger</i>	Low	As above.	Low
<i>XMT</i>	Low	As above.	

Consequences of having cement in the 9 5/8" x 13 3/8" casing annuli – discussion

If the along hole distance between the 9 5/8" and 13 3/8" shoes is short (200-300 mMD), it is conceivable that the TOC will be above the 13 3/8" shoe and could create an enclosed annuli filled with fluid. In deeper and warmer wells, this is a concern as thermal expansion of trapped fluid can increase the B-annulus pressure significantly and cause burst or collapse of exposed casing strings. In shallow reservoirs this is not a concern, as temperature increase is only about 13 K (4°C on seabed, 17°C in the reservoir).

5. Geomechanical Assessment

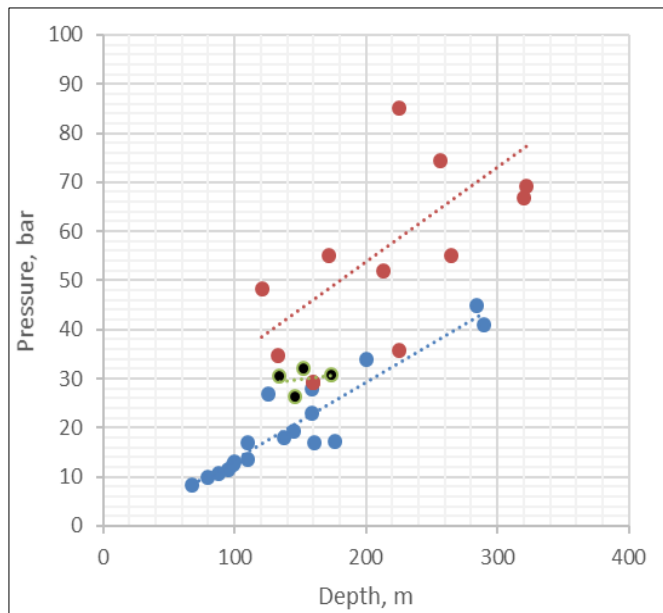
The formation fracture pressure is one of the most important factors for the integrity of the well. Hydraulic fracturing induced by sustained and excessive wellbore pressure could ultimately lead to the escape of reservoir fluids to the seabed. It depends on the in-situ stress state, the lithology and the pore pressure.

In this chapter, we will compare fracture pressures between other oil regions in Norway and the Barents Sea by normalising the leak-off test data obtained. We observe that fracture pressures recorded in the Barents region are higher than in the North Sea.

5.1 Challenges

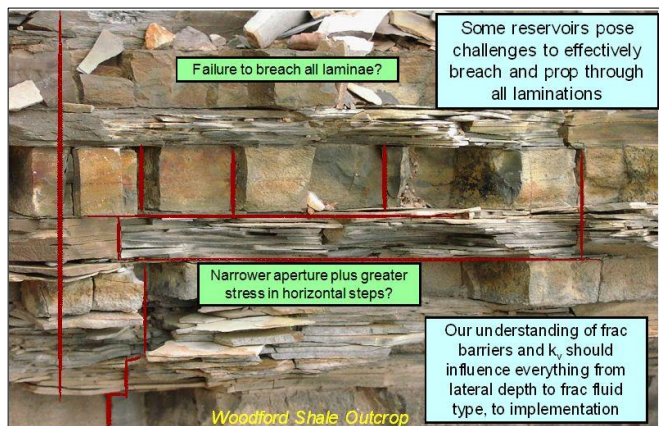
Challenge: What is the formation fracture pressure?

By analyzing leak-off data from the Barents Sea wells, lateral stresses / fracture pressures are higher than wells in the North Sea, possibly indicating “Reverse Fault Stress” syndrome. This means that the horizontal stresses are higher than the vertical stress. The consequence of this is that a fracture will preferentially propagate in a horizontal plane rather than upwards. This should reduce the risk of leaks to surface. It is recommended to perform a comprehensive study based on more wells and elimination of possible error in data.



Challenge: What is flow resistance in natural fractures?

Due to tectonic movements there are a considerable number of natural fractures in these older rocks formed by geological processes such as uplift and faulting. The fractures can vary considerably, often a crushed zone exists in the immediate fracture area. The hydraulic conductivity can also vary. The flow resistance depends on



Five Things You Didn't Want to Know about Hydraulic Fractures

By Vincent M.C.
 DOI: 10.5772/56066

these conditions. There exists no method to quantify the flow resistance due to these unknowns.

5.2 Shallow Fracture Pressure – Regional Comparison

High fracture pressures have been recorded in the Barents region.

Aadnøy (2010) developed a method which normalises the data to the sea floor. Initially it was developed for deep-water application, but the method has shown good results also for shallower water depths.

The fracture pressure is P_{wf} and the well depth D and the water depth is h_w . The airgap below the drillfloor is h_f . The fracture pressure is defined as the LOT. This can be either a leak-off test or a pressure integrity test (leak-to test).

The fracture pressure is:

$$P_{wf} = 0.098LOTxD = 0.098x1.03xh_w + P$$

Subtracting the water pressure, the fracture pressure from seabed is:

$$P = 0.098(LOTxD - 1.03h_w) \quad (2.1)$$

The seabed penetration is:

$$D_p = D - h_w - h_f \quad (2.2)$$

Below are shallow fracture pressures from some North Sea wells normalized to seabed as per formulas above.

Table 5.1: Shallow fracture data from the North Sea (Aadnøy, 2010)

Depth from seabed (m)	Net pressure (bar)	Source	Nomenclature
68	8.4	Soil	- Soil - fracture data measured from soil investigation studies, i.e. geotechnical studies.
80	10	Soil	
88	10.6	Sleipner	- Saga - shallow fracture data measured below the 30 in. casing. Treasure Saga used a Hydril annular preventer on the 30 in. to run shallow leak-off data.
95	11.5	Soil	
99	12.5	Saga	
100	13	Soil	
110	13.5	Soil	
110	17	Saga	- Sleipner - data from a previous study on shallow casings
126	27	Saga	
138	18	Soil	- Exploration - from an exploration well.
145	19.3	Saga	
159	23	Saga	
159	28	Saga	
200	34	Saga	
284	45	Exploration	
290	41	Sleipner	

In 2005, Norsk Hydro drilled several wells in the Peon shallow gas discovery in the northern part of the North Sea. Data from Peon is normalized to seabed in Table 5.2.

Table 5.2: Fracture data from Peon normalized to seabed (PSA 2017)

Depth from seabed (m)	Net pressure (bar)	Source
146	26,3	PEON
174	30,7	PEON
134	30,4	PEON
152	32,2	PEON

In the Barents Sea, several wells have penetrated shallow water or HC bearing reservoirs from approx. 130 - 490 m below seabed.

Table 5.3: Fracture data from Barents Sea normalized to seabed (PSA 2017)

Depth from seabed (m)	Net pressure (bar)	Well name
213	52,0	Wisting
453	121,6	Wisting
133	34,6	Wisting
257	74,4	Wisting
235	105,7	Bjaaland
225	35,8	Isfjell
320	66,7	Isfjell
225	85,2	Caurus Carn
265	55,0	Norvarg
172	55,1	Veveris
121	483	Veveris
489	74,8	Pingvin
160	29,2	Apollo
322	69,1	Apollo

The data from Table 5.1, Table 5.2 and Table 5.3 is shown in Figure 5.1.

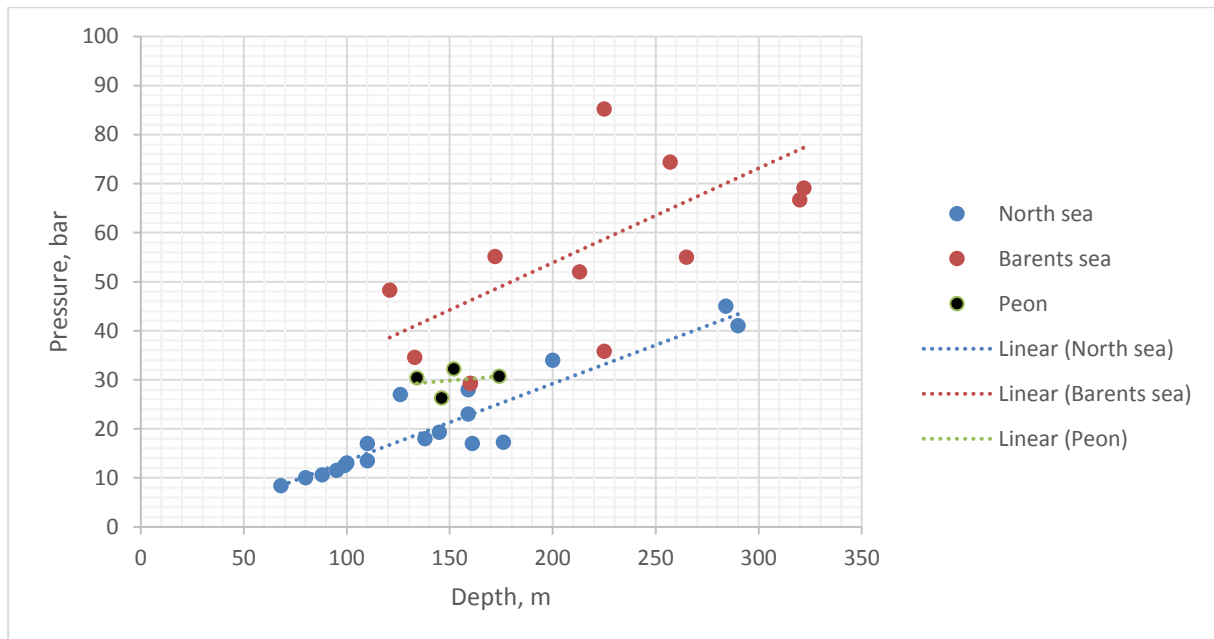


Figure 5.1: Fracture data normalized to seabed

It is observed that the fracture pressure for the Barents Sea wells is higher than the North Sea wells. There is, however, a considerable spread which may suggest that some of the data may be formation pressure integrity tests where the wellbore is not pressurized up to fracture. These will show up as low numbers. The main reason for high formation stresses is linked to the geologic history.

5.3 Fracture model for the Barents Sea

The original final well reports were not available, so the data has not been quality checked. Errors can be caused by using measurements from formation pressure integrity tests and reduction in formation strength caused by circulation losses during drilling. The results are based on preliminary data and can be revised when better data becomes available. The data from PSA (2017) is summarized as follows:

Table 5.4: Fracture data from the Barents Sea (PSA 2017)

Source	Water depth (m)	Well depth (mTVD-RKB)	LOT (FIT)(sg)	Depth from seabed (mTVD)
Wisting	398	636	1,48	213
Wisting	413	891	1,87	453
Wisting	417,5	576	1,36	133
Wisting	417,5	700	1,70	257
Wisting	417,5	1200	1,99	257

Source	Water depth (m)	Well depth (mTVD-RKB)	LOT (FIT)(sg)	Depth from seabed (mTVD)
Bjaaland	394	654	2,27	235
Isfjell	429	679	1,19	225
Isfjell	429	774	1,45	320
Caurus Carn	356	606	2,04	225
Norvarg	377	667	1,50	265
Veveris	347	554	1,69	172
Veveris	347	855	1,86	121
Pingvin	422	936	1,28	489
Apollo	444	629	1,20	160
Apollo	444	791	1,47	322

The wells listed in Table 5.4 are located in water depths varying from 347 m to 444 m. The model production and injection wells described in Chapter 3 have seabed at 450 m. In this case all wells in Table 4 will be depth normalized to 450 m. The resulting fracture curve can be applied directly to assess well integrity.

In the absence of detailed records, the following assumptions apply:

- normal pore pressure at shallow depth (1.03 SG)
- constant bulk density in the shallow layers, the same for all wells
- 25 m between the drillfloor and sea level in all wells
- same rock penetration below seabed for both model wells

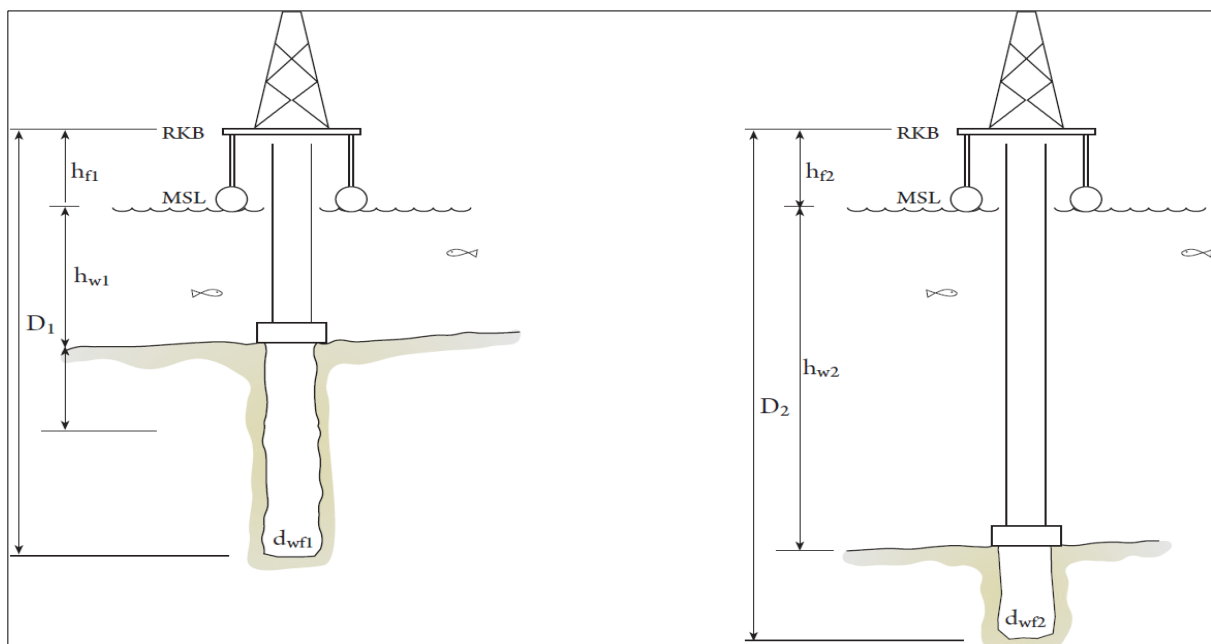


Figure 5.2: Depth references used when data is normalized to various water depths

Subscript 1 refers to reference, while subscript 2 refers to the prognosis. From Aadnøy (2010).

$$D_{wf2} = D_{wf1} + \Delta h_w + \Delta h_f$$

$$d_{wf2} = d_{wf1} \frac{D_{wf1}}{D_{wf2}} + \frac{d_{sw} \Delta h_w}{D_{wf2}} \quad (2.3)$$

The datum reference is the drill floor. The following definitions apply:

- h_f = air gap from drill floor to sea level (m)
- h_w = water depth (m)
- D = depth (m)
- D_{wf} = fracturing depth
- d = gradient with reference to water (s.g.)
- d_{sw} = relative density of sea water (s.g.)

COMMENT: The equations above are based on simplified assumptions. When more data such as overburden gradients and bulk densities becomes available, the full solution can be used.

Furthermore, the average horizontal stress is computed assuming isotropic conditions and normal pore pressure as follows;

$$\sigma_h = \frac{1}{2} (d_{wf} + d_{sw}) \quad (2.4)$$

Table 5.5: Fracture data from the Barents Sea is normalized to a water depth of 450 mRKB

Source	Normalized values			
	Water depth (mRKB)	Well depth (mRKB)	LOT (FIT) (sg)	Hor.stress (sg)
Wisting	450	688	1,45	1,24
Wisting	450	928	1,84	1,44
Wisting	450	608	1,34	1,19
Wisting	450	732	1,67	1,35
Wisting	450	1252	1,96	1,50
Bjaaland	450	710	2,17	1,60
Isfjell	450	700	1,19	1,11
Isfjell	450	795	1,44	1,24
Caurus Carn	450	700	1,91	1,47
Norvarg	450	740	1,45	1,24
Veveris	450	657	1,59	1,31

Source	Normalized values			
	Water depth (mRKB)	Well depth (mRKB)	LOT (FIT) (sg)	Hor.stress (sg)
Veveris	450	958	1,77	1,40
Pingvin	450	964	1,27	1,15
Apollo	450	735	1,20	1,12
Apollo	450	847	1,47	1,25

The results are shown in Figure 5.3. There is a considerable spread which can be explained by the fact that some of the low data points represent pressure integrity tests where the wellbore is not pressurized to initiate fracturing (LOT).

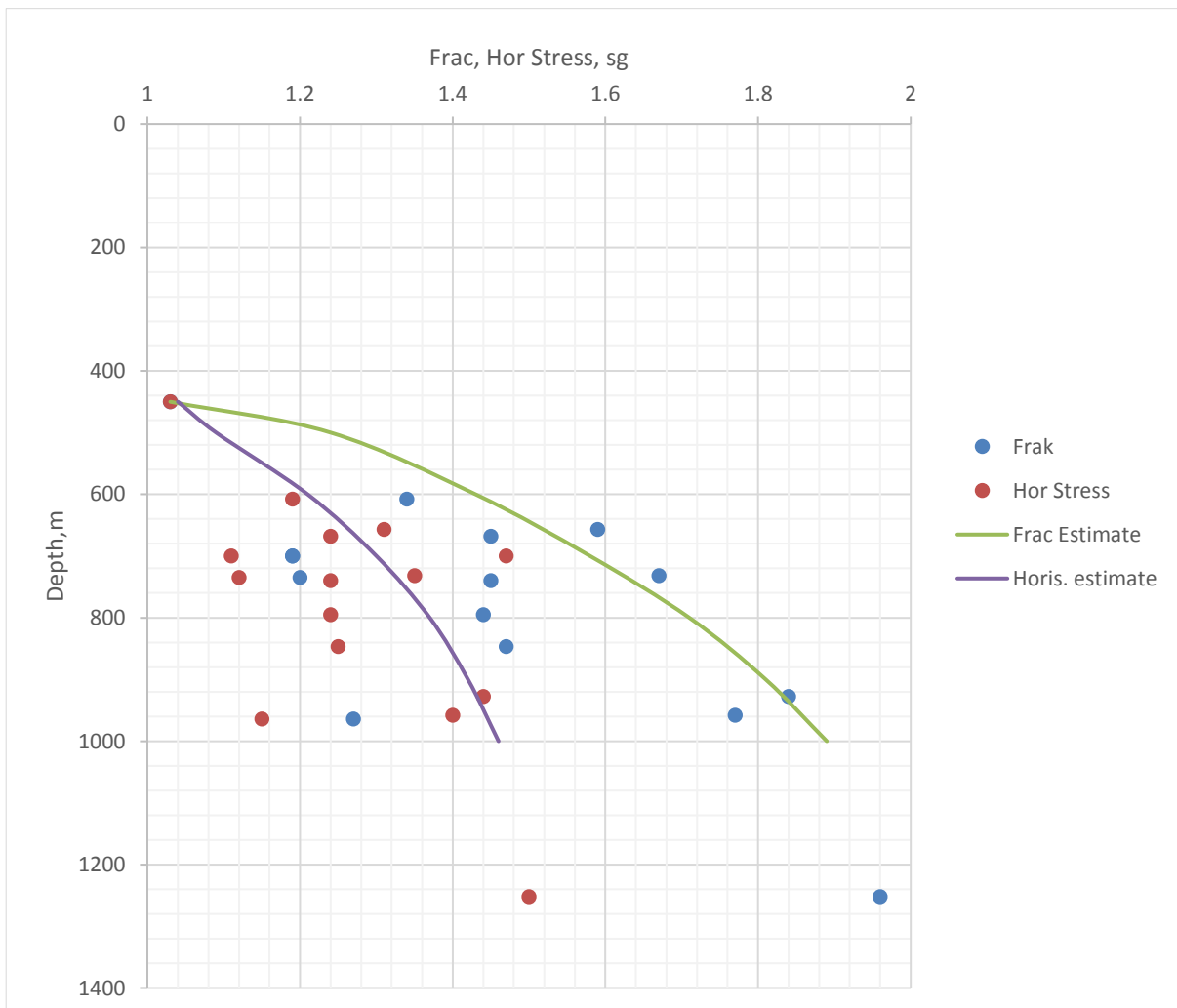


Figure 5.3: Fracture data from the Barents Sea normalized to a seabed depth of 450 mRKB.

For the prognosis shown $K = 2,65$.

From Figure 5.1 we observe that the pressure plot below seabed can be linear. The fracture model is defined as the seawater pressure plus the linear fracture resistance below seabed.

$$P = 0.098d_{wf}D = 0.098 \times 1.03 \times D_w + 0.098K(D - h_w - h_f)$$

$$\text{or: } d_{wf} = 1.03 \frac{D_w}{D} + K \frac{(D - h_w - h_f)}{D} \quad (2.5)$$

$$\text{and: } \sigma_a = \frac{1}{2} \left\{ 1.03 \left(\frac{D + h_w}{D} \right) + K \frac{(D - h_w - h_f)}{D} \right\}$$

The K is chosen to obtain the desired curve.

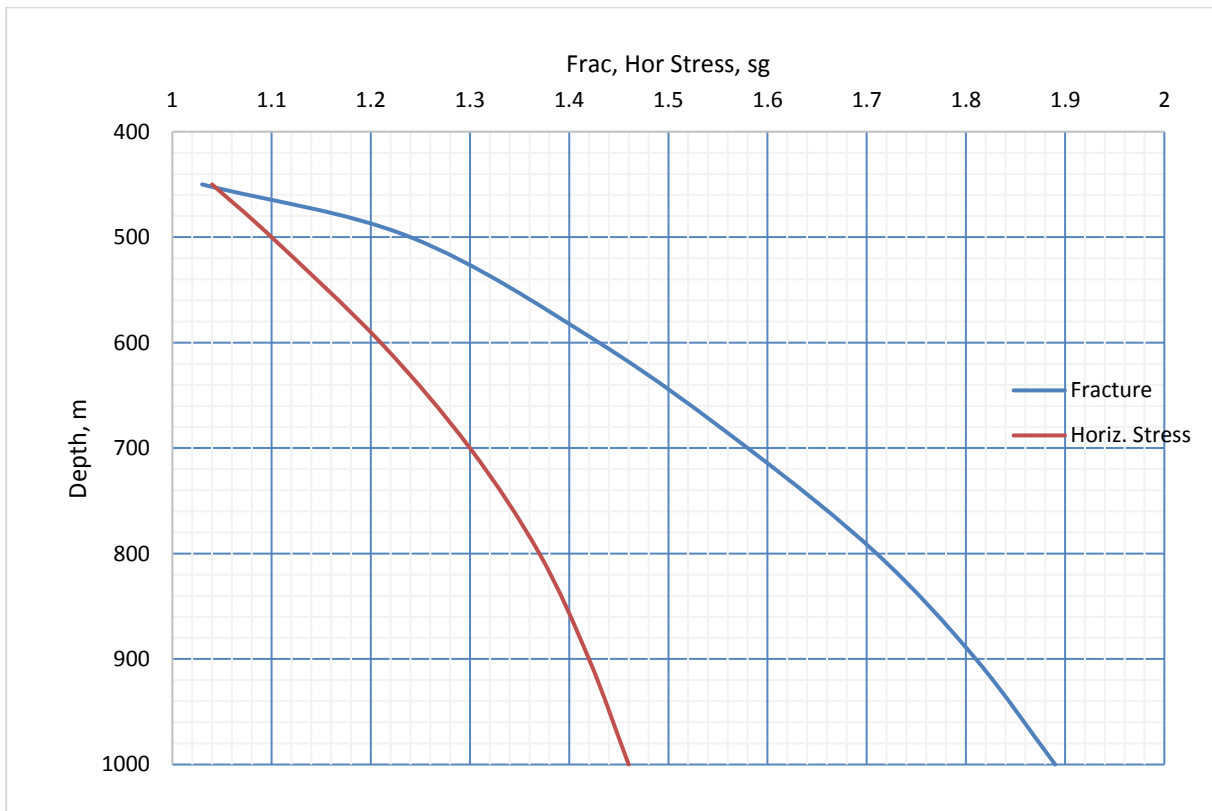


Figure 5.4: Fracture curve and horizontal stress curves for the model production and injection wells at water depth of 450 mRKB

Figure 5.4 will be used as a prognosis for fracturing for the two model wells. The horizontal stress curve will also be used for evaluation of the potential for upward leak to seabed.

Finally, the slope of the curve above was $K=2,65$. The overburden stress is an integration of the bulk rock density, which is in the order of 2.0 – 2.4 sg. The horizontal stresses appear to be much higher than the overburden stress. We conclude as follows:

- The in-situ stress state appears to be reverse fault stress state. The horizontal stresses exceed the vertical overburden stress.

5.4 Upward fracture growth

Appendix B discusses upward fracture growth in some detail. Here it is shown that fractures can be sealed by using a drilling mud. Leaks of reservoir fluids do not have filter cake and can more easily propagate to surface. Actually the presence of a filter cake in the mud reduces the risk of leaks to surface during the drilling operation.

One critical issue is the question if the fracture may grow to surface and create a leak. Keck (2002) defines barriers to upward fracture growth as follows:

- Stress barrier: If a higher stress state exists in a rock above the injection zone, upward growth may be arrested.
- Elasticity barrier: If there is higher stiffness in the rock above, fracture propagation may be limited or stopped. This could be a caprock.
- Permeability barrier: If the fracture propagates into a permeable rock, it may be arrested and not propagate further.
- Rock consolidation, in unconsolidated (shallow) sand reservoirs.

Valko and Economides (1995) provide a detailed review of the basic calculations of fracture growth. It is deterministic and supports the barriers defined above. However, in a correspondence Valko (2008) states:

“Regarding height containment: microseismics and other diagnostic tools have convinced us that height is controlled by everything except for stress contrast, modulus contrast, permeability contrast and whatever previously we assumed. I think at this point the best is that height is controlled by lamination and will be 20 – 80 % of total length.....”

Although the fundamental mechanics is well developed, Valko questions the exactness of the models from field observations. One reason can be lack of or poor input data to the models. He also suggests that we should look for lamination contrast. A caprock above a reservoir could give this contrast.

5.5 Does the Barents Sea have reverse fault stresses?

This analysis indicates the possibility of reverse fault stress state in the Barents Sea. This means that the horizontal stresses are higher than the vertical stress. The consequence of this is that a fracture will preferentially propagate in a horizontal plane rather than upwards. This should reduce the risk of leaks to surface.

5.5.1 The North Sea is a relaxed depositional basin

In the North Sea rocks from Jurassic age and older have been exposed to tectonic activity such as earthquakes during geologic times. The Bottom Cretaceous Unconformity defines a change. Cretaceous and younger sediments are in general deposited in a relaxed depositional basin environment. This means that there are no or little tectonic effects. This is called a normal fault stress state, where the horizontal stresses are smaller than the vertical stress. In this case a fracture will have an upward preference, it will try to propagate upwards. This is the situation for the leaks at Tordis,

Ringhorne and the other reported leaks in the southern parts of Norway. By defining σ_h as horizontal stress and σ_v as vertical stress we can deduce:

Table 5.6: Stress states versus fracture directions

Stress state		Area	Fracture propagation
Normal fault	$\sigma_h / \sigma_v < 1$	North Sea	Vertically
Reverse fault	$\sigma_h / \sigma_v > 1$	Barents Sea?	Horizontally

5.5.2 Characteristics of reverse fault stress states

There are many geological phenomena that may lead to horizontal stress exceeding the vertical stress. Tectonism is a broad definition often caused by earthquakes. Our understanding is that this is not the case in the Barents sea. The geologic history shows sediments that have been buried and later have been eroded away up to 2 km thickness. This is what we call denudation. We then assume that the horizontal stresses that existed during burial still exist after erosion of the overburden .

The denudation effect is well documented in hard rock environments. These are typically igneous rocks. Brown and Hoek (1978) summarize reverse fault stress states worldwide as measured in mines at shallower depths. As a follow-up of this report a project should be established to collect more data from the Barents Sea to further investigate the lateral stresses.

We conclude that it is highly likely that a reverse fault stress state exists, with a consequence that this may reduce upward fracture growth.

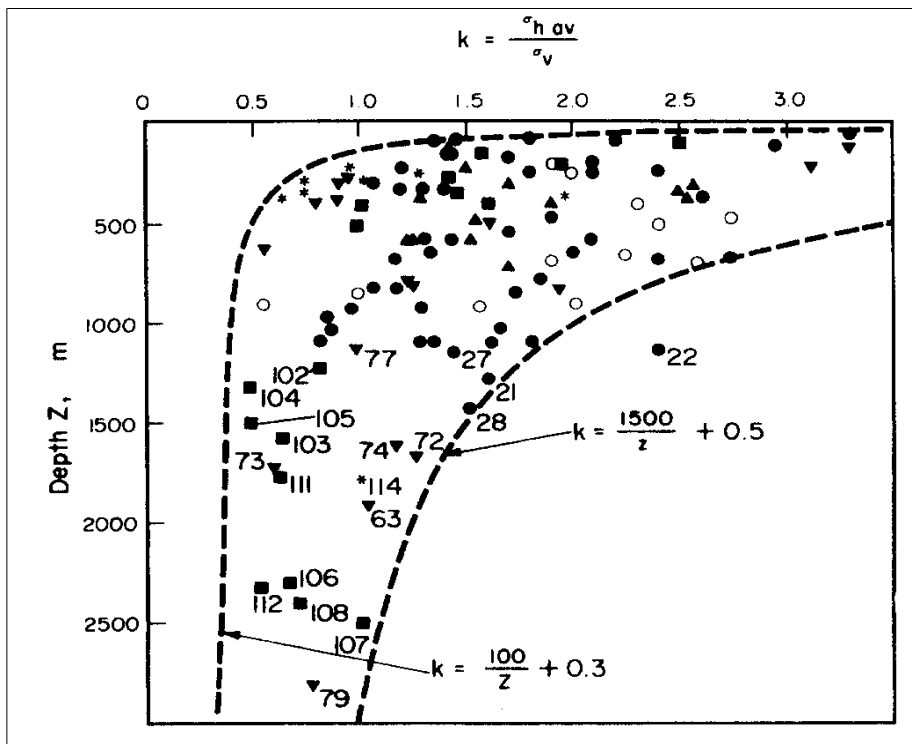


Figure 5.5: Stress ratio

Ratios lower than 1.0 indicate normal fault stress state, and higher than 1.0 indicate reverse fault stress state (Brown and Hoek 1978).

Furthermore, they report measurements from Scandinavia as follows:

#	Location	Type of rock	m	Mpa	σ_h / σ_v
Scandinavia					
80	Bleikvassli Mine, N. Norway	Gneiss and mica schist	200	6.0	1.92
81	Bleikvassli Mine, N. Norway	Gneiss and mica schist	250	7.0	2.00
82	Bidjovagge Mine, N. Norway	Pre-Cambrian rocks	70	2.8	4.64
83	Bjornevann, N. Norway	Gneiss	100	(2.7)	5.56
84	Sulitjelma, N. Norway	Phyllite	850	10.0	0.99
85	Sulitjelma, N. Norway	Phyllite	900	11.0	0.55
86	Ställberg, Sweden	Pre-Cambrian rocks	915	(24.7)	1.56
87	Vingesbacke, Sweden	Granite and amphibolite	400	(10.8)	4.99
88	Laisvall, Sweden	Granite	220	(5.9)	3.72
89	Malmberget, Sweden	Granite	500	(13.4)	2.41
90	Grängesberg, Sweden	Pre-Cambrian rocks	400	(10.8)	2.31
91	Kiruna, Sweden	Pre-Cambrian rocks	680	(18.4)	1.90
92	Stalldalen, Sweden	Pre-Cambrian rocks	690	(18.6)	2.58
93	Stalldalen, Sweden	Pre-Cambrian rocks	900	(24.3)	2.02
94	Hofors, Sweden	Pre-Cambrian rocks	470	(12.7)	2.74
95	Hofors, Sweden	Pre-Cambrian rocks	650	(17.6)	2.25

Figure 5.6: Reported stress ration from Scandinavia

The last column in Figure 5.6 is the stress ratio. It typically defines a reverse fault stress ($\sigma_h / \sigma_v > 1$) state for all locations except Sulitjelma (Brown and Hoek 1978).

The data above documents that denudation has played an important role in forming high horizontal stresses in hard rock environments. The question is if this is also valid for the sedimentary rocks of the Barents Sea area?

Amadei, B. and Stephansson, O. (1997) report high horizontal stresses in sedimentary basins in Ontario. Nøttvedt (2000) argues that in ridge push of the Barents Sea, lateral stresses in the order of twice the overburden stress may arise.

There exist many other geological studies of the Barents Sea area that suggest high horizontal (lateral) stress. These are mostly qualitative and do not give data useful for drilling design. For well construction purposes higher quantitative data is required. This is usually obtained from leak-off-tests.

We conclude that it is likely that reverse fault stress state exists in shallow layers of the Barents Sea area.

5.6 Flow capacity in natural faults

Natural faults often exist in older rocks due to tectonic movements. There exist no methods to define whether these faults are sealed or if they leak. However, if a reverse fault stress state exists, a high compressive horizontal stress will likely try to close these fractures.

One indicator is circulation losses if the wellbore approaches a larger natural fracture. Circulation loss might be the strongest indicator for a leaking fault. The loss rate may define the flow capacity of the fracture system.

Changes in reservoir pressure during production or injection may lead to activation of some fractures. However, a considerable fluid volume is most likely needed for this to occur.

5.7 Subsidence and reservoir compaction

With a small overburden of a few hundred meters also subsidence can occur for large reservoir depletion. In fields like Ekofisk the overburden arrests about half of the reservoir subsidence due to an overburden of several thousand meters. With only a few hundred meters it is likely that most of the reservoir subsidence is observed also on the sea floor. However this depends on the extent of the reservoir, the volume of produced fluids and also the properties of the rock.

There is a possible positive effect of this. In Ekofisk subsidence has led to an efficient reservoir drive mechanism resulting in much higher recovery. Reverse fault stresses might have similar positive effects on the recovery factor.

6. Methods for detection of fluid migration from reservoir to seabed

This chapter describes geophysical methods that potentially can be used to detect migration of fluids from the shallow reservoir and upwards to the seabed. It is envisioned that, in addition to general vertical migration, conduits are created by fracturing of overburden, re-activation of faults or failure in well barrier elements.

6.1 Challenges

Challenge: Can migration and accumulations of escaping reservoir fluids be detected before they reach the seabed?

Monitoring of producing reservoirs is done for many offshore fields, but direct monitoring of the overburden is not common. In principle this can be done, but careful feasibility studies should be performed to understand the local conditions for the actual field. In traditional monitoring acquisition repeatability is probably the largest source of error.

Challenge: Can leakage be detected at an early stage?

If leakage is to be detected at an early stage the surveys should be repeated often. Continuous monitoring with permanent equipment is most likely necessary to achieve this.

Challenge: Can leakage be quantified?

It is likely that leakage from the reservoir can be detected. However, it can be difficult to quantify the amount of gas or fluid leaking through the subsurface. To solve this problem several geophysical measurements can be used to measure different properties. When these results are combined in an integrated inversion and interpretation this problem could potentially be solved.

6.2 Introduction

Geophysical methods such as 4D seismic surveying are currently used for monitoring of hydrocarbon reservoirs.

If geophysical methods should be used for detailed monitoring of the overburden, the current techniques and work flows must be improved:

- Survey frequency should be increased and accuracy should be improved.
- To detect and understand subtle changes at an early stage a quantitative approach should be used.

The table below shows an overview of possible methods that could be used for frequent monitoring of the overburden.

Nomenclature

Geophysics: the branch of geology that deals with the physics of the earth and its atmosphere, including oceanography, seismology, volcanology, and geomagnetism.

Seismic: pertaining to, of the nature of, or caused by an earthquake or vibration of the earth, whether due to natural or artificial causes.

4D seismic; Mapping of seismic response in a cube (x, y, z) versus time (t)

Seismic inversion; is the process of transforming seismic reflection data into a quantitative rock-property description of a reservoir.

Figure 6.1: Nomenclature

Table 6.1: Possible methods used for monitoring of overburden

Technologies -> Features	Deployed on seabed			Deployed in well
	4D seismic	Passive seismic	Time lapse gravity	Distributed acoustic sensing
Detect initiation of fractures?	Yes	Yes	No	Yes
Detect new fractures?	Yes	Yes	No	
Detect flow of oil/gas/water in conduits?	Yes	Yes	No	Yes
Detect accumulation of escaping fluids in overburden?	Yes	Yes	Yes	
Indicate type of fluid?	Yes	Yes		
Frequency of sampling	Weekly to monthly			
Excepted time delay from data sampled to interpreted result=?	Today: Months Future: Days			

6.3 3D and 4D seismic data acquisition

3D seismic is the standard method for reservoir monitoring and 4D projects are performed in most geological and environmental settings. By repeating 3D seismic acquisition over a reservoir, it is possible to detect production-related changes and update the reservoir model. However, 4D surveys may also be useful for monitoring the strata above the reservoir; the overburden. One of the requirements for 4D marine seismic survey is to repeat the acquisition configuration as closely as possible. This is a significant challenge when collecting data with traditional acquisition equipment in the marine environment. 3D acquisition and imaging are normally repeated several times over the lifetime of a producing field.

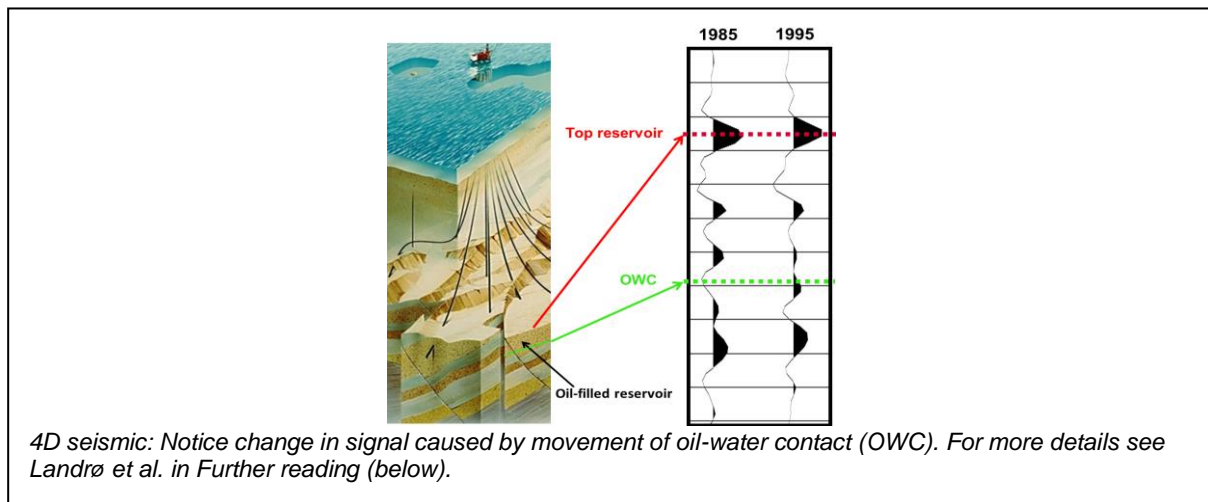


Figure 6.2: 4D Seismic

6.4 Status and future development of geophysical monitoring

Continuous monitoring is necessary to be able to detect leakage at an early stage. This can potentially give early warning forecasts from small changes in the subsurface. Continuous geophysical monitoring using controlled active sources will significantly improve the accuracy and will enabling detection of subtle but important subsurface property changes.

Compared to passive geophysical monitoring methods such as seismology, gravity and magnetotellurics (electromagnetic geophysical exploration technique), controlled-source geophysical monitoring will give significant improvement in quality.

However, active monitoring methods have a sparse sampling in calendar time, typically once a year. Reducing this time interval drastically by changing to more continuous geophysical monitoring will improve monitoring capabilities.

Traditionally, seismic monitoring exploits and measures changes in P-wave velocity and acoustic impedance. Adding information obtained from monitoring S-wave variations will increase monitoring capacity and accuracy.

The most advanced class of reservoir monitoring available today is Permanent Reservoir Monitoring (PRM), where a range of acoustic, temperature and pressure sensors are deployed on seabed and subsurface (downhole). In Norway, four (4) oil fields have been instrumented with acoustic sensors that are permanently buried at the seabed.

Continuous geophysical monitoring is also developing into an important tool for early warning of geohazards, such as earthquakes, volcanic eruptions and landslides. In addition, this method can be applied to CO₂-storage, hydrocarbon production, geothermal energy, energy storage systems and ground water resources. Most likely it can also be used for monitoring of active leakage from producing fields.

6.5 Continuous active marine seismic monitoring

Currently it is not common to use permanent acoustic sources in addition to permanent receivers. With permanent installed sources, it should be possible to perform continuous monitoring on a weekly or daily basis.

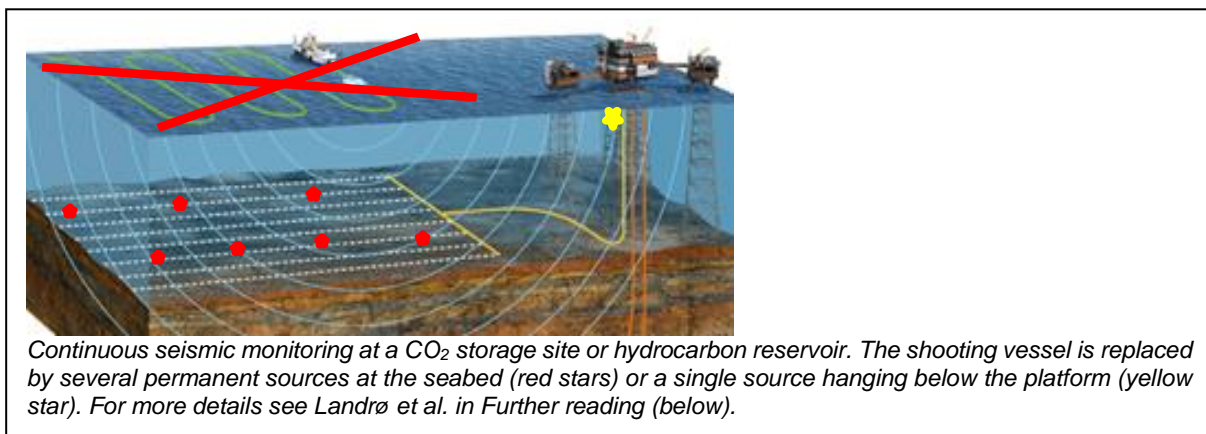


Figure 6.3: Seismic monitoring at a CO₂ storage site

Three types of permanent sources can be used:

- (1) Time lapse refraction “radar” with a single source hanging below the platform:
The signal will be dominated by shallow changes as for instance a thin gas layer that is emerging in a shallow sand layer.
- (2) Piezo-electric system of permanent sources on sea bed: This will give a detailed map of changes in the shallow subsurface, typically 100 meters below seabed. This is useful as an early warning system for leakage detection from a producing hydrocarbon field into the overburden and to the surface.
- (3) High-pressure air pipe lines at the sea bed: This solution might have the possibility to monitor changes at reservoir level, and is therefore the goal for continuous reservoir monitoring, enabling mapping detailed changes within reservoirs or producing hydrocarbon fields.

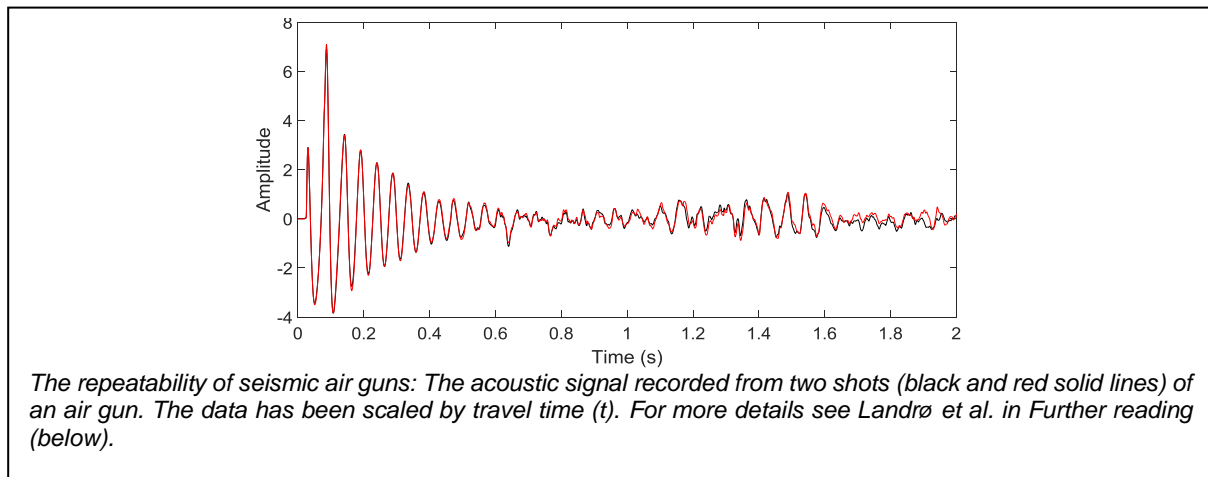


Figure 6.4: Repeatability of seismic air guns

Variations in the water layer (density, temperature, salinity) will influence the recorded seismic data. It will be a challenge to distinguish between water layer variations and subsurface variations relating to leakage or pressure changes.

6.6 Complex geophysical processing of time lapse data

Continuous recording of passive seismic data where the source is either a natural noise or manmade noise can be combined with full waveform inversion to extract information about the subsurface for long periods of time. The largest challenge here is the computational burden of the numerical model, which presently uses a 3D finite-difference approach to solve the elastodynamic equations.

6.7 Broadband seismic techniques for enhanced 4D seismic analysis

The advantage with broadband streamer acquisition is that the effect of the free surface, which creates notches in the frequency spectrum of the data (referred to as ghosts) is attenuated. While the receiver-side ghost problem is practically solved, handling the source ghost is still challenging. The use of variable source depth during acquisition has been proposed to achieve source-ghost variability.

If it is possible to increase the low frequency content in time lapse seismic (below 5 Hz), this could dramatically improve data quality of the 4D seismic. The main challenge in this respect is to design a marine source that can emit strong signals below 5 Hz.

6.8 Quantitative analysis and uncertainty assessment of time lapse data

In many monitoring projects, it is sufficient to detect that there has been a change. This is often referred to as qualitative time-lapse interpretation, and has turned out to be robust and very useful for hydrocarbon monitoring.

The next step is to estimate how much change or how to discriminate between various subsurface property changes. A classic example of this is to discriminate between pore pressure and fluid saturation changes.

Due to noise level and lack of precise relations between various parameters and properties, it is much more challenging to achieve quantitative time lapse geophysical results.

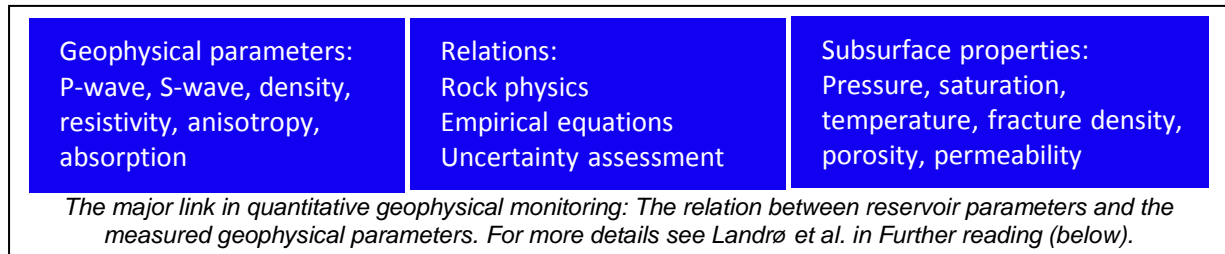


Figure 6.5: The major link in quantitative geophysical monitoring

Time lapse data is available both from repeated geophysical surveys and repeat monitoring in wells. The former has good areal coverage but poor accuracy and precision, while the latter has the opposite.

To combine the various data efficiently, the signal-to-noise characteristics of each data type must be quantified. The target properties - lithology classes, fracture density, pressure, temperature and fluid saturation – change in time and space, and the joint inversion of geophysical measurements and well data must take such spatial and temporal variations into account.

Both predictions and associated quantifications of uncertainties are required if statistically significant changes in the characteristics shall be identified. Spatio-temporal inversion methods can be used to assess this problem.

6.9 Combining various geophysical monitoring techniques

Presently, seismic is the most common technology used for subsurface monitoring. However, other geophysical techniques can offer very useful additional information. Time lapse gravity has emerged to become one of those. By combining the two, it is possible to constrain the inversion and thereby improve the results. Another interesting possibility is to combine time lapse seismic with time lapse electromagnetic surveying. Yet another major class of joint geophysics inversion is to combine passive (micro-earthquake) detection data with active seismic monitoring to develop improved imaging of changes in velocity and stress distribution.

6.10 Geomechanics and stress monitoring

Production of petroleum from reservoirs and injection of gas and water into reservoirs induces stress changes in the subsurface - not only within, but also above, around and beneath the area of pore pressure alteration. These stress changes are visible in 4D seismic. Examples of induced seismicity are found both in injection scenarios (like waste water storage or use of enhanced geothermal systems in North America) and during depletion (e.g. Groningen in the Netherlands). Seismological modelling requires knowledge of stresses, mapping of existing faults, and geomechanical modelling to

assess where faults could be re-activated and to what extent new faults may be generated.

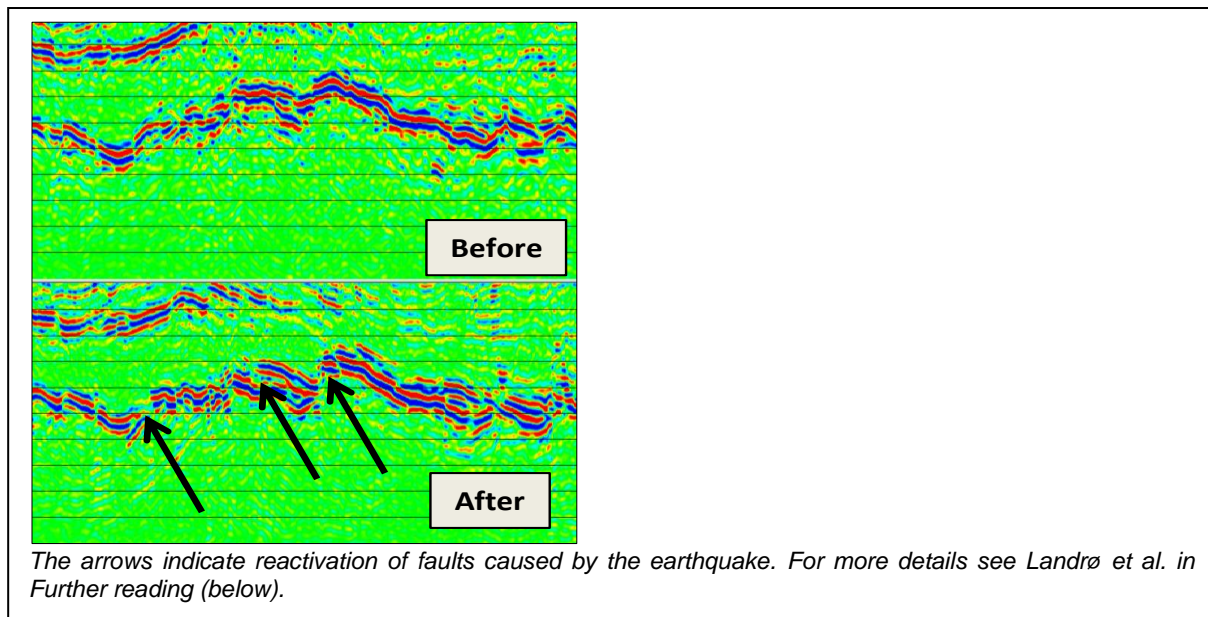


Figure 6.6: 4D seismic before and after the Tohoku earthquake

Laboratory experiments can be performed where P- and S-wave velocities and their associated stress sensitivities are measured at seismic and ultrasonic frequencies with rock samples brought to in-situ conditions. Combined with relevant rock physics models, this may enable real-time quantification of stress and pore pressure changes in the subsurface.

6.11 Passive seismic monitoring

Registration of micro seismic waves is used for monitoring and to control hydraulic fracturing of onshore wells for development of shale gas. When a crack develops, it generates a signal which is picked up by the geophones located on the surface in a defined pattern. Triangulation of received signals is used to determine the location and the direction of the crack. This method could also be used offshore.

6.12 Technologies deployed in wells

Distributed Acoustic Sensing (DAS) and Distributed Temperature Sensing (DTS) is based on sending light through a fiberoptic cable.

This rapidly evolving technology for permanent in-well and geophysical monitoring, can be used to detect useful in-well velocity data along the entire length of the well from wellhead to TD. The technology is rapidly improving and can give good images also compared to conventional borehole geophones in terms of signal to noise ratio and resolution. Permanently installed fiber-optic infrastructure can enable low-cost non-intrusive geophysical monitoring.

DAS instruments can detect P-waves and S-waves in addition to micro seismic events. Figure 6.7 illustrates a micro-seismic event recorded by DAS in a horizontal treatment well. From channel 200 located in the vertical section of the well we know the distance the event occurred away from the wellbore; that is, we have no azimuthal information. This gives a circle of possible origin locations. If the event is also recorded in the horizontal section of the well we will have another circle which will intersect the first circle at the only two possible origin locations. Depending on how deviated the trajectory is, we could narrow down to one location given the number of DAS channels /2/.

The system can also be used for leak detection in the wellbore due to changes in noise and/or temperature. This method is also used in production logging operations to detect flow pattern.

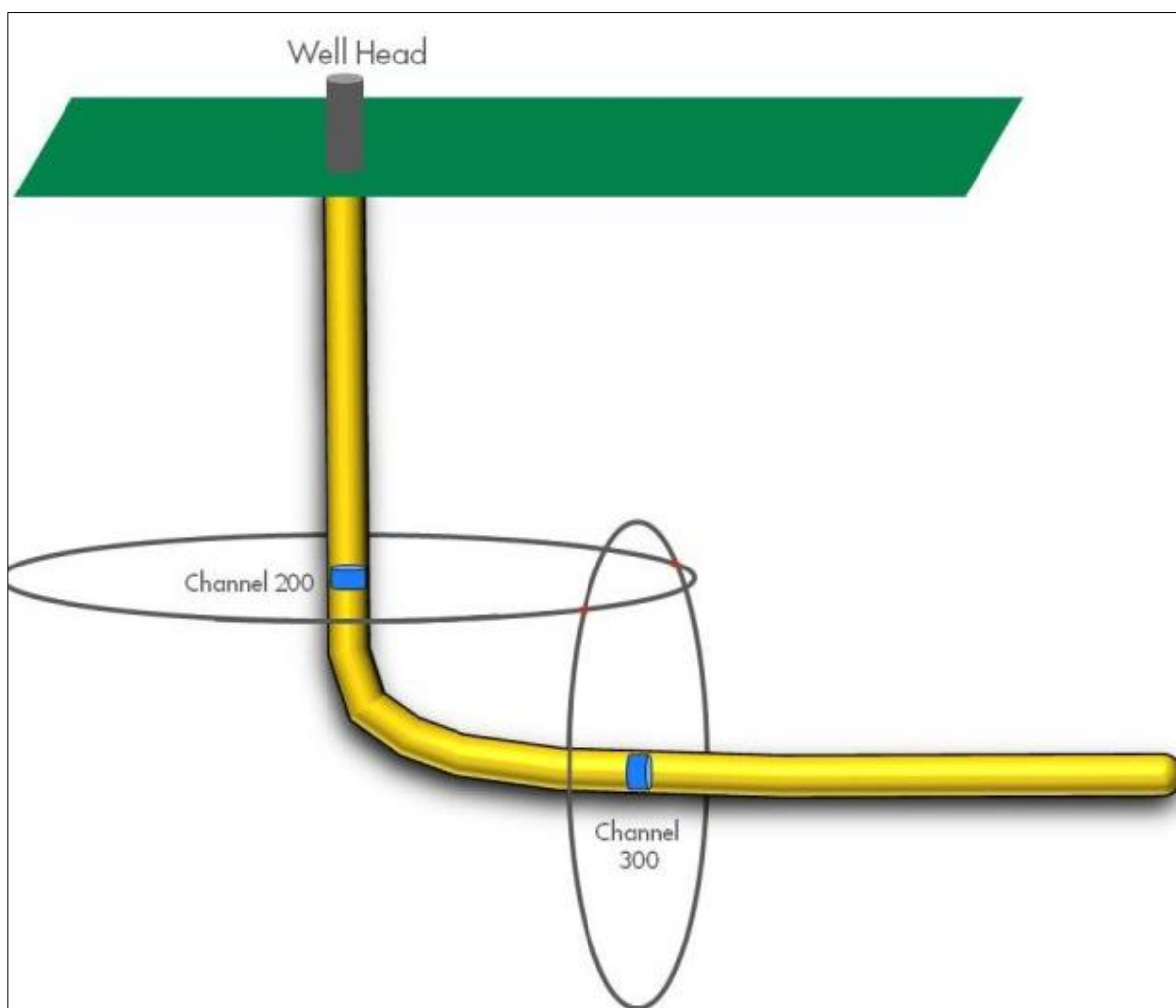


Figure 6.7: A micro-seismic event recorded on DAS/2/

7. Methods for detection of leaks from the reservoir at seabed

This chapter describes the methods that can be used for detection of reservoir fluids to seabed. It is envisioned that the migration of fluid described in the previous chapter has reached the seabed and mixes with the seawater. The escaping fluids can be oil, gas or injection seawater or a mixture of all these.

7.1 Challenges

Challenge: How to detect leak of injection water from seabed and into the sea column?

Injection water containing no oil or gas is very difficult to detect in the sea water column. Both surface vessels and autonomous underwater vehicles (AUVs) equipped with sensors and sensor systems can assist in detection and monitoring leakage to seabed from injection wells.

Multibeam and side scan sonar surveying are useful for detecting seepage of gas bubbles in water column which give strong acoustic backscatter properties.

Changes in seabed bathymetry (plume/crater) are likely to be detected if a significant amount of leakage takes place through conduits (fractures).

Interferometric side scan sonar is a new method/system mounted on the AUV for automatic gas seep detection and high-resolution imagery and bathymetry of the sea floor.

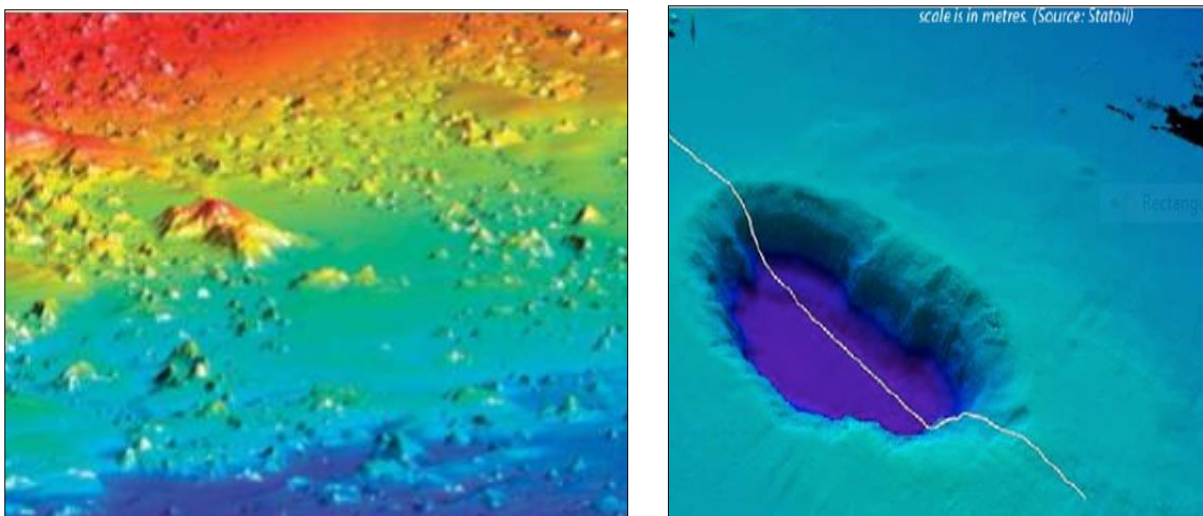


Figure 7.1: Seabed bathymetry

Challenge: Is continuous surveillance of a large seabed area feasible?

For limited sea bed areas, permanent leak detection systems located on the seabed allow for continuous online monitoring.

Both surface vessels and autonomous underwater vehicles (AUVs) equipped with proper sensors and sensor systems can assist in detection and monitoring leakage from injection wells. For surveys in 300 – 400 m water depth, an AUV should be able to map the changes in seabed bathymetry needed to identify potential leakage.

An AUV may be able to scan 2,5 km² / hr. A sea bed area of 50 km² (10 km x 5 km), which may be the size of a representative field in the Barents Sea will require 20 hours. Processing and interpretation of data typically requires 50% of the survey time. Therefore, performing the surveys once a week, allows time for data processing and interpretation of data.



Figure 7.2: AUV

Measurements of small concentration HC content in seawater column by UAV sensors is tedious and not efficient.

7.2 Introduction

Leakage from water injection wells to seabed may typically take place through the following conduits (see Figure 7.3):

1. Fractures created in the reservoir and overburden due to excessive injection pressure.
2. Natural fractures in the reservoir and overburden.
3. The well bore (annulus seals / cement, etc.).

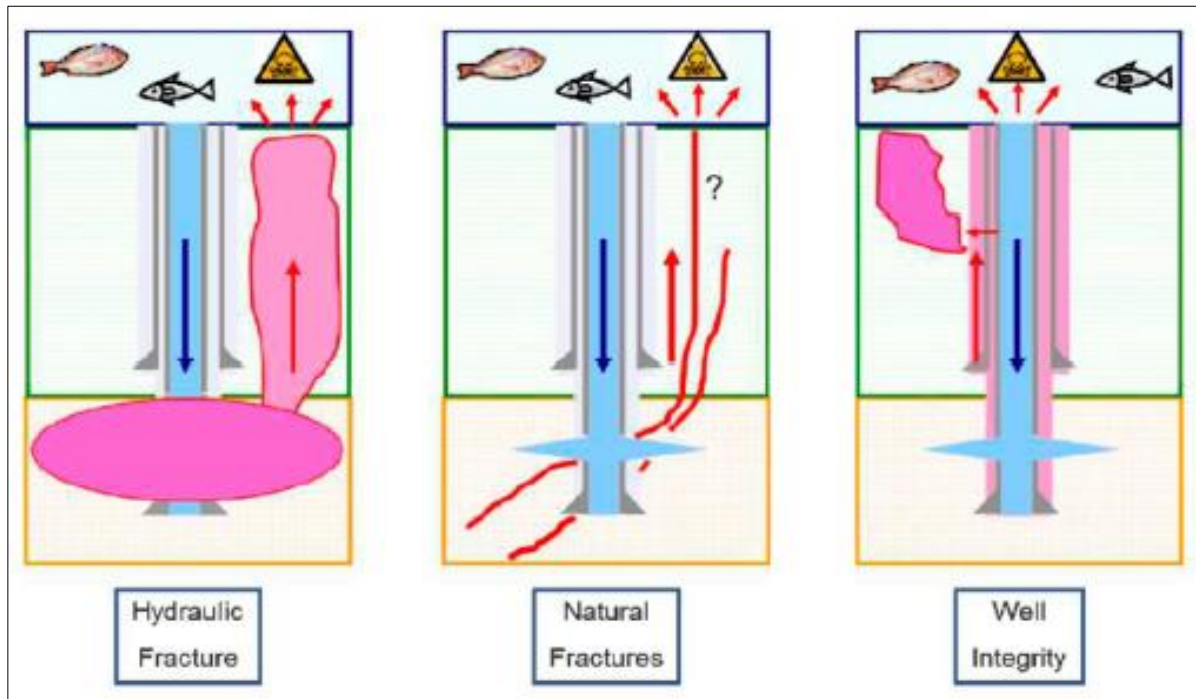


Figure 7.3: Potential leak paths to sea floor (Øfjord, G.D.,2013) (Source: Statoil)

The typical depth of water injection zones on the NCS is 2000 – 3000 m below the sea level. Leaks from injection wells to seabed due to excessive injection pressure are normally not a major problem. Leakage from the injection point or along the well trajectory may be diverted and trapped by overlying reservoirs and may not reach the seabed.

However, discoveries of shallow reservoirs located 250 – 400 m below the seabed in the Barents Sea have higher potential for leaks due to the short distance from the injection point or reservoir to the seabed and corresponding low formation strength of the overburden.

In this region there are also discoveries of karstified reservoir rocks. These carbonate rich rocks were subjected to chemical dissolution by fresh water after deposition. Such reservoirs are characterized by varying porosity and permeability, and occasionally large caves and channel systems. These karst formations and landscapes were buried in the Triassic period and later uplifted due to severe erosion. There is limited experience with such reservoir rocks from the NCS.

The table below shows incidents relating to injection on the NCS from 1997 to 2013.

Table 7.1: Incidents relating to injection on the NCS from 1997 to 2013 (Øfjord, G.D., 2013)

	Period for injection	Oil	Baseoil	Cuttings	Slop/ other chemicals	Black	Red
Åsgard	1997 - 2000						
Ringhorne	2002 - 2004				76 000 m ³ cuttings/ slop		
Visund	2004 - 2007			5 000 m ³			
Tordis (pwri)	2008	175 m ³					
Veslefrikk	1997 - 2009		48,5 m ³	3 450 m ³	93 000 m ³	1,6 m ³	348 m ³
Snorre B	2005 - 2009						81 tons
Oseberg C	2008 - 2009		4 559 tons	4 606 tons			19 tons
Oseberg Sør	Before 2006						
Grane	Depression confirms leakage						
Njord	1999 - 2006				3400 tons	5,8 tons	133 tons
Statfjord B	2000 - 2013		219 m ³		764 m ³		3,1 m ³

7.3 Examples of leakage from injection wells

Figure 7.4 shows the crater developed on the seabed close to the Tordis Field underwater installations caused by injection of produced water. The crater was about 7 m deep and 30–40 m wide.

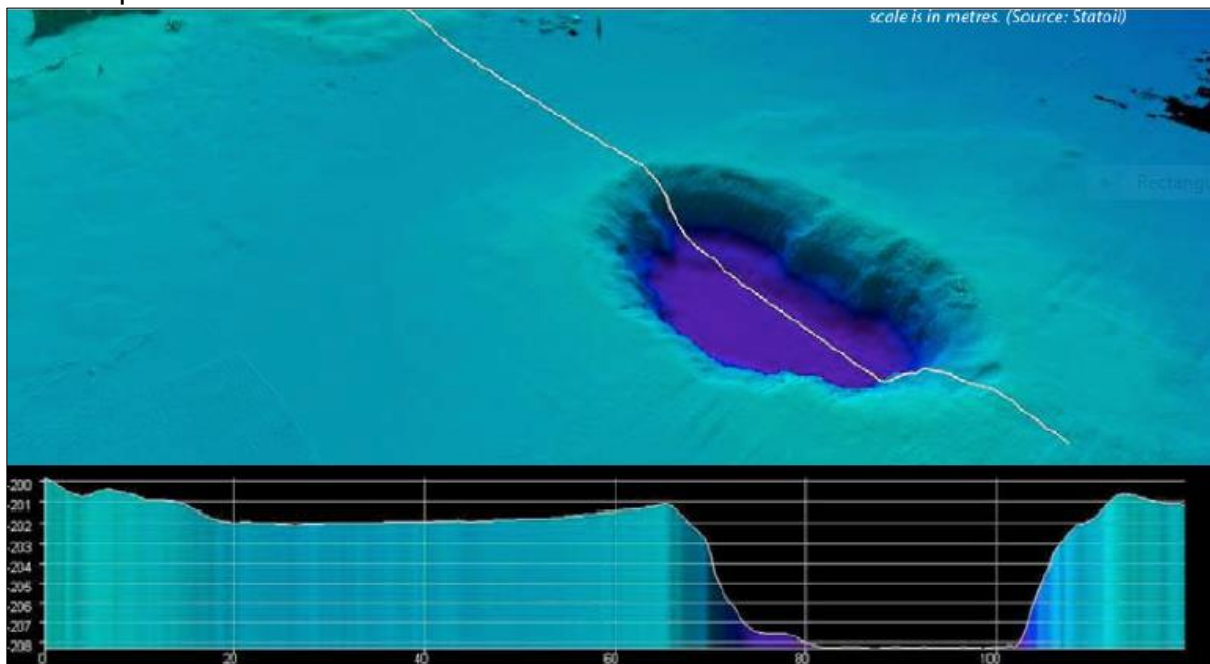


Figure 7.4: Illustration of seabed crater near Tordis - scale meters (Edvin, Tor & Øverland, Jon Arne) (Source: Statoil)

<http://www.npd.no/en/publications/norwegian-continental-shelf/no2-20091/faulty-geology-halts-project/>

7.4 Overview of technologies for detection of leaks from seabed

The following table shows an overview of available technologies and technologies under development for detection of leaks from the sea bed (injection water, oil and or gas). These methods will be described further in this chapter.

Table 7.2: Overview of technologies for detection of leaks from seabed

Technologies -> Features	Deployed from sea level			Deployed on sea bed
	Surface vessel	ROV	AUV	Permanent installation (Limited local area)
Detect changes in seabed topography (crater and potential)	M	M	M	-
Detect inj. water leaks (no HC)	T	T	T	T
Detect plume structure of oil	M	M	M	OI, S (50 m+)
Detect small gas leaks	M	M	M	OI, S (tens of meters)
Able to determine small amount of oil in water (Deep in the water column)	-	W, F	W, F	W, F
Frequency of data sampling	Weekly?	Weekly?	Weekly?	Continuous
Excepted time delay from data sampled to interpreted result	Continuous processing of data – Quick Interpretation	Continuous processing of data – Quick Interpretation	As a rule of thumb, 50% of the survey time after the AUV has been recovered ¹	Real time surveillance
Typical area coverage rate using multi beam sonar (km ² /hour)	1,8 ²	1,0 ³	2,6 ⁴	-

¹ Data processing may take place inside the AUV and status data can be transferred over acoustic links to the mothership.

² Multibeam sonar may have too low accuracy. Towed fish containing Multibeam + side scan sonar allows online data recovery, but the system is complicated to operate.

³ Most applicable for detailed survey of small area (Survey velocity typically 1-2 knots for inspection ROV vs. 3-5 knots for AUV). ROV not suitable for multibeam survey – less stable movement.

⁴ Hugin AUV. Area coverage rate depends on type of sensor system in use (Multibeam + side scan sonar)

Abbreviations:

M – Multibeam Echo Sounder, Side Scan Sonar, Interferometric Side Scan Sonar
S – Sonar (High frequency)
W – Water sampler
HC - Hydrocarbon
F – Fluorescence (Oil in Water, continuous measurements)
T – Temperature sampler (increased local temperature may indicate leakage - difficult)
OI – Optical imaging

7.5 Characterization of injection water and fluids leaking to sea

Treated seawater and produced water are used for reservoir pressure maintenance. The quality of injection water depends on the reservoir properties. Specific requirements relating to salinity level, particle size and particle distribution, contents of oil from produced water, and type of added chemicals, need to be assessed.

Injected water / formation water leakage to sea

Leakage of injected water into sea water is difficult to detect. Potential differences and key indicators may be:

1. Differences in salinity
2. Small amounts of oil in the water (from produced water and / or rests of residual oil in the reservoir)
3. Oil and gas from the reservoir in case of leakage through the cap rock
4. Small temperature difference
5. Chemical composition
6. Changes in seabed topography. A plume and/or crater is likely to be seen on the sea floor if a significant amount of leakage takes place through fractures etc.
7. Increased particle concentration in the water column and reduced visibility

Injected water may be treated for purpose of leak detection in the following manner:

1. Adding tracers (chemical or color based)
2. Adding gas / N₂ (gas in the water column is easier to detect)

7.6 Technologies for leakage detection at the seabed and/or in the sea water column

Surface vessel and long-range radar and aircraft systems are currently used to discover oil spills in the sea. Most leaks are not detected before oil is observed on the sea surface. The leak origin may be far away depending on the water depth and sea current. Systems for early leak detection are vital in all phases of offshore field development.

Leaks in the well due to well barrier element failures (i.e. cement), may be detected and controlled using proper instrumentation in the well and/or close to the subsea wellhead (i.e. pressure sensors, HC traps with sensors).

7.6.1 Active acoustic, multibeam technologies

Detection of leaks using active sonar is achieved through transmission of different acoustic pulses with various characteristics and analysis of the received echo from specific directions. When an acoustic wave interacts with fluid, gas, particles or plumes of other liquids it will be received with different characteristics than if it was interacting with seawater. The received signals will be affected by difference reflectivity in interface layers, impedance differences, resonance behavior, attenuation differences and flow phenomenon (Koldgaard, E.P., 2012).

New volumetric acoustic-based sonar systems permanently installed across the seabed infrastructure as well as critical hazard areas can mitigate leakage from complex subsea infrastructure and provide real time surveillance (Koldgaard, E.P., (2012).

Sonar is useful for seep detection as gas bubbles in water give strong acoustic backscatter properties. Interferometric side scan sonar is a new method/system mounted on AUVs for automatic gas seep detection and high-resolution imagery and bathymetry of the sea floor (Blomberg, A.E.A. et.al, 2017). Injection water containing no oil or gas is not easy to detect. However, changes in seabed bathymetry (plume/crater) are likely to be observed caused by significant amount of leakage through fractures.

7.6.2 Multibeam seabed survey using surface vessel

Multibeam survey is a highly efficient and accurate solution for seabed mapping. See Figure 7.5. <http://www.o-r-g.no/services/mbes>

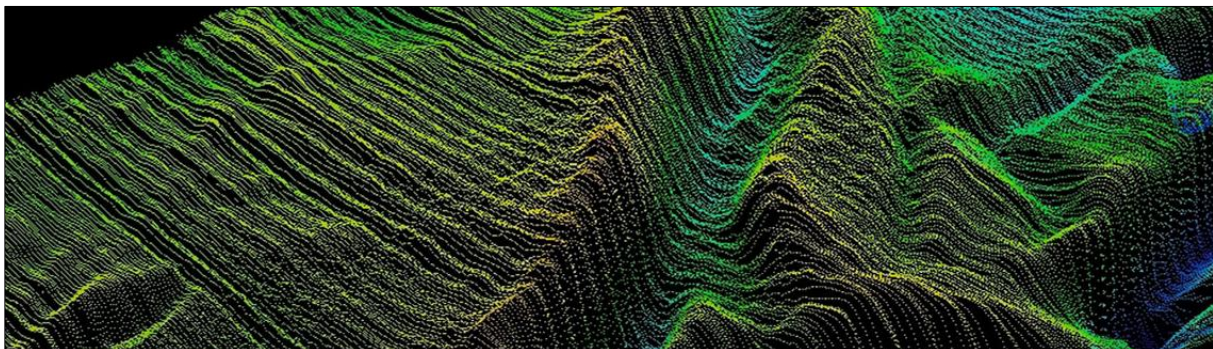


Figure 7.5: Hydrographic Survey (ORG Geophysical AS)

Time-lagged scanning allows changes of the topography to be observed and more detailed investigation may be carried out to identify potential leakage.

Typically, a vessel can scan 5 times the water depth at a velocity of 6 knots (11 km/t). With 50% overlap due to reduced data quality on each side, the effective seabed area scanned in 400 m of water is approximately 1.8 km² / hr. A typical field in the Barents Sea may cover an area of 50 km². The survey time will be in the order of 1 day. Continuous processing of data allows for quick Interpretation. The stand-by vessel can be utilized for this purpose as well as for performing measurements of the sea water column. More accurate bathymetry data can be provided using a submerged towed

Multibeam plus Side Scan Sonar. However, this arrangement is more complicated to operate.

Gas bubbles of a certain size in the sea water column can normally be identified using multi-beam sonar.

7.6.3 Autonomous Underwater Vehicle (AUV)

Clean Sea is an advanced robotic technology aimed at providing a cutting-edge and highly cost-effective solution for both environmental and asset integrity monitoring in oil and gas developments (Gasparoni, F. et.al., 2016). This technology is based on an AUV equipped with a modular interchangeable mission payload. Appendix C shows the standard and additional payload module. Environmental monitoring includes, among other things, temperature, salinity, turbidity, dissolved CH₄, PH, Fluorescence (oil in water), automatic water sampler, etc.

Different types of AUVs (Hugin and Remus) with a selection of sensor and sensor systems are commercially available.

[http://www.atmarine.fi/ckfinder/userfiles/files/HUGIN_Family_brochure_r2_lr\(1\).pdf](http://www.atmarine.fi/ckfinder/userfiles/files/HUGIN_Family_brochure_r2_lr(1).pdf)

The AUVs run survey missions of durations up to 2.5 days with all payload sensors (SSS, SBP, MBE and CTD) in operation simultaneously.

A standard HUGIN payload suite includes:

- Multibeam echosounder - Sidescan or synthetic aperture sonar
- Sub-bottom profiler - Conductivity temperature density (CTD)
- Turbidity sensor
- Acoustic Doppler current profiler (ADCP)

Payload sensors for specific applications can be added. Figure 7.6 below shows the Hugin AUV and Figure 7.7 shows the bathymetry from the Ormen Lange field. Figure 7.7 is mapped with HUGIN II and EM 3000 multibeam echosounder (NUI AS).



Figure 7.6: Hugin – AUV

[http://www.atmarine.fi/ckfinder/userfiles/files/HUGIN_Family_brochure_r2_Ir\(1\).pdf](http://www.atmarine.fi/ckfinder/userfiles/files/HUGIN_Family_brochure_r2_Ir(1).pdf)

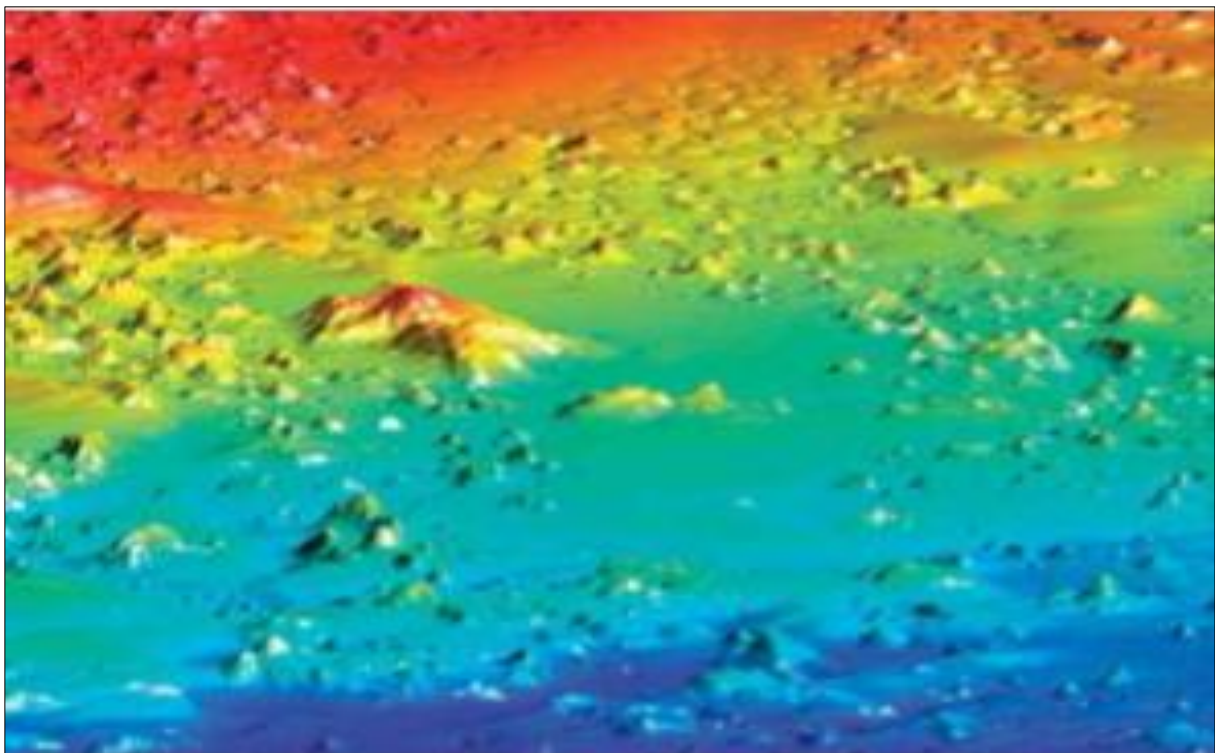


Figure 7.7: HUGIN bathymetry from the Ormen Lange field – year 2002 (NUI AS)

The AUV can be programmed to follow a selected pattern on the seabed. Typical scanning capacity of the seabed is 2,6 km²/hr. Cracks of a size less than 0,05 – 0,1m can be identified. By comparing the maps, or even by comparing each pixel with baseline surveys changes can be identified and further action taken.

Appendix D shows the product range for Remus and Hugin AUVs.

8. Relief Well Design

All blowouts and ensuing relief well operations are inherently different, with unique challenges that must be addressed to successfully regain control of the problem well. Designing a relief well usually requires multiple iterations before reaching the optimum plan (Wright). The primary objective that must be demonstrated is that the relief well can locate and intersect the target well and subsequently kill the blowing well by a pumping operation. In other words, the contingency plan should answer the following two questions; “can the relief well hit the target well?” and “can the relief well kill the blowout?”.

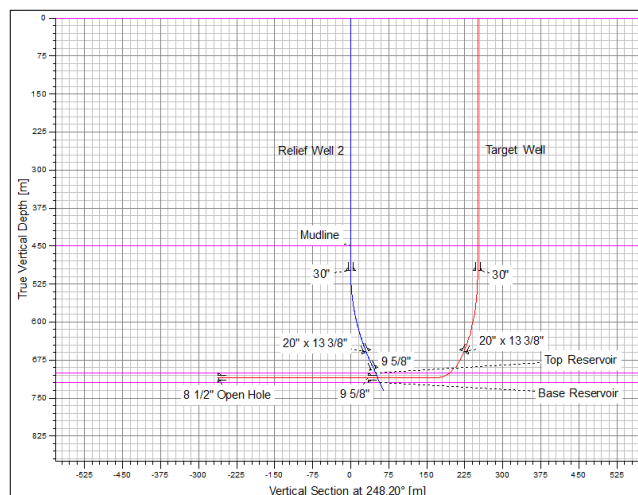
Drilling a relief well in the Barents Sea may be faced with many challenges including but not limited to procuring suitable drilling rigs, accurate wellbore surveying and placement, unconventional ranging and intersect strategy, and demanding dynamic kill requirements. The following chapter will focus on relief well specific challenges for a shallow intersect in the Barents Sea.

8.1 Challenges

Challenge: Can the blowing model well be intersected with a relief well?

Of 3 possible relief well trajectories, the vertical relief well is preferable as this may give the shortest time to intersect, consequently reducing the time that the reservoir is exposed and the duration of the blowout. The only successful vertical relief well drilled to a horizontal target was done on the Montara blowout, which was ultimately intersected by milling through the casing after 5 sidetracks.

For the model well, the intersection point can be the shoe of the 9 5/8" or the 7" production liner. This requires a direct intersect with high incident angle. Several plug backs and re-drills (sidetrack) to increase the accuracy of relative positioning through magnetic ranging before the final intersect must be expected. Pre-magnetization of the casing in the model well will reduce the number of sidetracks.

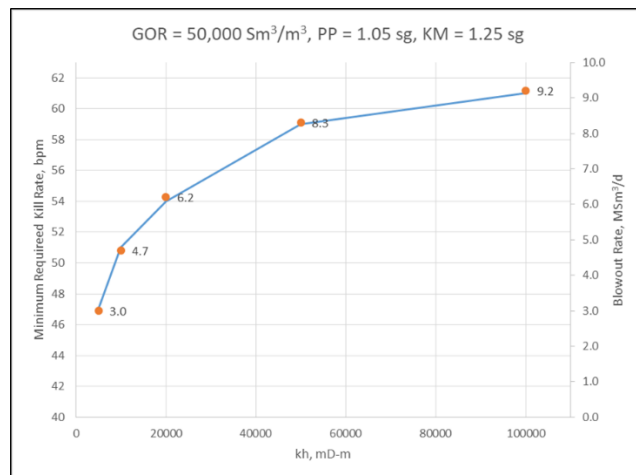


Challenge: Can the blowing well be killed dynamically?

The dynamic kill uses the increased hydrostatic head of a mixture of gas, oil, and mud in the blowing well together with the frictional pressure drop to increase the bottomhole pressure (BHP) and consequently stop the flow from the reservoir.

For a shallow reservoir, achieving the hydrostatic and frictional pressure during a dynamic kill is challenging. This, in combination with a prolific reservoir, large hole size, and high GOR, may lead to demanding kill operations.

Simulations (OLGA Well Kill) shows that the model well can be killed with a single relief well by pumping 50 – 60 BPM of 1,25 SG kill mud. However, full wellbore displacement could not be established since the relief well intersects the target well approximately 1200 m MD off-bottom. Intersecting the model well at a shallower depth does not significantly change the kill requirements. Higher pore pressures or a larger open hole could result in kill requirements exceeding the capabilities of a single relief well.



8.2 Model Well

In this study a relief well planning process for a hypothetical well representative for some of the areas in the Barents Sea will be outlined. The model well is an extended-reach well that will be drilled in 450 m of water with a TD at 710 m in the Wisting Field. The planned trajectory is shown Figure 8.1 and Table 8.1.

Table 8.1: Shallow horizontal well directional plan

Measured Depth m	Inclination deg	Azimuth deg	True Vertical Depth m	North m	Easing m	Vertical Section m	Dogleg (°/30m) deg/30m
0	0	0	0	0	0	0	0
500	0	0	500	0	0	0	0
830	90	0	710	210	0	210	8.18
2000	90	0	710	1380	0	1380	0

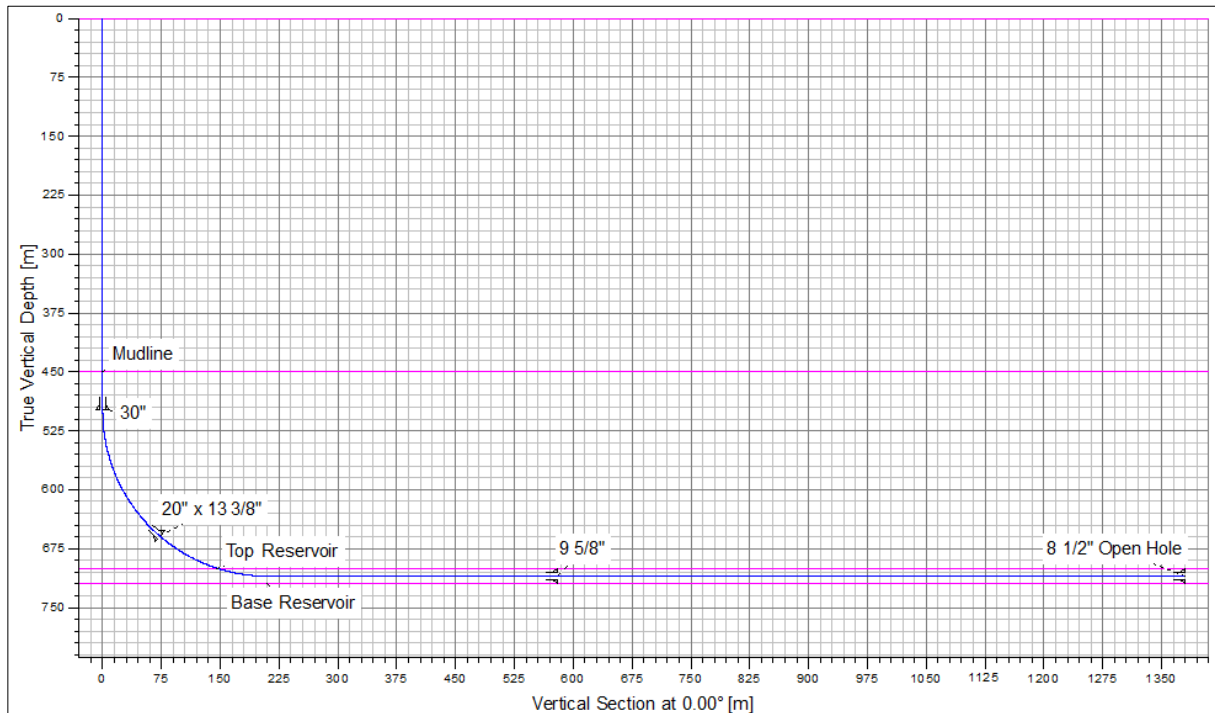


Figure 8.1: Model production/injection well profile

The assumptions for the reservoir and fluid properties and the flow scenarios are presented in appendices A.1 Background information and input data – reservoir fluid and A.3 Scenarios.

8.3 Downhole Ranging Techniques

Determining the distance and direction to adjacent wellbore(s) is a critical task while drilling relief wells or preventing wellbore collisions. Because of the cumulative and systematic errors inherent in MWD or gyroscopic tools, the measured survey coordinates of a wellbore will have increasing uncertainty with depth, which is referred to as the “cone of uncertainty”. With MWD surveying and In-Field Referencing (IFR) the model well will have an uncertainty ellipse of 19.5 m diameter (Figure 8.2). Similarly, the relief well will also have positional uncertainty. Hence for blowout intervention, to accurately steer a relief well to an intersection by relying on the survey data of the target well alone is practically impossible. Instead, the homing-in process must be accomplished by a downhole ranging technique.

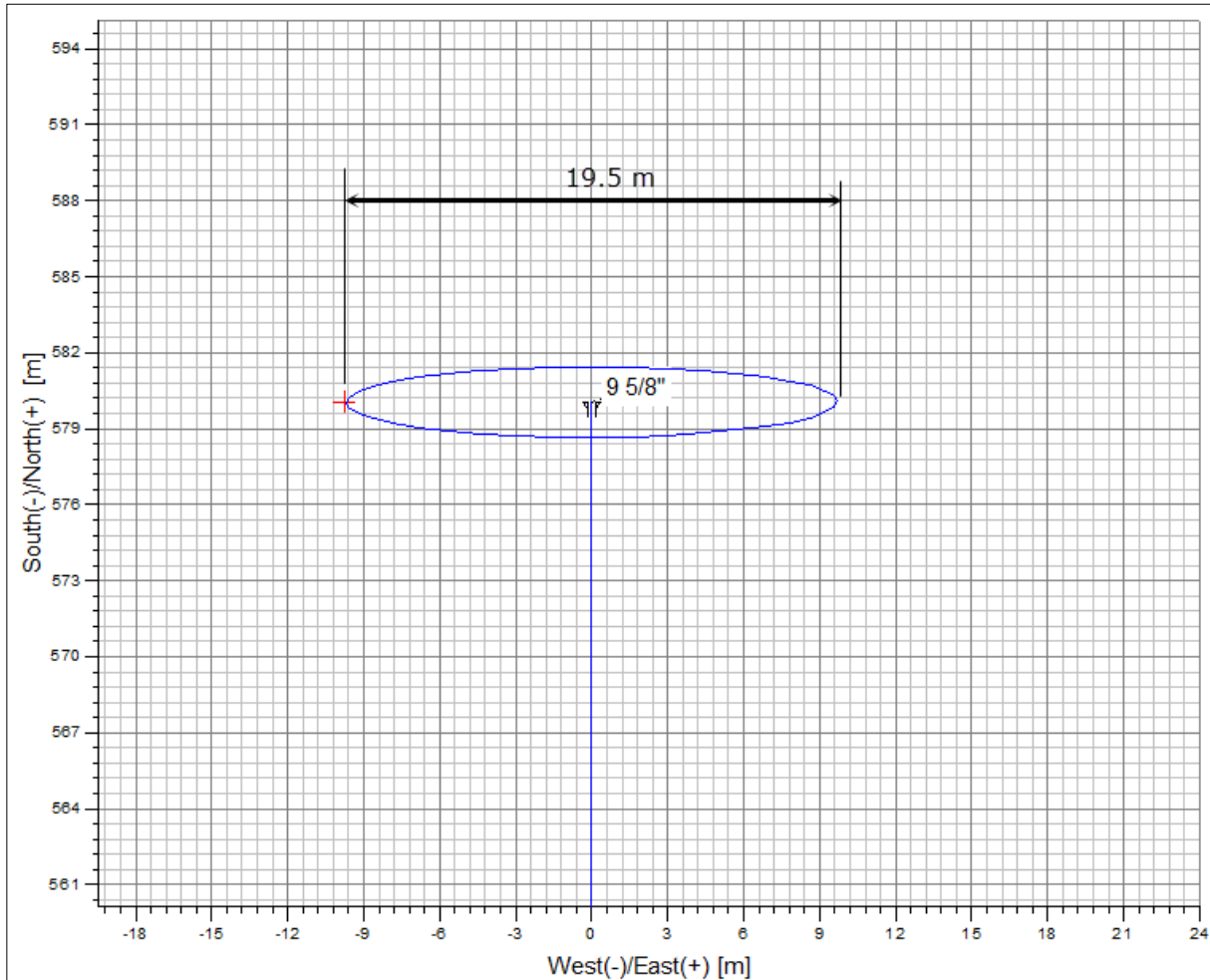


Figure 8.2: Wellbore positional uncertainty ellipse at the 9 5/8" casing shoe

For relief well operations, the target well is typically not accessible, thus an access independent downhole ranging method must be used. The two most commonly used methods are:

- Active Electromagnetic Ranging
- Passive Magnetostatic Ranging

8.3.1 Active Electromagnetic Ranging

The first-generation active electromagnetic ranging tools have two main downhole components are 1) a current injector and 2) a magnetic field-sensor package consisting of two-axis AC magnetometers mounted in the radial plane of the tool (West, Kuckes and Ritch, 1983). The two main components are separated by an insulated bridle. As illustrated Figure 8.3, the electrode is used to inject a uniform alternating current into the surrounding formations. If there is an adjacent wellbore, the current will short-circuit and travel up and down on the casing or drillpipe. A fluctuating electromagnetic field will be created which surrounds the target well. The magnetometer sensors will measure this field and the data is transmitted to surface where it is interpreted to produce a distance and direction to the target well.

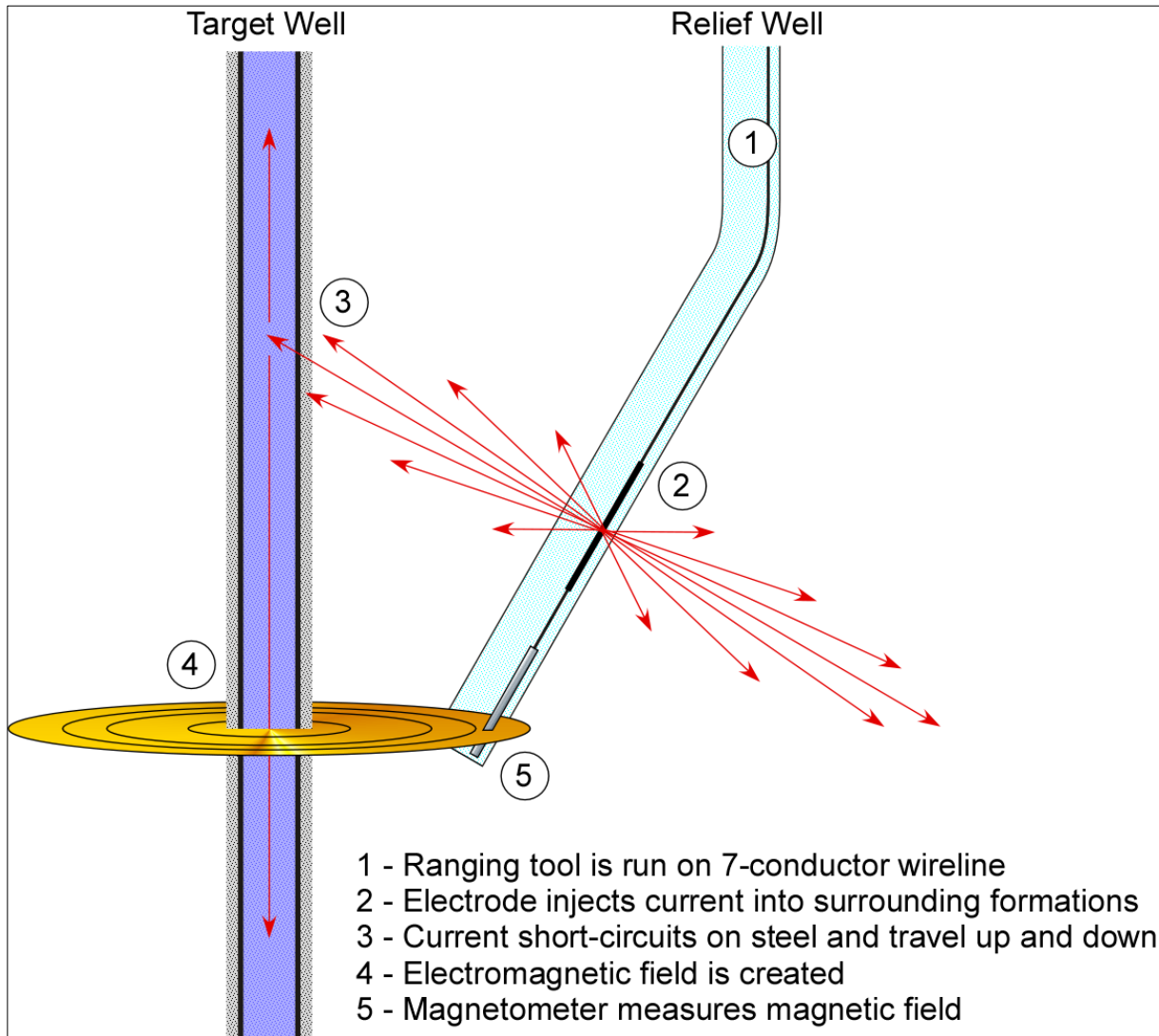


Figure 8.3: Principle of electromagnetic ranging with downhole injection in openhole

The maximum detection range of active electromagnetic ranging will depend on the ability to get current flow on the target well. Some factors that may affect detection range include (but are not limited to):

- Tool type, excitation method and configuration
- The conductivity of surrounding geologic formations
- Wellbore geometry
- The mud type in the relief well
- Incident angle between target well and relief well

Another factor that may significantly reduce the detection range of this technique is the end-of-pipe effect. As noted earlier, if current travels through a casing string it will create an electromagnetic field. However, when the current approaches the casing shoe, it will go to ground and the electromagnetic field will diminish until it completely disappears at the end.

The ranging service provider will have proprietary models that can be used to estimate the maximum detection range for a given tool and well scenario. Based on the authors practical experience on actual relief wells, the maximum detection range of active electromagnetic ranging was often around 40 m.

In the recent years, ranging inside drillpipe has been made practical and successfully been used on several projects to significantly reduce the time to range and drill a relief well. The principles of operation are the same as described for openhole tools, but it requires the use of NMDC and gap subs in the BHA. The detection range will typically be less than open-hole ranging, thus this method will often be used after the target well has been located and the relief well is paralleling the target well at close distance.

For the model well and this study, active electromagnetic ranging is assumed to be the primary ranging method due to its detection range and accuracy. However, some challenges that may arise include:

- To align the relief well with the horizontal target well, it will likely be necessary to pump down wireline tools through open-ended pipe using a side-entry sub at surface. This will be time consuming and has the potential for resulting in significant down time.
- When attempting to range close to the 9 5/8" casing shoe, the end-of-pipe effect may significantly reduce the ability to measure an electromagnetic field.

8.3.2 Passive Magnetostatic Ranging

Passive-magnetostatic ranging (PMR) can be used as the primary ranging technique or in parallel with active electromagnetic ranging. By analyzing magnetic interference in the MWD raw data, the direction and distance to the target well can be estimated.

Every joint of casing or drillstring will have a positive and a negative pole at opposite ends. The detection range of PMR will depend on the strength of these poles located in the target well. The best way to facilitate homing in on the target well using PMR is to pre-magnetize the target-well casing joints to increase the pole strengths. This can be done by inducing current in a solenoid coil wrapped over the casing joint before it is run in the hole. Another way to increase pole strength is to connect two poles of the same polarity, e.g. two casing joints where the opposing South poles are made-up together.

For this study, PMR have applications for high inclinations such as when the relief well attempts to parallel the horizontal section of the target well. This could eliminate the need for wireline operations and reduce the ranging time.

PMR can also be used close to the 9 5/8" casing shoe where end-of-pipe effect will limit or prevent the use of active electromagnetic ranging. This is particularly important for a direct approach or a toe-to-heel approach, which will be elaborated further in the relief well examples.

Because PMR may be applicable for these projects, considerations should be given to pre-magnetize the target well 9 5/8" casing string. Depending on the relief well

approach—as will be discussed—either solely the 9 5/8" shoe track, or the shoe track plus some number of additional joints could be used to range on and should be pre-magnetized.

8.3.3 Ranging techniques in development

A recent study assessed the feasibility of drilling a relief well using a surface seismic method for continuous ranging while drilling (Evensen, Sangesland, Johansen 2014). This method may fill a current industry gap for detecting wellbores without steel while also reducing the time to drill relief well. With a deeper intersect below the last casing shoe, the kill requirements may be less demanding. At the time of this study, the method is not commercially available.

Another new ranging concept in development is the Active Acoustic Ranging, which uses a Sonic Scanner tool to detect acoustic reflections (Poedjono). This method may also enable detection of wellbores without steel. The theoretical ranging distance is 50 m. The Sonic Scanner tool is commercially available and should operate to a max 180°C / 1380 bar. The Active Acoustic Ranging service is currently in field testing, but not yet available commercially.

8.3.4 Cross-by and triangulation

For a given depth, the downhole ranging tool should produce a distance and a direction measurement to the target well. The distance to the target will often have relatively high uncertainty compared with the direction measurement. Before attempting to align the relief well with the target well, it is recommended to drill past the target well (cross by) and use a triangulation technique to minimize the total positional and ranging uncertainties. Figure 8.4 is a simplified illustration of how the positional uncertainty box is significantly reduced with triangulation as compared to drilling directly to the target.

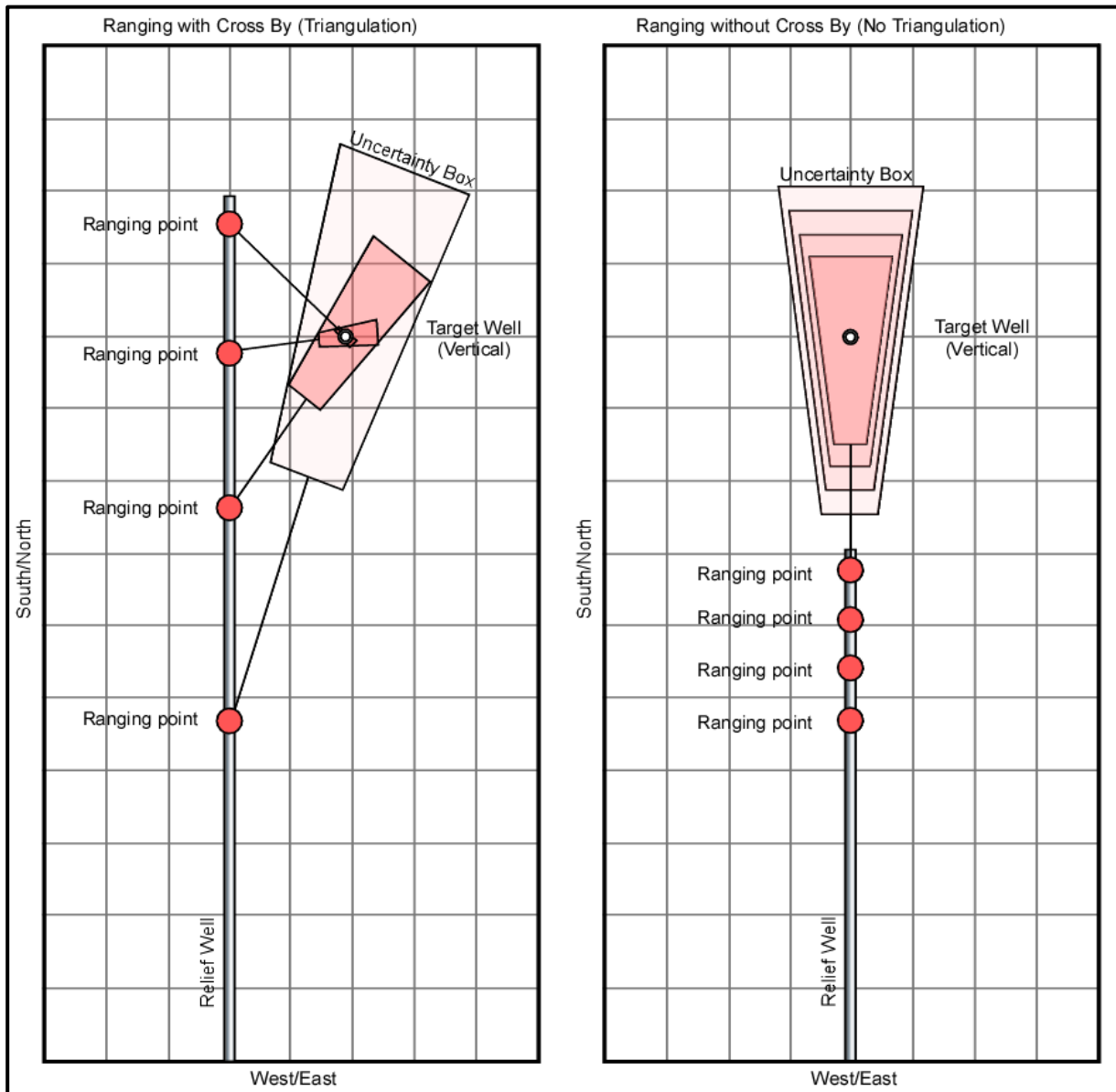


Figure 8.4: Triangulation after cross-by reduces the positional uncertainty box

8.3.5 Direct relief-well approach

Due to MD/TVD limitations or other criteria, there may not be enough room for a cross-by. Instead the relief well will be drilled directly to the target where intersecting on the first attempt will rely more on the wellbore-survey uncertainty, wellbore-positioning accuracy, ranging-run results, luck etc. If the relief well is not aligned to hit the target, the recommended plan forward may be to drill past the target well by + 30 m, which will allow for triangulation of its position. Once an accurate fix of the target well has been obtained, the survey data will be tied to this reference point to estimate deeper wellbore locations. As illustrated in Figure 8.5, the bit can then be pulled back before sidetracking and intersecting the target wellbore in the openhole.

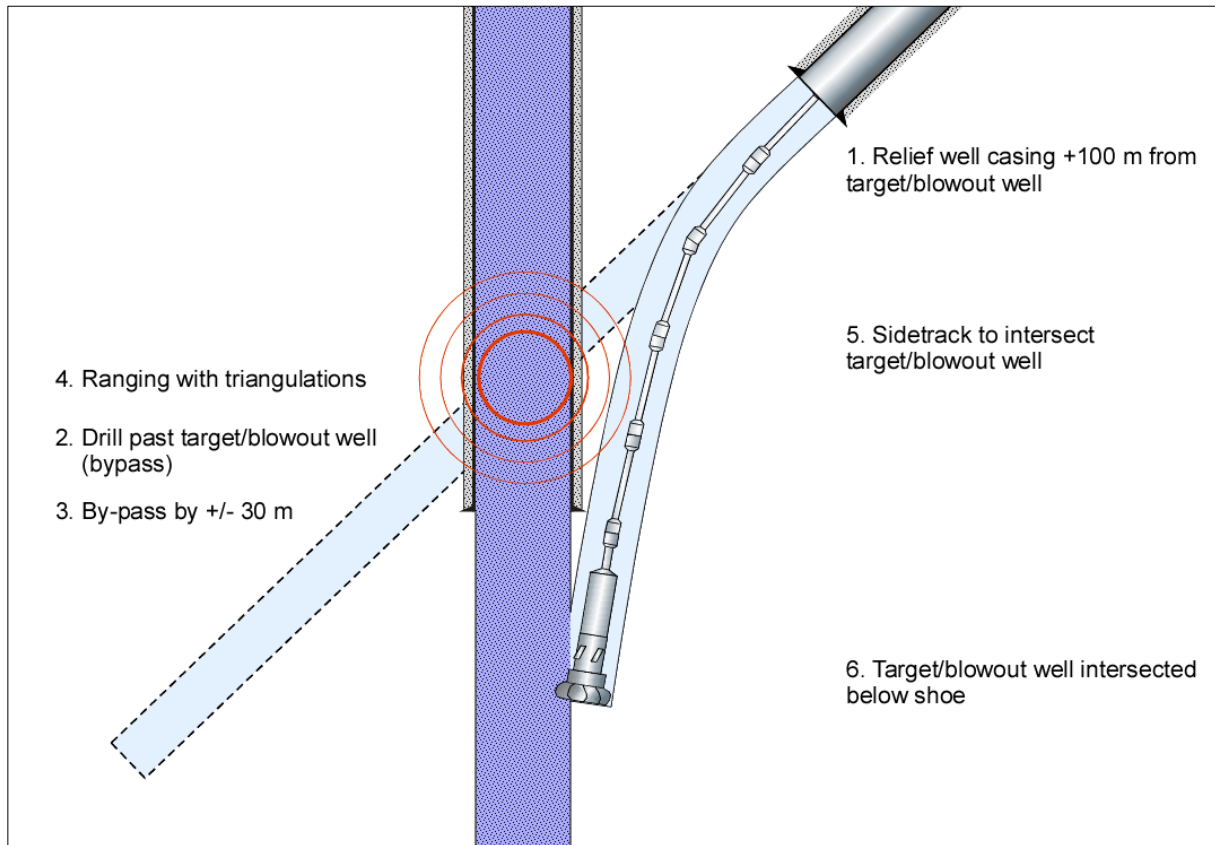


Figure 8.5: Example ranging strategy for a by-pass and plug-back intersect

To complicate matters, a direct intersect close to a casing shoe will severely limit the use of active electromagnetic ranging techniques due to end-of-pipe effects. For this scenario, it is important to pre-magnetize the casing shoe to assure the relief well locates the target well.

8.4 Relief Well Trajectories

A conventional S-shaped relief well trajectory is planned to approach the target well at a relative low incidence angle before performing search and locate with a downhole ranging technique. Subsequently, the relief well will drill past the target well for a cross-by to allow detailed triangulations of the target well position. Once an accurate fix of the target well is obtained, the relief well will parallel the target well to the planned kill point. This section is also used to align the relief well with the target well, before intersecting at a low attack angle ($<8^\circ$). The relief-well design will usually be planned with conservative directional drilling parameters, e.g. low build/drop rates, as low a sail angle as possible and room to allow for triangulation.

With a shallow kill point, there may not be enough room for a conventional relief well approach with low incident angle and a cross-by. As an example, consider a planned vertical well with three hydrocarbon-bearing hole sections as illustrated in Figure 8.6. A conventional relief well strategy with cross-by and a parallel section may be possible for a relief well drilled to the 9 $\frac{5}{8}$ " casing shoe. For an intersect at the 13 $\frac{3}{8}$ " casing shoe, the TVD window that allows directions steering is too narrow for a conventional

relief well approach. In the most extreme cases, the relief well must be drilled as a fish-hook to hit its target (Ralowski 2016). Achieving such a trajectory will likely encounter many challenges including running casing, hole stability, cuttings transportation, torque and drag etc.

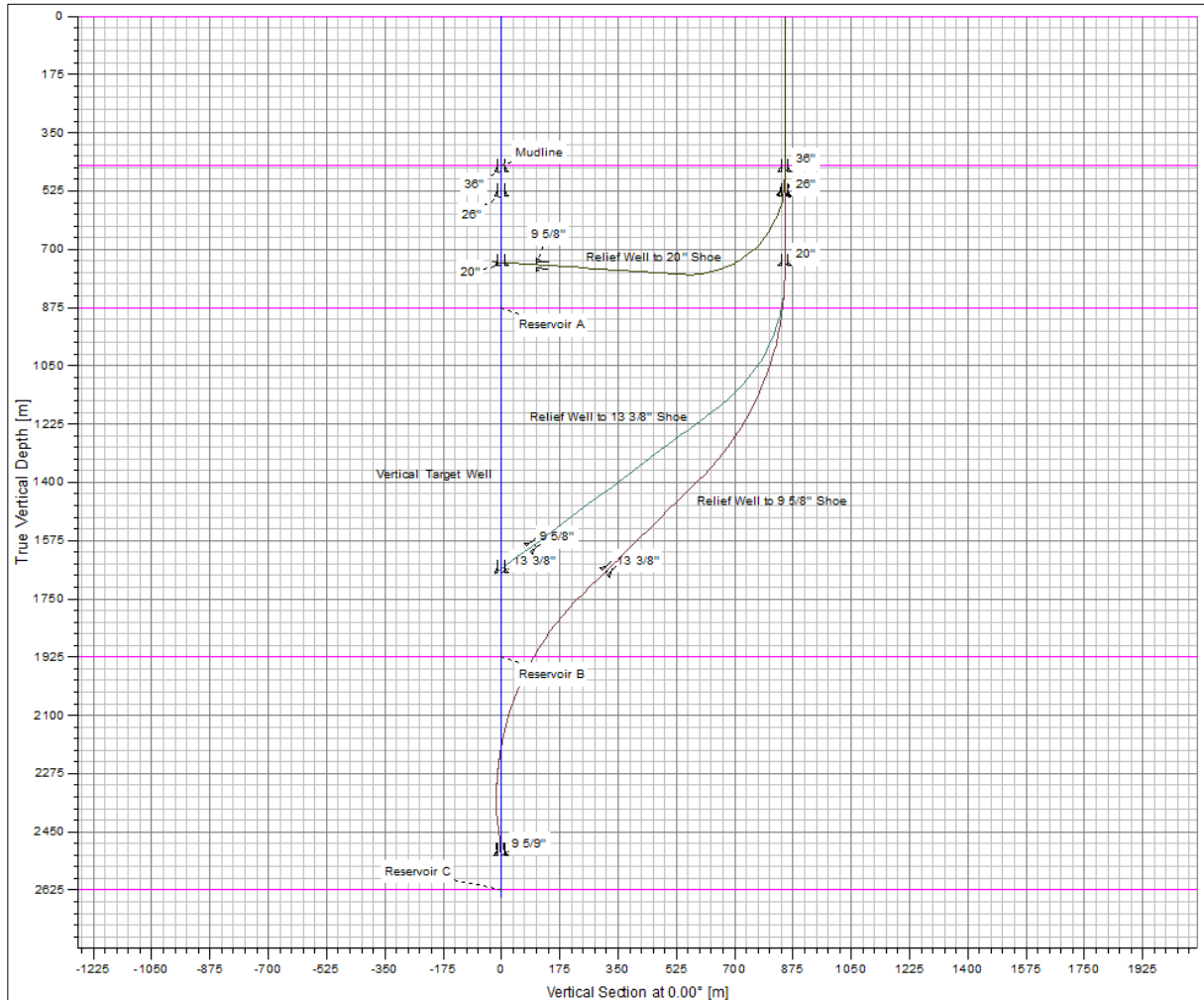


Figure 8.6: Relief well trajectories for kill points at different depths

8.5 Surface Site Selection

Historically, regulator and insurance requirements and industry guidelines often suggested a relief well to be spudded at least 500 m away (safety zone) from the blowing well. The distance may vary greatly, but will often lie in the range of 1000 m \pm 500 m around the blowout itself (when H₂S is not present) and 500 m between relief-well rigs. The relief-well intervention of the Marathon Steelhead Platform, in a water depth of 60 m, used a surface site of approximately 125 m away from the target-well location. The opposite extreme is the Montara relief well which was spudded approximately 2025 m from the blowout.

Before spudding any well, the surface location must be assessed based on the environmental constraints such as bathymetry, shallow hazards, shipping lanes, subsea production and associated equipment etc. A relief-well surface location from a

single subsea location will have additional environmental constraints based on the blowout scenario and must also facilitate the relief-well trajectory.

Magnetic surveying uses the measurement of the geomagnetic field to infer the orientation of the wellbore. At high latitudes, such as the Barents Sea, the horizontal component of the geomagnetic field is reduced, which increases the effect of internal interference from the drill string and external interference from crustal magnetic anomalies and ionospheric disturbance fields. For a relief well that will be drilled with inclinations above 70°, it is usually preferred that the surface location is not placed directly in an East/West location from the target.

For this study, three locations that may be used for drilling relief wells are described in Table 8.2 and Figure 8.7.

Table 8.2: Proposed relief-well surface locations

Geographic Reference System				
Geodetic System	Universal Transverse Mercator			
Geodetic Datum	EDM Common Offshore			
Map Zone	Zone 35 N			
Surface Sites	Geographic Location		Map Location	
	Latitude	Longitude	Northing (m)	Easting (m)
Target_Surface_Site	73° 26' 30.830 N	24° 15' 40.080 E	8151997.24	412900.00
RW_Site_1	73° 26' 27.100 N	24° 17' 5.604 E	8151847.29	413649.77
RW_Site_2	73° 26' 48.626 N	24° 15' 42.881 E	8152547.07	412949.99
RW_Site_2	73° 27' 5.157 N	24° 16' 12.513 E	8153046.92	413234.90
Relief Well	Distance from Potential Spill		Bearing from Potential Spill	
RW1 (RW_Site_1)	765 m E		101° N	
RW2 (RW_Site_2)	552 m N		5° N	
RW3 (RW_Site_3)	1346 m NE		21° N	

8.5.1 Relief Well Intersect Target

In the event of an actual blowout, the most important tool for selecting kill point is normally the diagnostics from hydraulic modeling which should be started immediately.

To locate and accurately navigate a relief well to the point of intersect, the target wellbore must have steel, such as casing or drillpipe, for the ranging operations to work. A deep intersection point is generally preferable as it will ensure maximum frictional forces and hydrostatic head in the blowing well. The primary kill point for contingency planning is therefore often chosen just below the deepest casing shoe. If the drillpipe is out of the hole, this will be the deepest point where ranging operations can be performed with conventional techniques.

For this study, the relief well target was chosen at the 9 5/8" casing shoe (Table 8.3). A disadvantage of this target is that the relief well is drilled through the reservoir sand. If this becomes an unacceptable risk, then a target above the reservoir should be

considered, however, this will dramatically change the directional plan of the relief wells and make the kill operation more demanding.

Table 8.3: Intersection point used for relief well design

Blowout scenario	Last casing/liner	Intersection point [m MD RKB]	Intersection point [m TVD RKB]
8 1/2" hole section	9 5/8"	1200	710

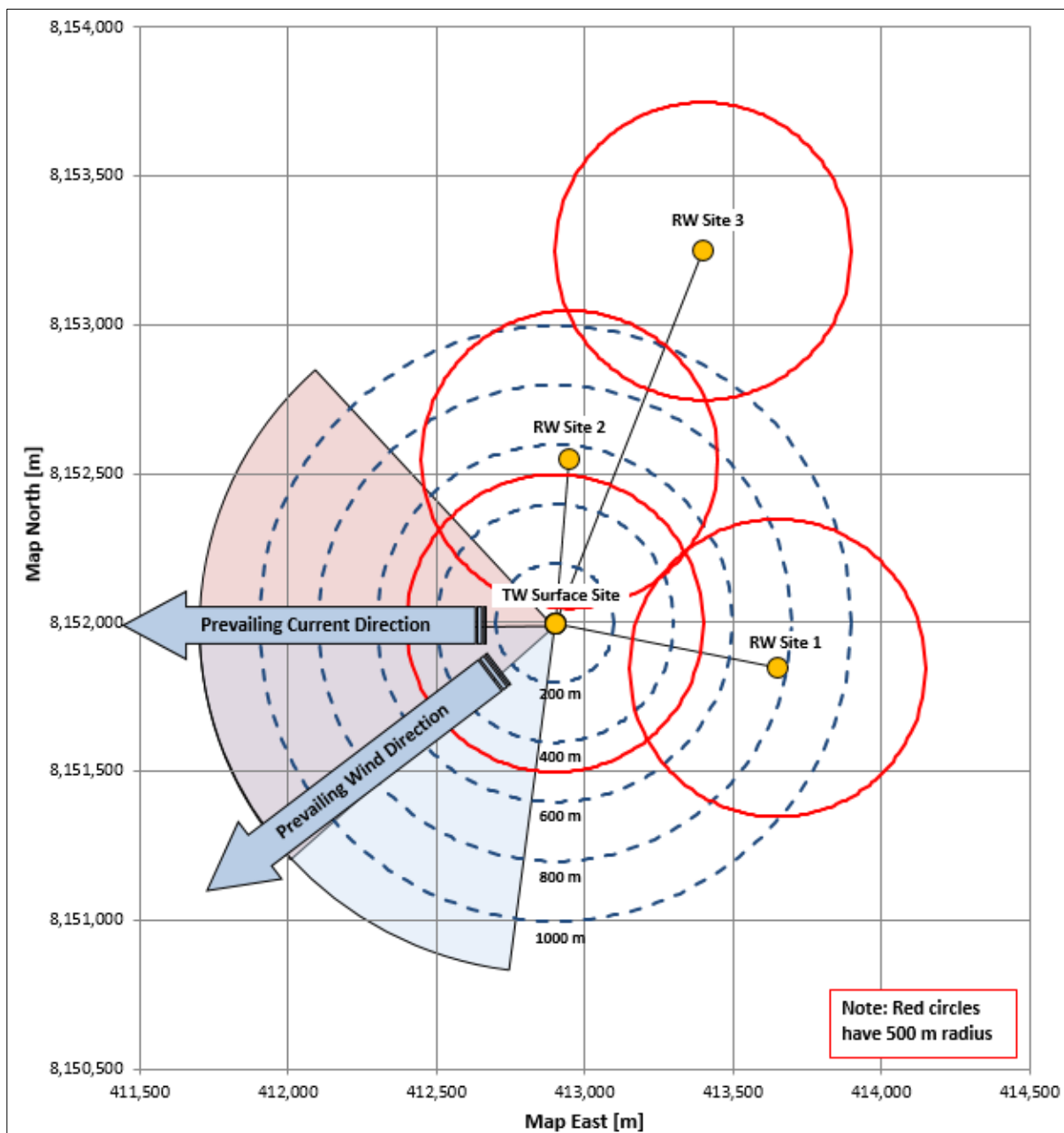


Figure 8.7: Proposed relief well sites with possible wind and current exclusion zones

8.6 Relief Well Design

When attempting to intersect a near horizontal well, there are in theory three types of approaches that can be used to drill the relief well to its target:

- Parallel heel-to-toe approach
- Direct approach
- Parallel toe to heel approach

8.6.1 Relief well 1 – Parallel heel-to-hoe approach

With a heel-to-toe approach, the relief well will attempt to locate the horizontal target well close to the heel and subsequently parallel it to the kill point closer to the toe.

The preferred ranging strategy is active electromagnetic ranging due to increased detection range and accuracy. However, to align the relief well with a horizontal target well, it will likely be necessary to pump down wireline tools through open-ended pipe using a side-entry sub at surface. This will be time consuming and has the potential for resulting in significant down time. Once the target well has been located, passive magnetostatic ranging may be used in the parallel section to reduce wireline operations and save time. Considerations may therefore be given to pre-magnetize the target well casing string that could potentially be used for ranging operations.

Relief well 1 is drilled from RW_Site_1. The directional plan is shown in Table 8.4 and details of the plan is illustrated in Figure 8.8 through Figure 8.10. The directional drilling parameters of the relief well should be similar to the target well. The kick-off point and build rates should always be assessed based on local directional knowledge. In the ranging section, the doglegs should be low ($<3^{\circ}/30\text{m}$) to reduce wireline noise and to allow for directional adjustments based on ranging results.

The first-iteration casing program for the relief-well follows the same basic design—casing size and TVD setting depths—as the target wells with some modifications. A 7" contingent kill liner may be used if there is a chance for the open-hole to collapse when hydraulic communication to the target well is achieved.

The relief well will be aligned with the target well, before setting a final casing/liner 30 m before the intersect. Subsequently the relief well will be drilled straight ahead to make the intersect just below the target wells 9 5/8" casing shoe. In this case, the intersect occurs in open hole, however, if it is necessary to penetrate a drillpipe, the primary means of communication will be to use a concave mill. The back-up method is to use perforation guns.

Table 8.4: Relief well 1 – parallel heel-to-toe approach

Measured Depth m	Inclination deg	Azimuth deg	True Vertical Depth m	North m	Easing m	Vertical Section m	Dogleg (°/30m) deg/30m
0	0.0	0.0	0	-150	750	0	0.0
500	0.0	0.0	500	-150	750	0	0.0
825	90.0	283.8	707	-101	549	177	8.3
1009	90.0	283.8	707	-57	370	334	0.0
1663	90.0	0.0	707	420	-4	936	3.5
1691	89.2	1.2	707	449	-4	956	1.5
1798	89.2	1.2	709	555	-2	1030	0.0
1841	88.0	3.0	710	599	0	1060	1.5
1843	88.0	3.0	710	600	0	1061	0.0

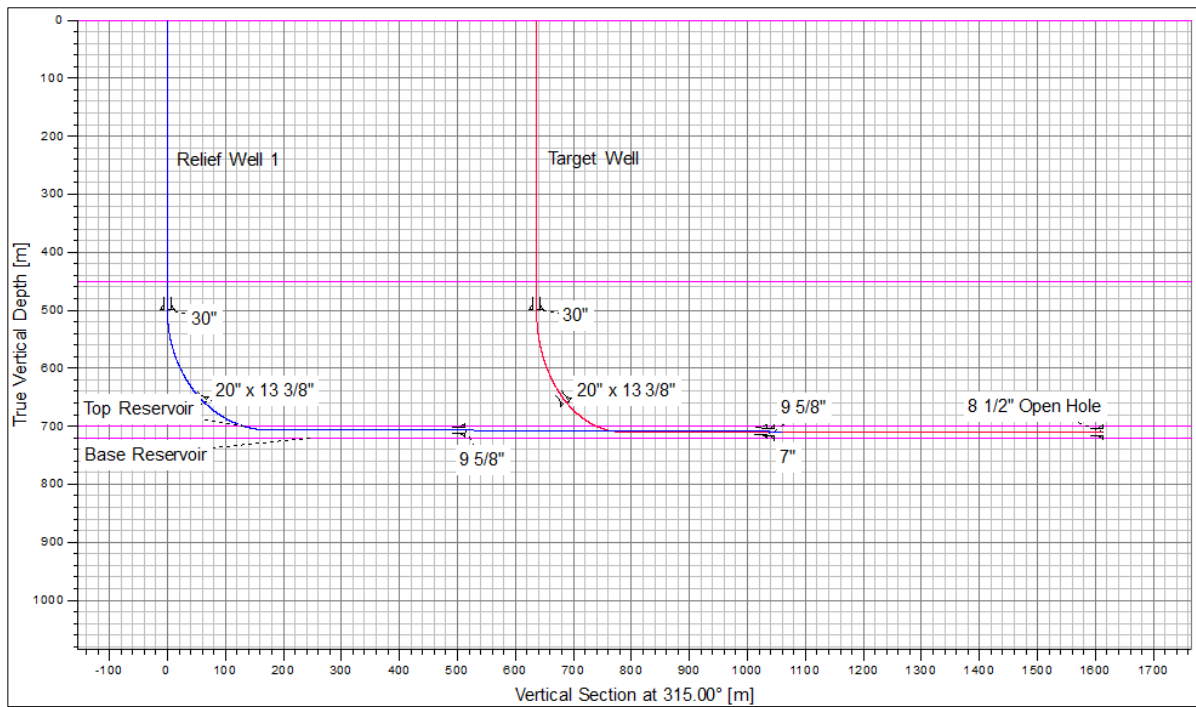


Figure 8.8: Relief well 1 vertical section view

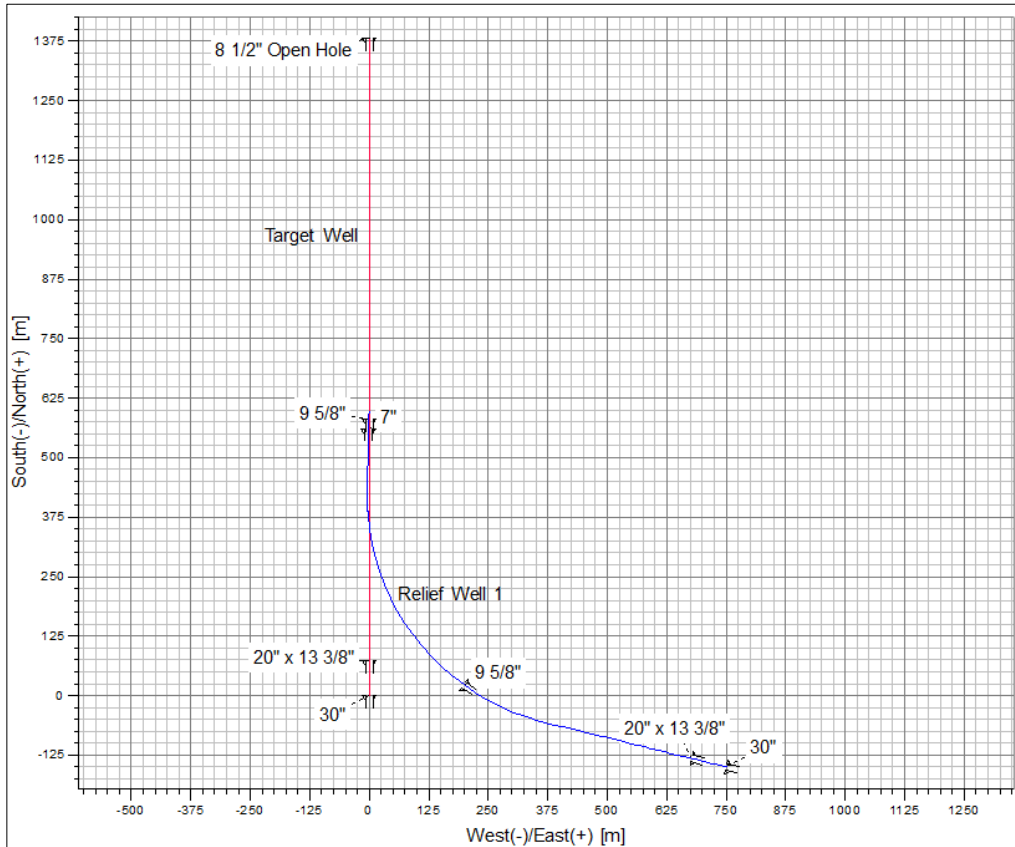


Figure 8.9: Relief well 1 horizontal plan view

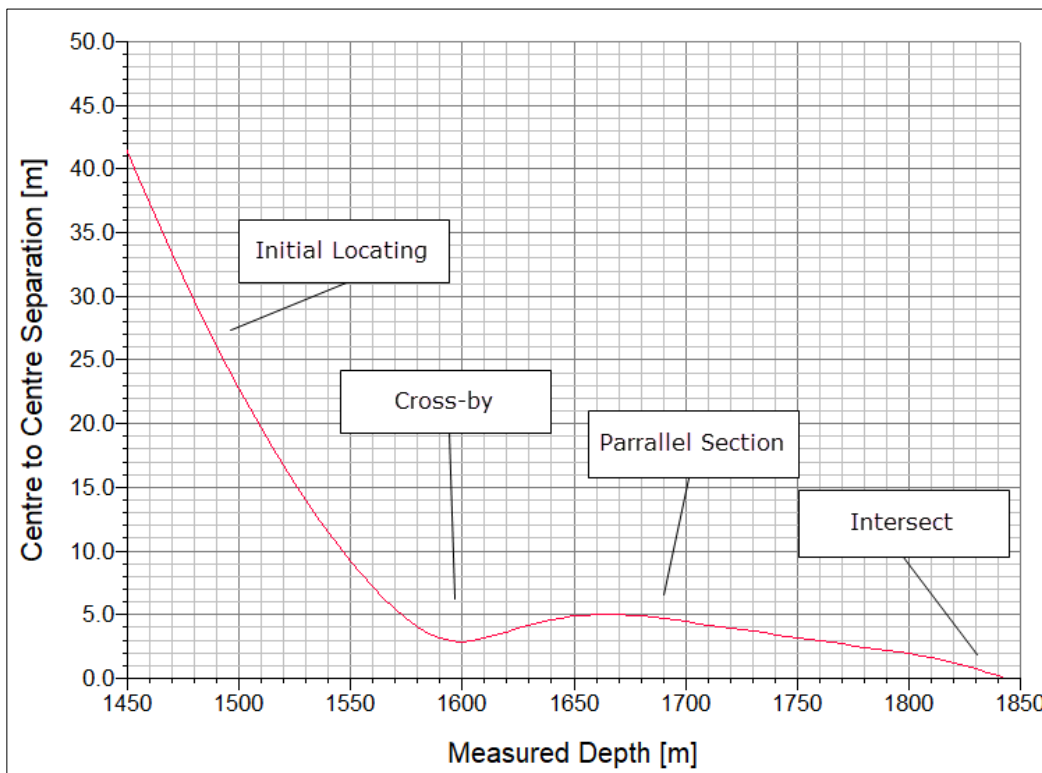


Figure 8.10: Relief well 1 ladder view

8.6.2 Relief well 2 – Direct approach

A relief well using a direct approach is drilled to the kill point without paralleling the target well, instead, it usually intersects with a large attack angle. This method is applicable when intersecting extended-reach wells and for shallow intersects. The advantage is that the relief-well surface location may in some cases be moved further from the spill site. The drawbacks are that active electromagnetic ranging may be limited and the chance of missing the target on the first attempt increases. There are two reasons for this: First off, the electromagnetic tool can only detect a target well in the radial plane, that is, to the side of the wellbore and not ahead of the bit. Secondly, end-of-pipe effect could be significant when intersecting close to the 9 5/8" shoe.

If the relief well misses and drills past the target well sufficiently away from the 9 5/8" shoe, detailed electromagnetic ranging with triangulation may be possible. The relief well will subsequently be plugged back and sidetracked for another intersect attempt, with higher likelihood of success. This was the strategy used on the Montara blowout, which was ultimately intersected by milling through the casing after 5 sidetracks.

With a by-pass close to the shoe, PMR ranging will likely be used. In this case, it is important that the shoe has been pre-magnetized to increase the detection range and accuracy of this method.

A direct approach is used for Relief well 2 drilled from RW_Site_2. The directional plan is shown in Table 8.5 and details of the plan are illustrated in Figure 8.11 and Figure 8.12.

With a parallel approach, the directional driller will have opportunities to do ranging runs and make small corrections to the trajectory of the bit to assure alignment with the target well. This is not the case for a direct approach at a high attack angle. The success in this case will rely on good surveys of the surface locations and wellbores to get as close as possible. After the by-pass, locating the wellbore and side-tracking, a successful intersect on the second attempt will also rely on the ability to drill directionally with high accuracy in the formation and directly place the bit in a target only about 24 cm (9 5/8") wide.

Table 8.5: Relief well 2 – direct approach

Measured Depth m	Inclination deg	Azimuth deg	True Vertical Depth m	North m	Easing m	Vertical Section m	Dogleg (°/30m) deg/30m
0	0.0	0.0	0	550	50	0	0.0
500	0.0	0.0	500	550	50	0	0.0
691	25.5	248.2	685	534	11	42	4.0
719	25.5	248.2	710	530	0	54	0.0
749	25.5	248.2	737	525	-12	67	0.0

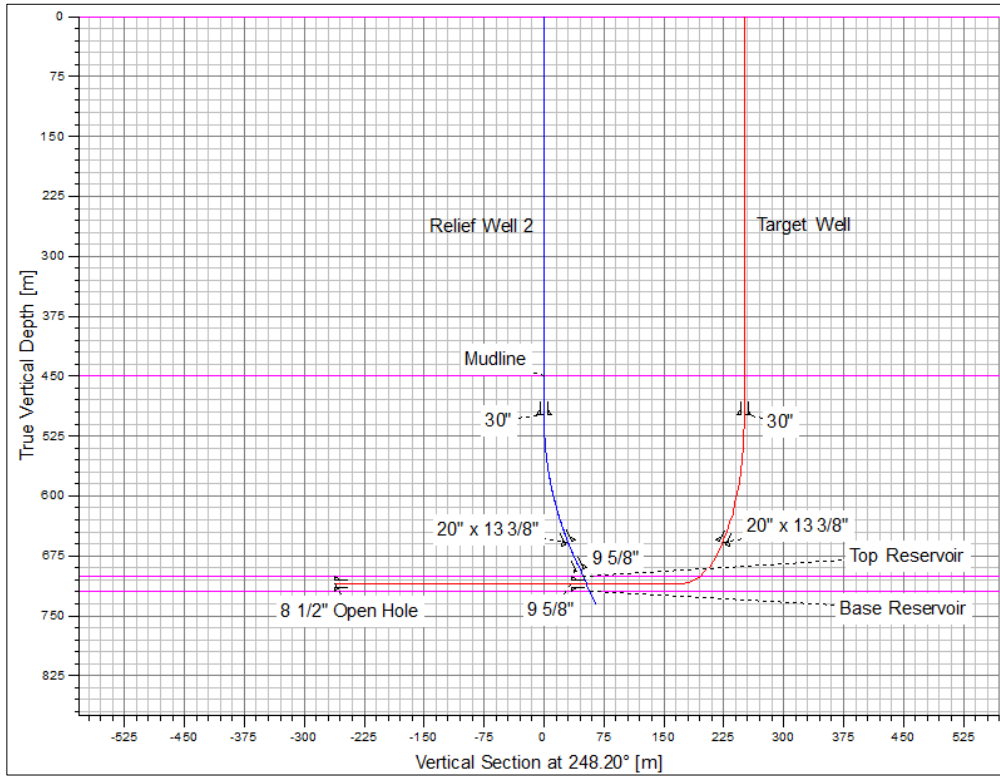


Figure 8.11: Relief well 2 section view

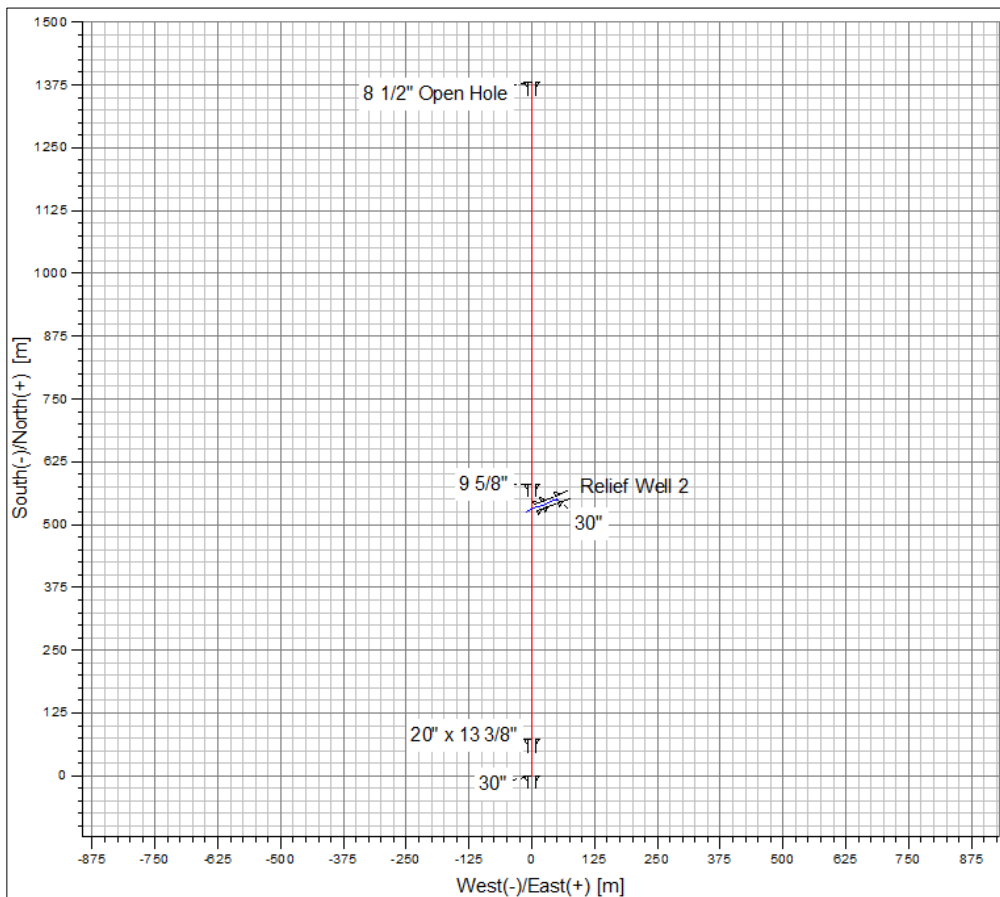


Figure 8.12: Relief well 2 plan view

8.6.3 Relief well 3 – Parallel toe-to-heel approach

As opposed to the parallel heel-to-toe approach used for in the relief well 1 directional plan, the parallel toe-to-heel approach will locate the target well closer to the toe, parallel in the “opposite” direction and finally intersect closer to the heel. This strategy may be applicable when the relief well surface site needs to be located as far from the spill as possible.

A potential challenge with this approach is that the EOU will typically be greater at the toe. Furthermore, the initial ranging must start sufficiently away from the 9 5/8” casing shoe to not be affected by the end-of-pipe effect.

A toe-to-heel approach is used for Relief well 3 drilled from RW_Site_3. The directional plan is shown in Table 8.6 and details of the plan are illustrated in Figure 8.11 through Figure 8.15.

Table 8.6: Relief well 3 – parallel toe-to-heel approach

Measured Depth m	Inclination deg	Azimuth deg	True Vertical Depth m	North m	Easing m	Vertical Section m	Dogleg (°/30m) deg/30m
0	0.0	0.0	0	1050	335	0	0.0
500	0.0	0.0	500	1050	335	0	0.0
837	90.9	219.2	712	883	199	207	8.1
954	90.9	219.2	710	792	125	320	0.0
1346	90.0	180.0	707	430	-4	704	3.0
1384	89.1	178.3	708	391	-4	739	1.5
1443	89.1	178.3	709	332	-2	792	0.0
1466	88.0	178.0	709	310	-1	813	1.5
1496	88.0	178.0	710	280	0	840	0.0

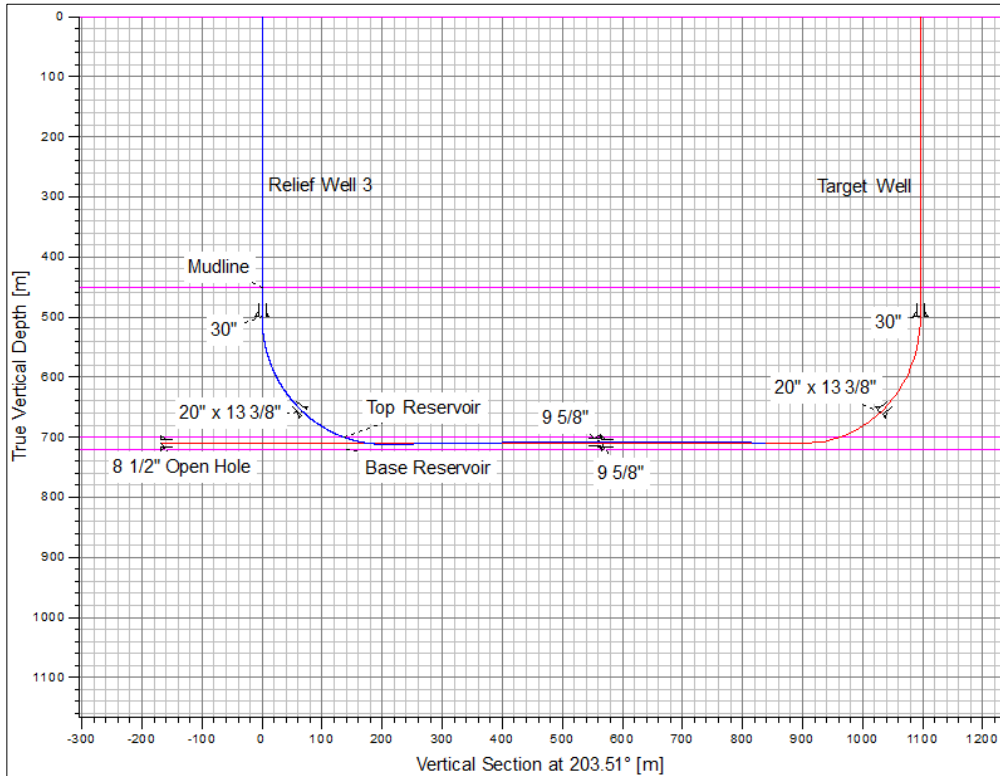


Figure 8.13: Relief well 3 section view

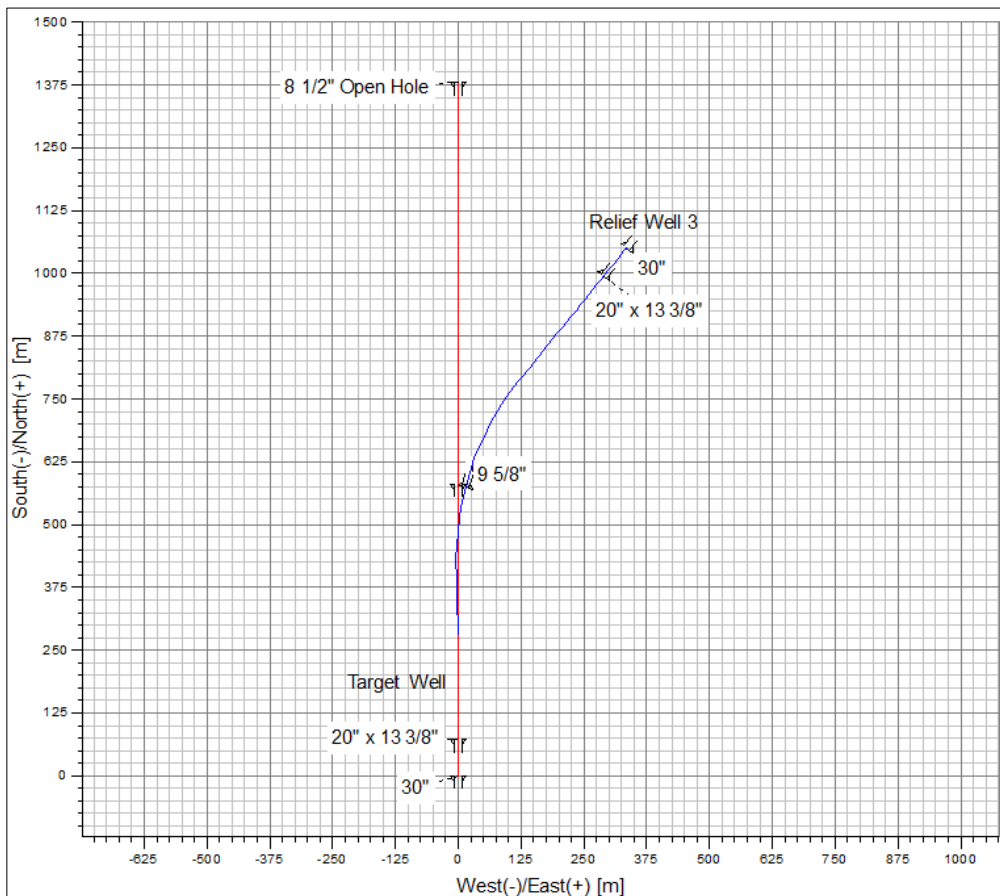


Figure 8.14: Relief well 3 plan view

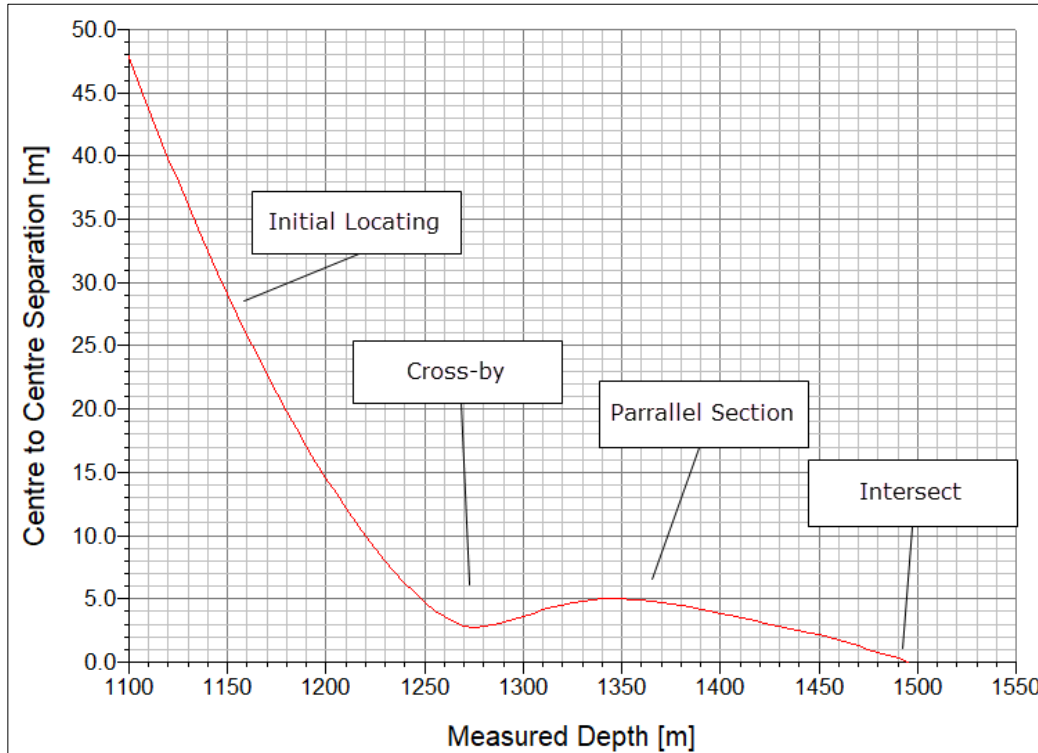


Figure 8.15: Relief well 3 ladder view

8.7 Ranging and Positional Uncertainty Analysis

The first ranging run and initial locating must be chosen to prevent an accidental premature intersect and ensure that the relief well does not drill past the target well without detecting it. After the initial locating, ranging will be used to steer towards the intersect.

The surveying methodology and assumptions used for the model well in this study are:

- Anti-collision modelling using “closest approach 3D” and elliptical conic error surface
- A 2.796 sigma confidence level
- A combined 3 m surface positional uncertainty between the blowout and relief well
- Surveying methodology consisting of MWD+IFR+MS.
- 40 m detection range of ranging tool.

By plotting the ellipses of uncertainty in the plan view, an estimate of the combined uncertainty for the relief well and target well can be obtained. As seen in Figure 8.16 to Figure 8.18, with both relief well and target well located at the opposite sides of their ellipses, the maximum separation at the cross-by is less than the estimated 40 m detection range of the ranging tool. That is, the likelihood of the relief well drilling past the target well without detecting it is low.

This is a conservative analysis. There are several methods for positional uncertainty analysis and ranging strategies that would be used in the event of an actual blowout which may significantly improve the ability to locate the target well. The purpose for a contingency plan is simply to demonstrate that likelihood of the relief well not finding the target well is low.

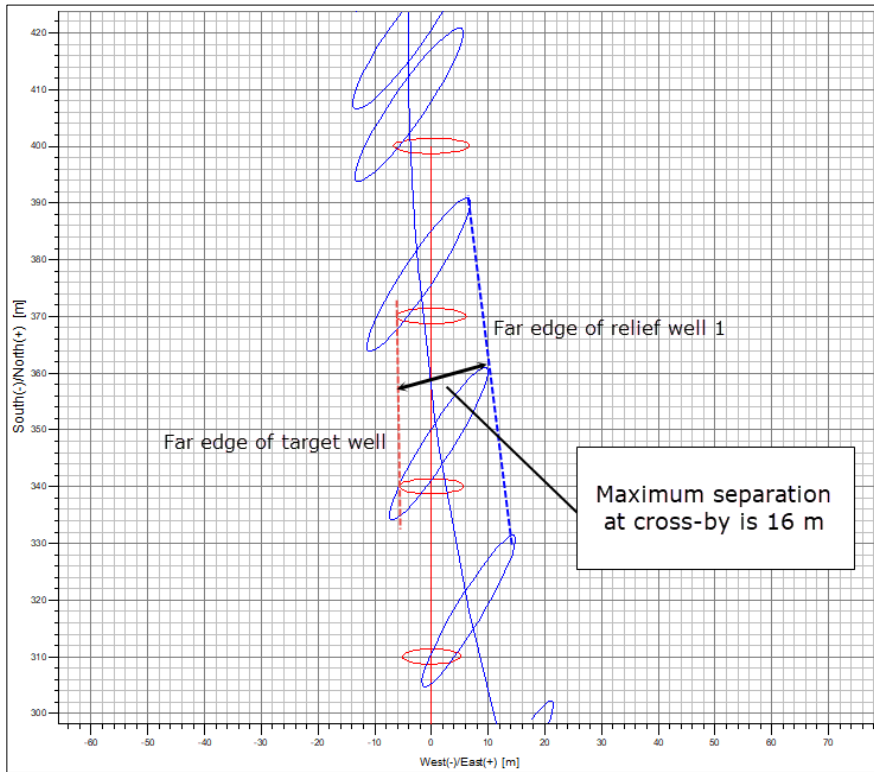


Figure 8.16: Maximum separation at cross-by depth for relief well 1

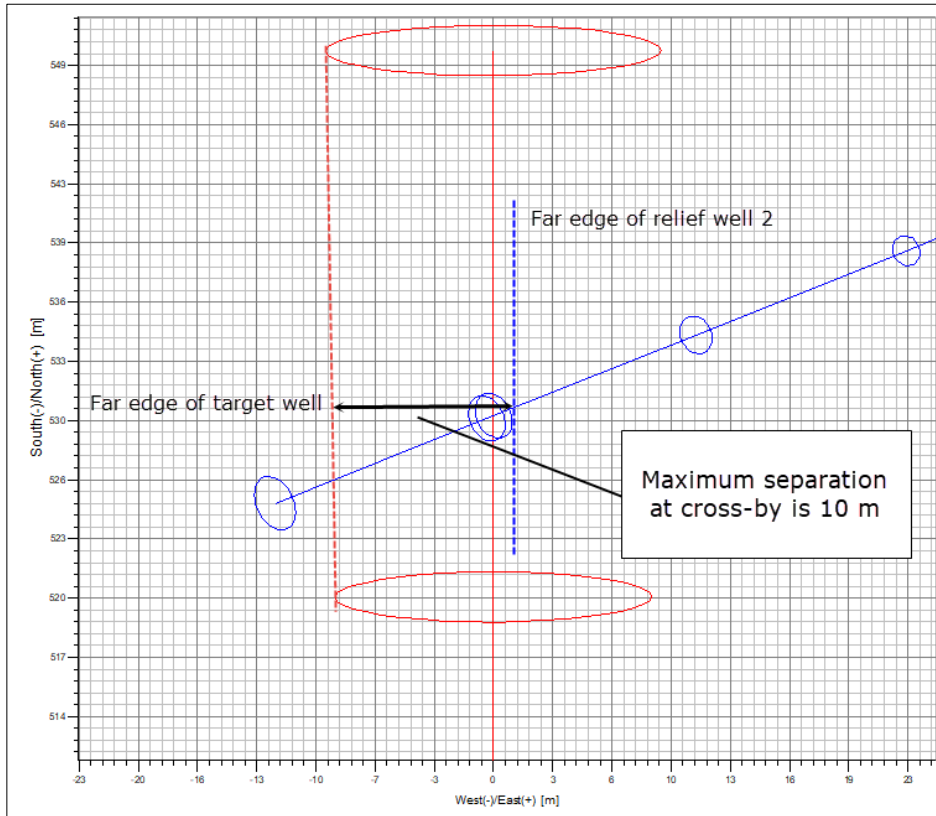


Figure 8.17: Maximum separation at cross-by depth for relief well 2

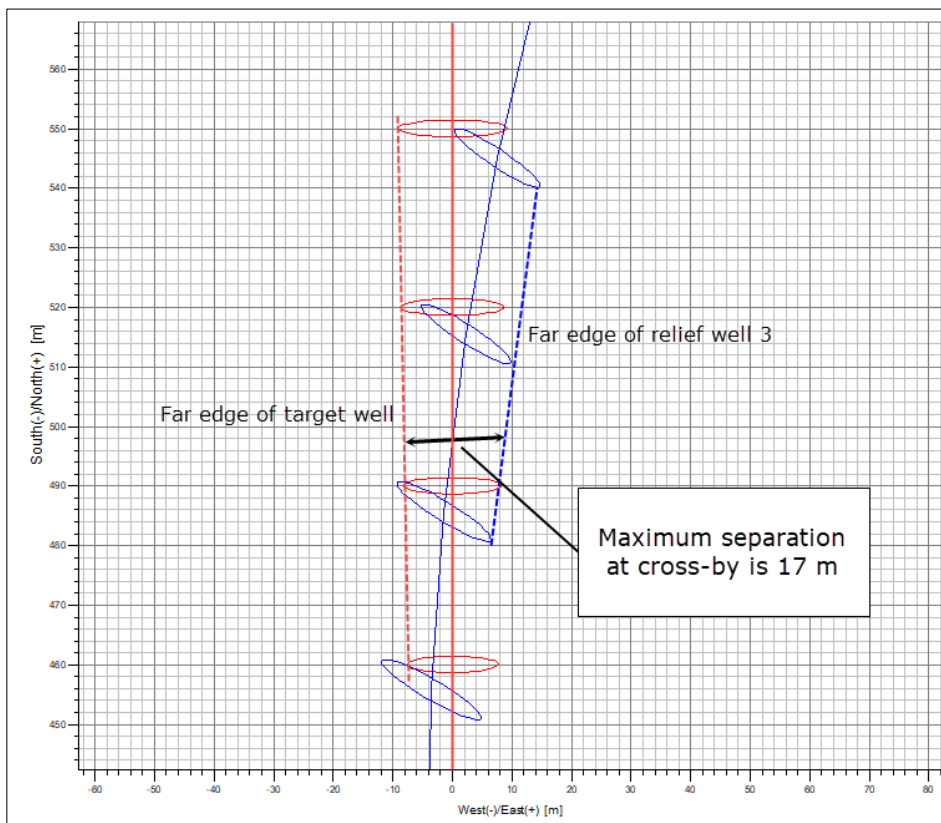


Figure 8.18: Maximum separation at cross-by depth for relief well 3

8.8 Dynamic Kill Method

The dynamic-kill technique has been established as the preferred method for killing a blowout after intersecting with a relief well. The dynamic kill uses the increased hydrostatic head of a mixture of gas, oil, and mud in the blowing well together with the frictional pressure drop to increase the bottomhole pressure (BHP) and consequently stop the flow from the reservoir (Blount and Soeiinah 1981).

For a shallow reservoir, achieving the hydrostatic and frictional pressure during a dynamic kill is challenging. This, in combination with a prolific reservoir, large hole size, and high GOR, may lead to demanding kill operations.

For very prolific/hard-to-kill blowouts, the pump rate necessary to be delivered at the intersection point can be beyond what can normally be pumped from a single relief well rig. This will trigger options to optimize the capacity of the relief well or planning two or more relief wells.

Based on the defined scenarios in this study, the well could be killed with a single relief well. However, full wellbore displacement could not be established since the relief well intersects the target well approximately 1200 m MD off-bottom. Based on additional simulations, intersecting the target well at a shallower depth does not significantly change the kill requirements. Detailed dynamic kill analysis is presented in Appendix A.5 Dynamic kill requirements. It should be noted that assuming higher pore pressures or a larger open hole could result in kill requirements that exceed the capabilities of a single relief well.

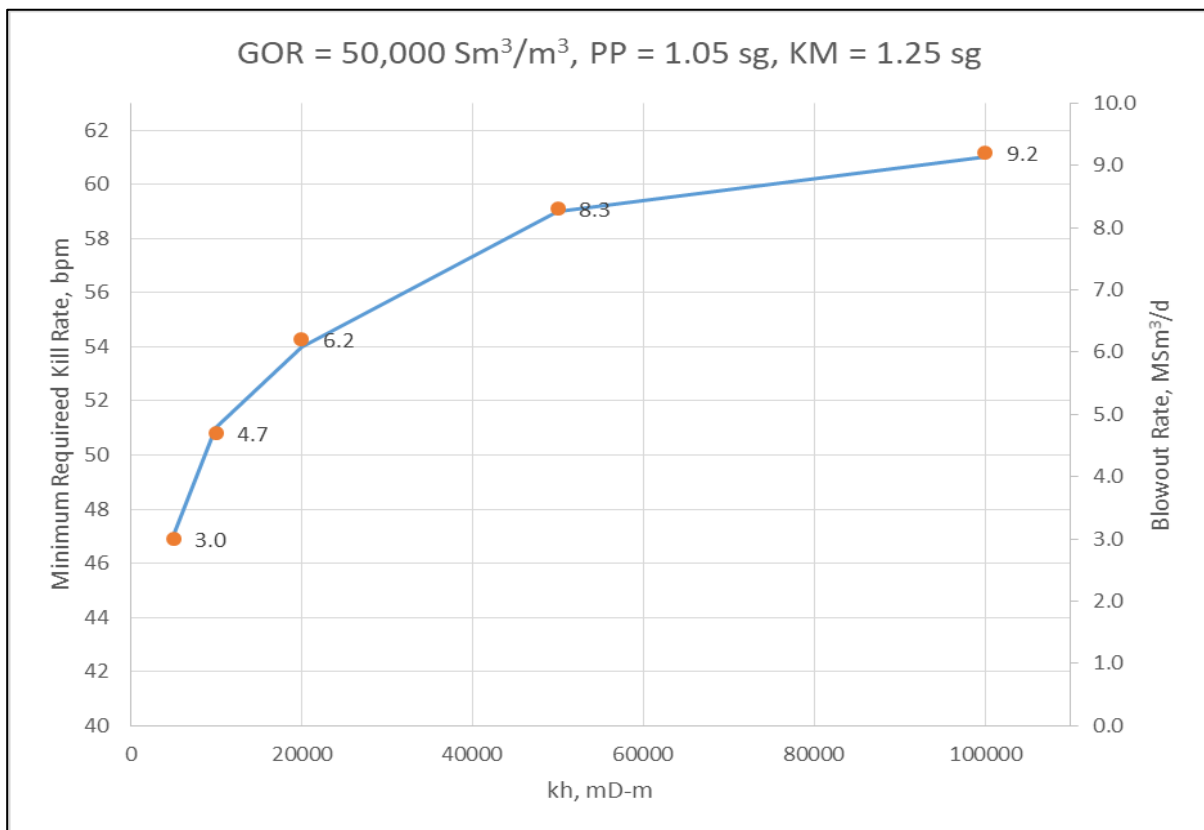


Figure 8.19: Minimum required kill rate for the defined scenarios

8.8.1 Challenges with Multiple Relief Wells

A kill operation with two relief wells is recognized as being a challenging operation. Two or more drilling rigs for the specific operation must be mobilized, each drilling a relief well from an approved surface location. Furthermore, both relief wells will have to successfully locate and intersect the blowing wellbore. The blowing well must be killed through a simultaneous coordinated kill operation. Complex operations are in general also more time consuming, which in the event of a blowout will increase the total volume of oil and gas released to the environment. There is also no actual experience in the industry with drilling multiple relief wells in an offshore environment.

Because of the limited experience and the potential challenges, a permit to drill a well that may require two or more relief wells would be difficult to achieve. In some cases, the planned well design can be revised to lower the pumping requirements within the capability of a single relief well. Some examples include setting the last casing string deeper to allow a deeper relief-well intersect, using a smaller diameter casing to increase friction during the dynamic kill, setting additional casing strings to isolate sands, or drilling a smaller hole size to lower the flow potential of potentially flowing sand(s). In these cases, the planned well design is driven by dynamic kill requirements. An example of this is the Chevron Wheatstone project (Upchurch et al. 2015), where additional casing strings were set to allow a deeper relief well intersect and increase friction pressure in the blowout well during a dynamic kill.

Setting additional casing strings may come at a high cost as it requires rig time, introduces additional risk, and could affect production rates. That is, wells designed with smaller casing and, as a result, smaller production tubing will flow at lower rates per well than with larger tubing sizes (Hartman et al. 2003). This may have significant impact on the overall field development cost by increasing the number of wells required to produce at a given rate. The cost increase of a standard well design can be on the order of USD 50 million per well higher than for a big-bore well.

8.9 Relief Well Injection Spool

The Relief Well Injection Spool (RWIS) provided by Trendsetter Inc. is a device that can greatly increase the pumping capacity of a single relief well. The RWIS is installed on the relief-well wellhead beneath the BOP to provide additional flow connections into the wellbore. Using high-pressure flex lines, the inlets enable pumping units from separate floating vessels, in addition to the relief well rig, to deliver a high-rate dynamic kill through a single relief well.

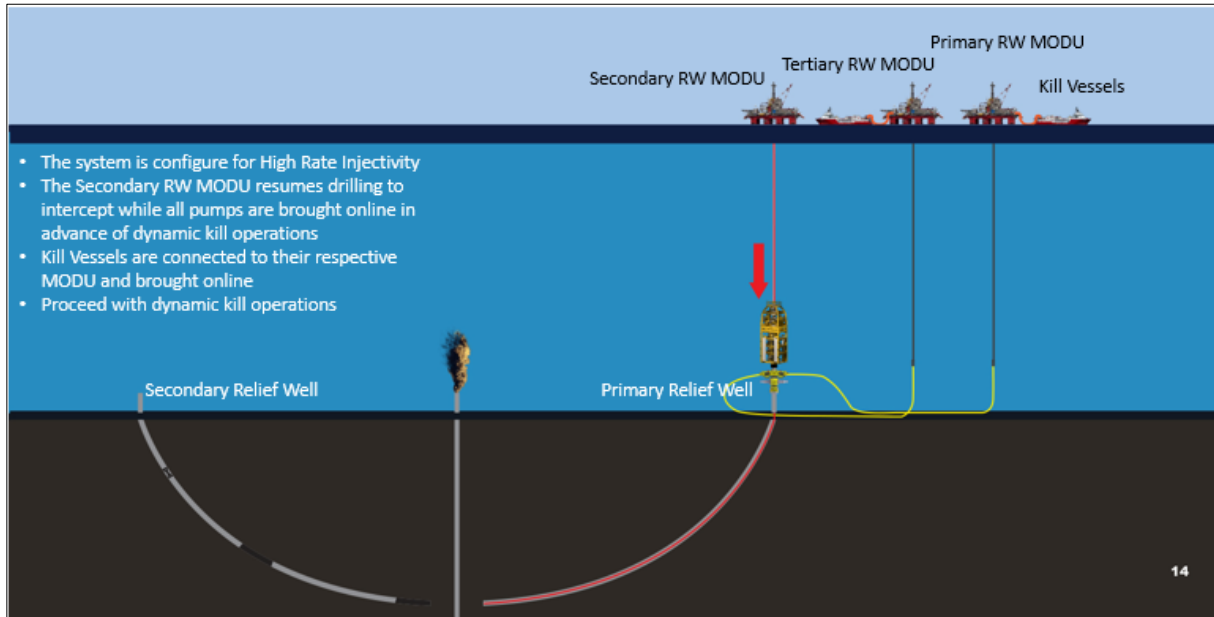


Figure 8.20: Relief well injection spool hardware configuration

The RWIS is designed with only components that are already used and proven in deepwater environments. The design is also relatively lightweight and modular, which allows the RWIS to be transported on land, offshore, and by air freight.

In the event of a blowout, relief-well drilling can commence immediately as soon as a suitable rig has been identified and mobilized. While the relief well is drilling, the RWIS will be transported to the location. A high-rate dynamic kill is achieved by simultaneously pumping down the relief-well rig and the support vessel(s) through the RWIS.

Reference List

- Aadnøy, B.S. 2010. Modern Well design – Second Edition. CRC press – Taylor and Francis Group. ISBN 978-0-415-88467-9.
- Aadnøy, B.S. & Looyeh, R. 2010. Petroleum Rock Mechanics – Drilling operations and Well design. Elsevier Gulf Publishing Company. ISBN 978-0-12-385546-6.
- Amadei, B. and Stephansson, O. 1997. Rock Stress and its Measurement. *Springer Science and Business Media* ISBN 0412447002.
- Asher, B. 2012. Brazil Berates Chevron for Frade Oil Spill, But Production to Restart., July 19, 2012. [http://www.rigzone.com/news/oil_gas/a/119441/Brazil Berates Chevron for Frade Oil Spill But Production to Restart](http://www.rigzone.com/news/oil_gas/a/119441/Brazil_Berates_Chevron_for_Frade_Oil_Spill_But_Production_to_Restart)
- Bjørlykke, K. & Jahren, J. 2015. Sandstones and Sandstone Reservoirs. In: *Bjørlykke, K., Jahren, J., Petroleum Geoscience. From Sedimentary Environments to Rock Physics - Second Edition*, 119-149.
- Blomberg, A. E. A., et. al 2017. Automatic Detection of Marine Gas Seeps Using an Interferometric Sidescan Sonar». *IEEE Journal of Oceanic Engineering*. Vol. 42, NO 3, July.
- Blount, E.M. and Soeiinah, E. 1981. Dynamic Kill: Controlling Wild Wells a New Way. *World Oil* (10), 109-126.
- Brown, E.T and Hoek, E. 1978. Trends in Relationships between measured In-Situ Stresses and Depth. *Int. J. Rock Mech. Min. Sci. & Geomech. Abstr.* Vol 15, pp. 2011 – 205.
- Clemens, T., Kienberger, G., Persaud, M., Suri, A., Sharma, M. M., Boschi, M. & Øverland, A. M. 2017. Optimizing Water-Injection Design in a Shallow Offshore Reservoir. *SPE Production and Operations*. SPE 180143.
- Davison, J.M., van den Bogert, P., Schutjens, Ita, J. and Fokker, P. 2013. Geomechanical Technology for Seal Integrity Analysis: The Three-Step Approach. Paper IPTC 17057 presented at the International Petroleum Technology Conference, Beijing, China 26 – 28 March 2013.
- Eidvin, T and Overland, J.A. 2009. Faulty geology Halts project. Norwegian Petroleum Directorate Report: <http://www.npd.no/en/publications/norwegian-continental-shelf/no2-20091/faulty-geology-halts-project>
- England, P. & Molnar, P. 1990. Surface uplift, uplift of rocks, and exhumation of rocks. *Geology* 18, 1173-1177.
- ERCB Staff Review and Analysis (2010). Total E&P Canada Ltd. Surface steam release of May 18, 2006 Joslyn Creek SAGD Thermal Operation. Energy Resources Conservation Board, Feb. 11, 2010.
- Evensen, K., Sangesland, S., Johansen, S.E. et al. 2014. Relief Well Drilling Using Surface Seismic While Drilling. Presented at the IADC/SPE Drilling Conference and Exhibition, Fort Worth, Texas, 4-6 March. SPE-167994-MS
- Faleide, J., I., Bjørlykke, K. & Gabrielsen, R., H. 2010. Geology of the Norwegian Continental Shelf. *Petroleum Geoscience: From Sedimentary Environment to Rock Physics*, 467-499.
- Fjeldskaar, W. & Amantov, A. 2016. Om årsakene til erosjonen i Barentshavet – del 2.
- Gasparoni, F., et.al. 2016. Clean Sea – Underwater Robotic Technology for Environmental and Asset Integrity Monitoring in Deep and Ultra-Deep Water. SPE-179361-MS.
- Gou, Q., Geehan, T. and Ovalle, A. 2007. Increased Assurance of Drill Cuttings Reinjection: Challenges, Recent Advances, and Case Studies. *SPE Drilling and Completion*, June 2007.
- Gradstein, F., M., Ogg, J., G., Schmitz, M. & Ogg, G. 2012. The Geologic Time Scale 2012. *Elsevier*.
- Hartmann, R., Møllerstad, H., Bysveen, J., and Rygg, O.B. 2003. Blowout Contingency for Deep Water High Rate Subsea Gas Wells. Presented at the IADC International Deepwater Drilling Conference, Rio de Janeiro, Brazil, 12-13 November
- Henriksen, E., Bjørnseth, H. M. & Heide, T. K. 2011. Uplift and erosion of the greater Barents Sea: impact on prospectivity and petroleum systems. *Artic Petroleum Geology, geological Society, Chapter 17*, 271-281.
- Hepsø, V., et.al. 2012. Integrated Environmental Monitoring in Daily Operations. SPE 150054, 2012.
- Japsen, P. & Chalmers, J. A. 2000. Neogene uplift and tectonics around the North Atlantic: Overview. *Elsevier: Global and Planetary Change 24 (2000)* 165-173.
- Keck, R.G. 2002. Drill Cuttings Injection: A Review of Major Operations and Technical issues. By SPE 77553 presented at the 2002 SPE Annual Tech. Conf. and Exhibition, San Antonio, TX, 29 Sept. 2 Oct.
- Koldgaard, E. P. 2012. Leakage Detection Utilizing Active Acoustic Systems. OTC 23709.

- Lander, R. H. & Walderhaug, O. 1999. Predicting porosity through simulating sandstone compaction and quartz cementation *AAPG bulletin* 83 (3), 433-449.
- Landrø, M., P. Rodriguez, T. Røste and M. Thompson, 2013. Using permanent arrays for shallow monitoring, Second EAGE Workshop on Permanent Reservoir Monitoring, Th-01-02, Expanded Abstracts.
- Marion, D. P. 1990. Acoustical, mechanical, and transport properties of sediments and granular materials. *Ph.D. thesis, Stanford University, Department of Geophysics.*
- Mondol, N. H., Bjørlykke, K., Jahren, J. & Høeg, K. 2007. Experimental mechanical compaction of clay mineral aggregates – Changes in physical properties of mud- stones during burial. *Marine and Petroleum Geology* 24(5), 289–311
- NORSOK D-010, *Well Integrity in Drilling and Well Operations*, Rev. 4. June 2013. Lysaker, Norway; Standards Norway, 36.
- NPD 2016. Factpages, Norwegian Petroleum Directorate. Accessed 2016-09-01.
- Nøttvedt, A.(ed.) 2000. Dynamics of the Norwegian Margin. *GSL Special Publications*, SP 167. ISBN 1-86239-056-8.
- PSA 2017. Information over leak-off-pressures in the Barents Sea area compiled from NPD website
- Poedjono, B. Active Acoustic Ranging. <http://www.iscwsa.net/download/f56b650c-b648-11e6-a0ee-e117362139ff/>
- Sorkhabi, R. 2015. Ph.D, Fracture, Fracture Everywhere - Part II, How and why do fractures occur in rocks? . *GEO ExPro*, Vol. 11, No. 3.
- Storvoll, V., Bjørlykke, K. & Mondol, N. H. 2005. Velocity-depth trends in Mesozoic and Cenozoic sediments from the Norwegian Shelf. *AAPG Bulletin*, 89, 359-381
- Ralowski, M. 2016. Design of a hypothetical relief well for a shallow reservoir, possible challenges. University of Stavanger Master Thesis. https://brage.bibsys.no/xmlui/bitstream/handle/11250/2409333/Ra%C5%82owski_Miko%C5%82aj.pdf
- Upchurch, E.R., Falkner, S., House, A., et al. 2015. Blowout Prevention and Relief Well Planning for the Wheatstone Big-Bore Gas Well Project. Presented at the Annual Technical Conference and Exhibition, Houston, 28-30 September. SPE-174890-MS.
- Valko, P. 2008. Personal communication.
- Valko, P. and Economides, M.J. 1995. Hydraulic Fracturing Mechanics. John Wiley and Sons, 1995, ISBN 0 471 95664 3.
- West, C.L., Kuckes, A.F., and Ritch, H.J. 1983. Successful ELREC Logging for Casing Proximity in an Offshore Louisiana Blowout. Presented at the SPE Annual Technical Conference and Exhibition, 5-8 October, San Francisco, SPE-11996-MS
- Wright, J.W., Ely, J.W. and Flak, L. Part 1-Strategy and Planning: Emergency Management Tools such as Prior Remedial Contingency Planning and a Designated Task Force Help Those Responsible for Emergencies Perform Critical Tasks Confidently, Effectively and Efficiently. <http://www.jwco.com/technical-literature/tech.htm>
- Ybray, D., Galiyeva, G. and Ibragimov, F. 2011. Caprock Integrity Study in Kashagan. Paper presented at the 10th Offshore Mediterranean Conference and Exhibition, Ravanny, Italy, March 23-25, 2011.
- Zhang, Z. Wang, J. and Yale, D.P. 2012. Overburden Stability.
- Øfjord, G. D. 2013. Injection incidents in the NCS and Regulation changes. Force seminar on Injection Safety, December 4th

Further Reading

- ANDERSEN, M. S., NIELSEN, T., SØRENSEN, A. B., BOLDREEL, L. O. & KUIJPERS, A. 2000. Cenozoic sediment distribution and tectonic movements in the Faroe region. *Global Planet. Change*.
- ARCHIE, G. E. 1941. The Electrical Resistivity Log as an Aid in Determining Some Reservoir Characteristics Dallas Meeting.
- AVSETH, P. 2015. Explorational Rock Physics: The link between Geological Processes and Geophysical Observables. In: Bjørlykke, K., Jahren, J., *Petroleum Geoscience. From Sedimentary Environments to Rock Physics - Second Edition*, 455-489.
- AVSETH, P. & DRÆGE, A. 2011. Memory of rocks - how burial history controls present day seismic properties. Example from Troll East, North Sea. In: 2011 SEG Annual Meeting. Society of Exploration Geophysics.
- AVSETH, P. & LEHOCKI, I. 2016. Combining burial history and rock-physics modeling to constrain AVO analysis during exploration. *The leading edge*, June 2016, 528-534.
- AVSETH, P., MUKERJI, T. & MAVKO, G. 2005. Quantitative seismic interpretation: Applying rock physics tools to reduce interpretation risk. Cambridge University Press.
- AVSETH, P. & VEGGELAND, T. 2015. Seismic screening of rock stiffness and fluid softening using rock physics attributes. *The Leading Edge* 33 (4), SAE85-SAE93.
- AVSETH, P., VEGGELAND, T. & LEHOCKI, I. 2014. Combined burial history and rock physics modeling of quartz-rich sandstones - Norwegian shelf demonstrations. SEG Technical Program Expanded Abstracts 2014. Society of Explorational Geophysics, 2809-2813.
- BACHRACH, R. & A. NUR, 1998, High-resolution shallow-seismic experiments in sand, Part I: Water table, fluid flow, and saturation, *Geophysics*, **63**, 1225-1233.
- BAIG, I., FALEIDE, J., I., JAHREN, J. & MONDOL, N. H. 2016. Cenozoic exhumation on the southwestern Barents Shelf: Estimates and uncertainties constrained from compaction and thermal maturity. *Marine and Petroleum Geology* 73, 105-130.
- BATZLE, M. & WANG, Z. 1992. Seismic properties of pore fluids. *Geophysics* 57 (11), 1396-1408.
- BHUYIAN, A. H., M. LANDRØ & S. E. JOHANSEN, 2012, 3D CSEM modeling and time-lapse sensitivity analysis for subsurface CO₂ storage, *Geophysics*, **77**, E343-E355
- BREVIK, I., CALLEJON, A., KAHN, P., JANAK, P. & EBRON, D. 2011. Rock physicists step out of the well location, meet geophysicists and geologists to add value in exploration analysis. *The Leading Edge* 30 (12), 1382-1391.
- BRIGAUD, F., VASSEUR, G. & CAILLET, G. 1992. Thermal state in the north Viking Graben (North Sea) determined from oil exploration well data. *GEOPHYSICS*, VOL. 57, NO. 1, 69-88.
- BULAT, J. & STOKER, S. J. 1987. Uplift determination from interval velocity studies, UK, southern North Sea. Brooks, J., Glennie, K.W. (Eds.), *Petroleum Geology of North West Europe*. Graham and Trotman, London, 293-305.
- BUSSAT, S., 2015, Using ambient noise for real-time (hourly) overburden monitoring, Expanded Abstract, Third EAGE Workshop on Permanent Reservoir Monitoring, Oslo, Th A02.
- CANNON, S. 2016. *Petrophysics: A Practical guide*. West Sussex, John Wiley & Sons, Ltd.
- CASTAGNA, J. P. & SMITH, S. W. 1994. Comparison of AVO indicators: A modeling study. *Geophysics* 59 (12), 1849-1855.
- CASTANGA, J. P. & SMITH, S. W. 1994. Comparison of AVO indicators: A modeling study. *Geophysics* 59 (12), 1849-1855.
- CGG HRS-9/R2.
- CHALMERS, J. A. 2000. Offshore evidence for Neogene uplift in central West Greenland. *Global Planet. Change* 24, 311-318.
- CLAUSEN, O. R., NIELSEN, O. B., HUUSE, M. & MICHELSEN, O. 2000. Geological indications for Palaeogene uplift in the eastern North Sea Basin. *Global Planet. Change* 724, 175-187.
- DALLAND, A., WORSLEY, D. & OFSTAD, K. 1988. A lithostratigraphic scheme for the Mesozoic and Cenozoic succession offshore mid- and northern Norway. *NPD-Bulletin No. 4*, 65.
- DIX, C. H. 1955. Seismic velocities from surface measurements. *Geophysics* 20 (1), 68-86.
- DONG H., NGUYEN T., D., & DUFFAUT K., 2013, Estimation of seabed shear-wave velocity profiles using shear-wave source data, *J. Acoust. Soc. Am.*, **134**, 176-184
- DORÉ, A. G. 1992. The base Tertiary surface of southern Norway and the northern North Sea. *Nor. Geol. Tidsskr.* 72, 259-265.

- DORÉ, A. G. & JENSEN, L., N. 1996. The impact of late Cenozoic uplift and erosion on hydrocarbon exploration. *Global and Planetary Change* 321. Special Issue: Impact of glaciations on basin evolution: data and models from the Norwegian Margin and adjacent areas.
- DRÆGE, A., DUFFAUT, K., WIİK, T. & HOKSTAD, K. 2015. Linking rock physics and basin history - Filling gaps between wells in frontier basins. *The Leading Edge* 33 (3), 240-246.
- DVORKIN, J. & NUR, A. 1996. Elasticity of high-porosity sandstones: Theory for two North Sea data sets. *Geophysics* 61 (59), 1363-1370.
- DVORKIN, J., NUR, A. & YIN, H. 1994. Effective properties of cemented granular materials. *Mechanics of materials* 18 (4), 351-366.
- EVANS, D., MCGIVERON, S., MCNEILL, A. E., HARRISON, Z. H., ØSTMO, S. R. & WILD, J. B. L. 2000. Plio-Pleistocene deposits on the mid-Norwegian margin and their implications for late Cenozoic uplift of the Norwegian mainland. *Global Planet. Change* 24, 233-237
- FIEDLER, A. & FALEIDE, J. I. 1996. Cenozoic sedimentation along the southwestern Barents Sea margin in relation to uplift and erosion of the shelf. *Glob. Planet. Change*, 12, 75–93
- GALLAGHER, K. 2012. Uplift, denudation, and their causes and constraints over geological timescales. *Principles of Geologic Analysis*, 10, 30.
- GASSMANN, F. 1951. Über die elastizität poröser medien. *Vierteljahrsschrift der Naturforschenden Gesellschaft in Zurich* 96, 1-23.
- GATEMANN, J. H. M. 2016. Relationship between burial history and seismic signatures in the Horda Platform area, Norwegian North Sea. Master Thesis, Department of Geosciences, University of Oslo.
- GLØRSTAD-CLARK, E., FALEIDE, J. I., LUNDSCHIENB, B. A. & NYSTUENA, J. P. 2010. Triassic seismic sequence stratigraphy and paleogeography of the western Barents Sea area. *Marine and Petroleum Geology* 24 (7), 1448–1475.
- GREEN, P. F. 1989. Thermal and tectonic history of the East Midlands shelf onshore UK and surrounding regions assessed by apatite fission track analysis. *J. Geol. Soc. London* 146, 755-774.
- HAAVIK, K. E. & M. LANDRØ, 2015, Variable source depth acquisition for improved marine broadband seismic data, *Geophysics*, **80**, A69-A73.
- HANSEN, K. 2000. Tracking thermal history in East Greenland: an overview. *Global Planet. Change* 24, 303-309.
- HANSEN, S. 1996. Quantification of net uplift and erosion on the Norwegian Shelf south of 66°N from sonic transit times of shale. *Norsk Geologisk Tidsskrift*, Vol. 76, 245-152.
- HERMANRUD, C., WENSAAS, L., TEIGE, G. M. G., BOLAS, H. M. N., HANSEN, S. & VIK, E. 1998. Shale porosities from well logs on Haltenbanken (offshore mid-Norway) show no influence of overpressuring. In: LAW, B. E., ULMISHEK, G. F. & SLAVIN, V. I. (eds.) *Abnormal pressures in hydrocarbon environments: AAPG Bulletin*.
- JAPSEN, P. 2000. Investigation of multi-phase erosion using reconstructed shale trends based on sonic data. *Sole Pit axis, North Sea. Global Planet. Change* 24, 189-210.
- JENSEN, L. N. & SCHMIDT, B. J. 1992. Late Tertiary uplift and erosion in the Skagerrak area; magnitude and consequences. *Nor. Geol. Tidsskr.* 72, 275-279.
- JOHANSEN, S. E. & GABRIELSEN, P. T. 2015. Interpretation of Marine CSEM and Marine MT Data for Hydrocarbon Prospecting. In: Bjørlykke, K., Jahren, J., *Petroleum Geoscience. From Sedimentary Environments to Rock Physics - Second Edition*, 515-544.
- JOHNSON, C. & GALLAGHER, K. 2000. A preliminary Mesozoic and Cenozoic denudation history of the North East Greenland onshore margin. *Global Planet. Change* 24, 261-274.
- JORDT, H., FALEIDE, J. I., BJØRLYKKE, K. & IBRAHIM, M. T. 1995. Cenozoic sequence stratigraphy of the central and northern North Sea Basin: tectonic development, sediment distribution and provenance areas. *Mar. Pet. Geol.* 12, 845-879.
- KENNETT, B. 1979. Theoretical reflection seismograms for elastic media. *Geophysical Prospecting*, 27, 301-321.
- KHUTORSKOI, M. D., VISKUNOVA, K. G., PODGORNYYKH, L. V. & AKHMEDZYANOV, V. R. 2008. A temperature model of the crust beneath the Barents Sea: Investigations along geotraverses *Geotectonics* 42 (2), 125-136.
- LABERG, J. S., ANDREASSEN, K. & VORREN, T. O. 2012. Late cenozoic erosion of the high-latitude southwestern barents sea shelf revisited. *Bull. Geol. Soc. Am.*, 124, 77–88.
- LANDRØ, M., O.A. SOLHEIM, E. HILDE, B. O. EKREN & L.K. STRØNEN, 1999, The Gullfaks 4D seismic study, *Petroleum Geoscience*, **5**, 213-226.
- LANDRØ, M., 2001, Discrimination between pressure and fluid saturation changes from time lapse seismic data, *Geophysics*, **66**, 836-844.

- LI, Y., DOWNTON, J. & XU, Y. 2014. AVO Modeling in Seismic Processing and Interpretation II. Methodologies. Recorder, 29.
- LIDMAR-BERGSTRØM, K., OLLIER, C. D. & SULEBAK, J. C. 2000. Landforms and uplift history of southern Norway. Global Planet. Change 24, 211-231.
- MARCUSSEN, Ø., MAAST, T. E., MONDOL, N., H., JAHREN, J. & BJØRLYKKE, K. 2009. Changes in physical properties of a reservoir sandstone as a function of burial depth – The Eive Formation, northern North Sea. Marine and Petroleum geology (2010) 1-11.
- MATHIESEN, A., BIDSTRUP, T. & CHRISTIANSEN, F. G. 2000. Denudation and uplift history of the Jameson Land Basin, East Greenland — constrained from previous maturity and new apatite fission track data. Global Planet. Change B 24, 275-301.
- MATHWORKS R2015a. Matlab. 1994-2016: The MathWorks, Inc.
- MAVKO, G. 1987. In: Bourbie et al 1987, Acoustics of porous Media, Gulf Publishing Co.
- MEUNIER, J., F. HUGUET, & P. MEYNIER, 2001, Reservoir monitoring using permanent sources and vertical receiver antennae: The Cere-la-Ronde case study, The Leading Edge, **20**, 622-629
- MIENERT, J., L. AMUNDSEN & M. LANDRØ, 2015, Gas Hydrates, Part VII, GeoExpro, **12**, April, 46-48.
- MINDLIN, R. D. 1949. Compliance of Elastic Bodies in Contact. Journal of Applied Mechanics 16, 259–268.
- MORK, M. B. E. 1999. Compositional variations and provenance of Triassic sandstones from the Barents Shelf. Journal of Sedimentary Research 69 (3), 690-710.
- NPD 2014. Lithostratigraphic summary for the North Sea.
- NYLAND, B., JENSEN, L., N., SKAGEN, J., SKARPNES, O. & VORREN, T. 1992. Tertiary uplift and erosion in the Barents Sea: magnitude, timing and consequences. Struct. Tect. Model. its Appl. Petrol. Geol., 153–162.
- OHM, S. E., KARLSEN, D. A. & AUSTIN, T. 2008. Geochemically driven exploration models in uplifted areas: Examples from the Norwegian Barents Sea. AAPG bulletin 92 (9), 1191-1223.
- QUEISSER, M. & S. SINGH, 2010, Time lapse seismic monitoring of CO2 sequestration at Sleipner using time domain 2D full waveform inversion, 80th Annual International Meeting, SEG, Expanded abstracts, 2875-2879.
- RAKNES, E. B., & B. ARNTSEN, 2015, A numerical study of 3D elastic time-lapse full-waveform inversion using multicomponent seismic data, Geophysics, **80**, R303-R315.
- RAKNES, E. B., W. WEIBULL & B. ARNTSEN 2015, Seismic imaging of the carbon dioxide gas cloud at Sleipner using 3D elastic time-lapse full waveform inversion, International Journal of Greenhouse Gas Control, 8, 42: 26-45.
- RICHARDSEN, G., VORREN, T. & TØRUDBAKKEN, B. O. 1993. Post-Early Cretaceous uplift and erosion in the southern Barents Sea: a discussion based on analysis of seismic interval velocities. Norsk Geologisk Tidsskrift. Vol. 73, 3-20.
- RIDER, M. 2000. The geological interpretation of well logs. Rider-french Consulting.
- RIIS, F. 1996. Quantification of Cenozoic vertical movements of Scandinavia by correlation of morphological surfaces with offshore data. Global Planet. Change 12, 331-357.
- ROHRMAN, M., VAN DER BEEK, P., ANDRIESSEN, P. & CLOETINGH, S. 1995. Meso-Cenozoic morphotectonic evolution of southern Norway: Neogene domal uplift inferred from apatite fission track thermochronology. Tectonics, 700-714.
- ROSS, C. P. & KINMAN, D. L. 1995. Nonbright-spot AVO: Two examples. Geophysics 60 (5), 1398–1408.
- ROSS, C. P. & KINMAN, D. L. 1995b. Nonbright-spot AVO: Two examples. Geophysics 60 (5), 1398-1408.
- ROUTH, P., G. PALACHARLA, I. CHIKICHEW & S. LAZARATOS, 2012, Full wavefield inversion of time-lapse data for improved imaging and reservoir characterization, SEG Expanded Abstracts.
- RUTHERFORD, S. R. & WILLIAMS, R. H. 1989. Amplitude-versus-offset variations in gas sands. Geophysics 54 (6), 680–688.
- SAWAZAKI, K. & R. SNIEDER, 2013, Time-lapse changes of P- and S-wave velocities and shear wave splitting in the first year after the 2011 Tohoku earthquake, Japan: Shallow subsurface, Geophys. J. Int., **193**, 238-251.
- SCHLUMBERGER 2015.
- SHUEY, R. 1985. A simplification of the Zoeppritz equations. Geophysics 50 (4), 609–614.
- STUEVOLD, L. M. & ELDHOLM, O. 1996. Cenozoic uplift of Fennoscandia inferred from a study of the mid-Norwegian margin. Global Planet. Change 12, 359-389.

- THYBERG, B., JAHREN, J., WINJE, T., BJØRLYKKE, K. & FALEIDE, J. I. 2009. From mud to shale: rock stiffening by micro-quartz cementation. *First Break*, Vol. 27, 53-59.
- VÅGNES, E., FALEIDE, J. I. & GUDLAUGSSON, S., T. 1992. Glacial erosion and tectonic uplift in the Barents Sea. *Norsk Geologisk Tidsskrift* 72 (3), 333-338.
- WALDERHAUG, H. P. 2012. Petrography, diagenesis and reservoir quality of the Triassic Fruholmen, Snadd and Kobbe formations, southern Barents Sea. Master Thesis, Norwegian University of Science and Technology.
- WALDERHAUG, O. 1996. Kinetic modeling of quartz cementation and porosity loss in deeply buried sandstone reservoirs. *AAPG bulletin* 80 (5), 731-745.
- ZHANG, F., C. JUHLIN, M. IVANDIC, & S. LUTH, 2013, Application of full waveform inversion to monitor CO2 injection: Modeling and a real data example from the Ketzin site, Germany, *Geophysical Prospecting*, **61**, 284-299.
- ØDEGAARD, E. & AVSETH, P. 2004. Well log and seismic data analysis using rock physics templates. *First Break* 22 (10), 37-43.

A. Blowout and Kill Simulations

A.1 Background information and input data – reservoir fluid

Some key fluid data after fluid characterization in PVTsim NOVA using the SRK-Peneloux equation of state is shown in Table A.1. All properties at standard conditions are based on a single stage flash.

Table A.1: Key fluid data after characterization

Fluid data	Gas
GOR, Sm ³ /Sm ³ (single stage flash)	50 000
Gas density at standard conditions, kg/Sm ³	0.861
Oil density at standard conditions, kg/Sm ³	782
Saturation point pressure, 16 °C), bar	212
Gas viscosity at res. cond. (73 bar, 16 °C), cP	0.0135
Gas compressibility at res. Cond. (73 bar, 16 °C), -	0.8334

A.2 Background information and input data - reservoir data

The key properties of the producing sand for the base case evaluated is presented below.

Table A.2: Key reservoir data

Hole section	8½"
Top reservoir depth, m TVD	710
Reservoir temperature, °C	16
Reservoir pressure, bar	73
Reservoir pressure, sg	1.05
Expected net pay, m TVD	20
Avg. horizontal permeability, k, mD	500
Reservoir radius, m	1000

A.3 Scenarios

All blowout scenarios have been simulated with exit point to seabed.

The scenarios have been simulated with the following key assumptions:

- Mud completely removed from the wellbore
- Flow to ambient conditions at surface and seabed
- No reduction in flow rate or pressure due to depletion

- Open hole section does not collapse

Since this study is not conducted for a specific well, a most likely scenario is defined based on the expected average reservoir properties in the region. However, to cover a wide range of possible variations in flow potential, sensitivity analysis is carried out over the product of permeability and net pay thickness (kh). The “kh” range in this study falls between 5000 to 100000 mD-m with the most likely case at 10000 mD-m. It is assumed that it is unlikely to have a “kh” value greater than 100000 mD-m.

Figure A.1 shows a schematic of the wellbore.

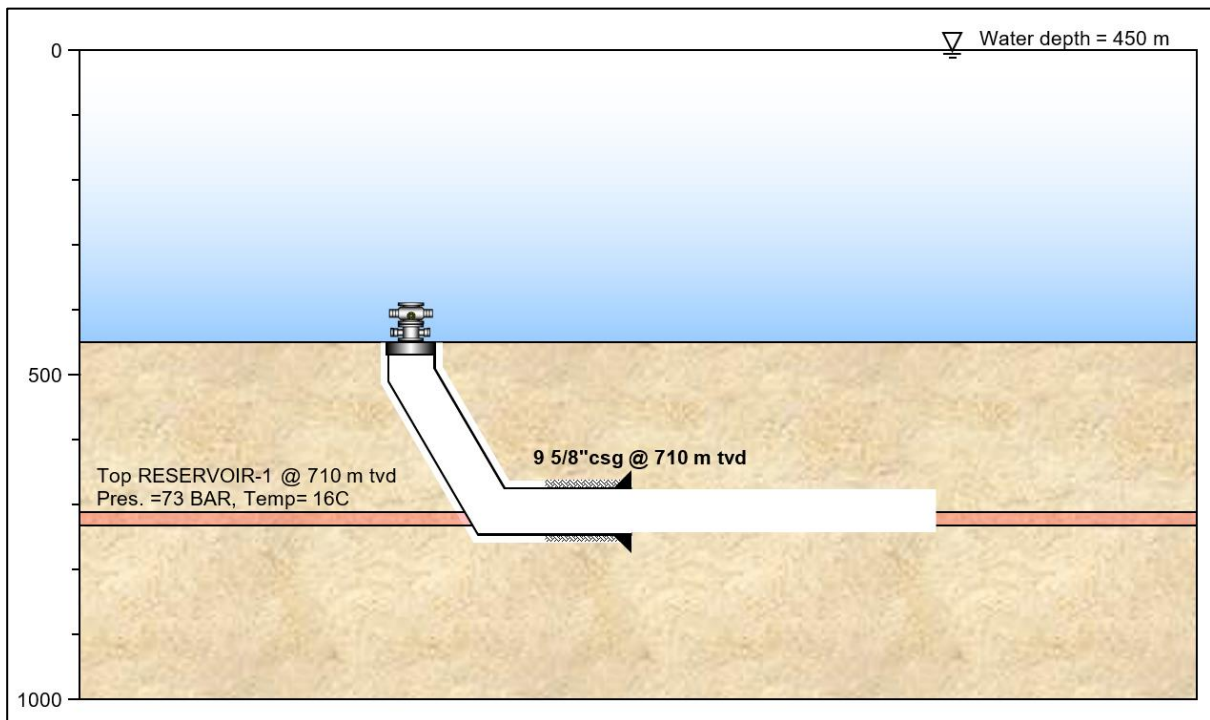


Figure A.1: Schematic of blowout scenario

A.4 Blowout Results

The blowout simulations were run with the inflow performance relation (IPR) as the inlet condition. The simulations assume unrestricted blowout to seabed with ambient seawater pressure as the outlet condition (46.5 bar and 4° C).

Table A.3: Blowout results

Blowout scenarios	FBHP [bar]	Gas rate [MSm ³ /d]
kh = 5000 mD-m	51.0	3.0
kh = 10000 mD-m (most likely case)	54.8	4.7
kh = 20000 mD-m	59.7	6.2
kh = 50000 mD-m	65.8	8.3
kh = 100000 mD-m	68.9	9.2

The flowing pressure profiles along the blowing wellbore are illustrated in Figure A.2.

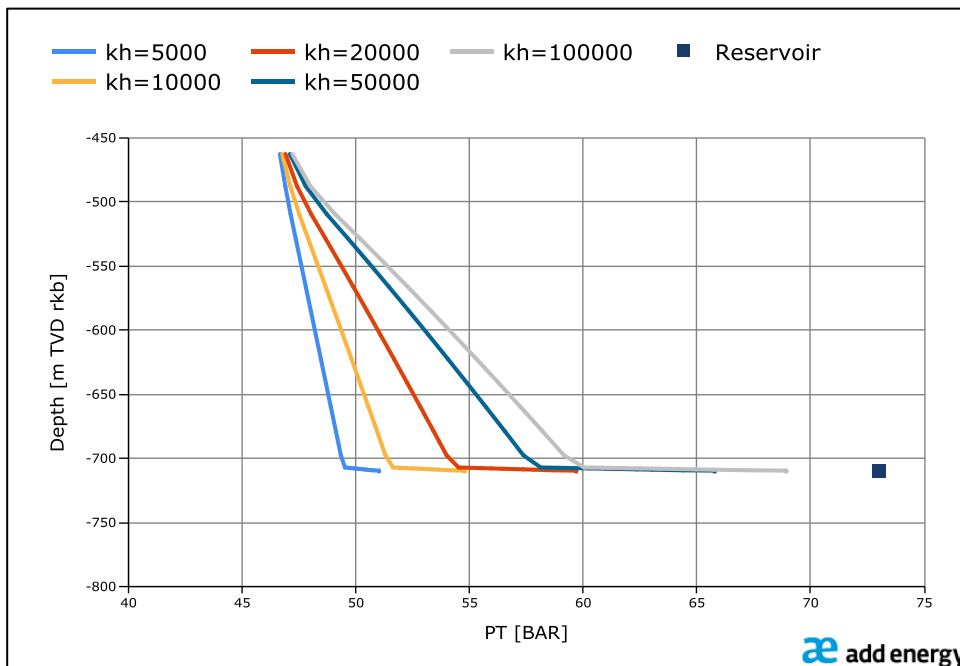


Figure A.2: Flowing pressure profiles

Considering the fairly high “kh’ values, because of a low-pressure differential between the pore pressure and the seabed hydrostatic ($\Delta p_{max} = 26$ bar), the flow potential is low. Also, sensitivity over higher GOR values showed no significant change in the estimated rates.

A.5 Dynamic kill requirements

A.5.1 Relief well casing design

The kill fluid is pumped down two kill and choke lines, and further down the annulus of the relief well to the intersection point. The relief well casing design is usually similar to the design of the blowout well, but hydraulic requirements might call for an optimized casing design with respect to flowing capacity. For this study, the design is similar to the design of the blowout well. The following assumptions were applied:

- Two 4 ½" kill and choke lines
- Intersection below at the casing shoe at 710 m TVD.
- 10 m of 8 ½" open hole section is drilled from the relief well casing shoe down to the intersection point
- The relief well drillstring consists of a 5" drillpipe and 60 m of 6 ½" BHA

Kill mud selection

It is assumed that, when balanced to the surface, the maximum pore pressure at 701 m TVD is 1.05 sg EMW while the FG at the same depth assumed to be 1.3 sg EMW. Because of the dual gradient system with discharge at the seabed, the minimum mud weight for balancing the pore pressure is 1.1 sg EMW. When balancing to the seabed, the fracture gradient is 1.77 sg EMW.

A.5.2 Kill requirements

The kill requirements are summarized in Table A.4.

Table A.4: Kill requirements

Blowout scenario	Intersection Depth [m TVD]	Kill Mud [sg]	Kill Rate [bpm]	Pump Pressure [bar]	Pump Power [hhp]	Mud Volume [m ³]
kh = 5000 mD-m	710	1.25	47	112	1866	400*
kh = 10000 mD-m (most likely case)			51	133	2413	
kh = 20000 mD-m			54	150	2877	
kh = 50000 mD-m			59	181	3789	
kh = 100000 mD-m			61	194	4206	

*Volume required to dynamically kill the well, full wellbore displacement could not be achieved

A.5.3 Kill requirements discussion

Based on OLGA-Well-Kill simulations, the well could be killed with a single relief well in all the scenarios. The pumping requirements for the worst case ($kh=100000$ mD-m) is shown in Figure A.3. As shown, three P-220 pumps with 8.5"-9.0" liners would provide enough power to kill the well with a single relief well.

Full wellbore displacement could not be established since the relief well intersects the target well approximately 1200 m MD off-bottom. Hence, there would be about 20 m³ (1/3 of the wellbore volume) hydrocarbons trapped in the wellbore after the well is killed.

Based on additional simulations, intersecting the target well at a shallower depth does not significantly change the kill requirements.

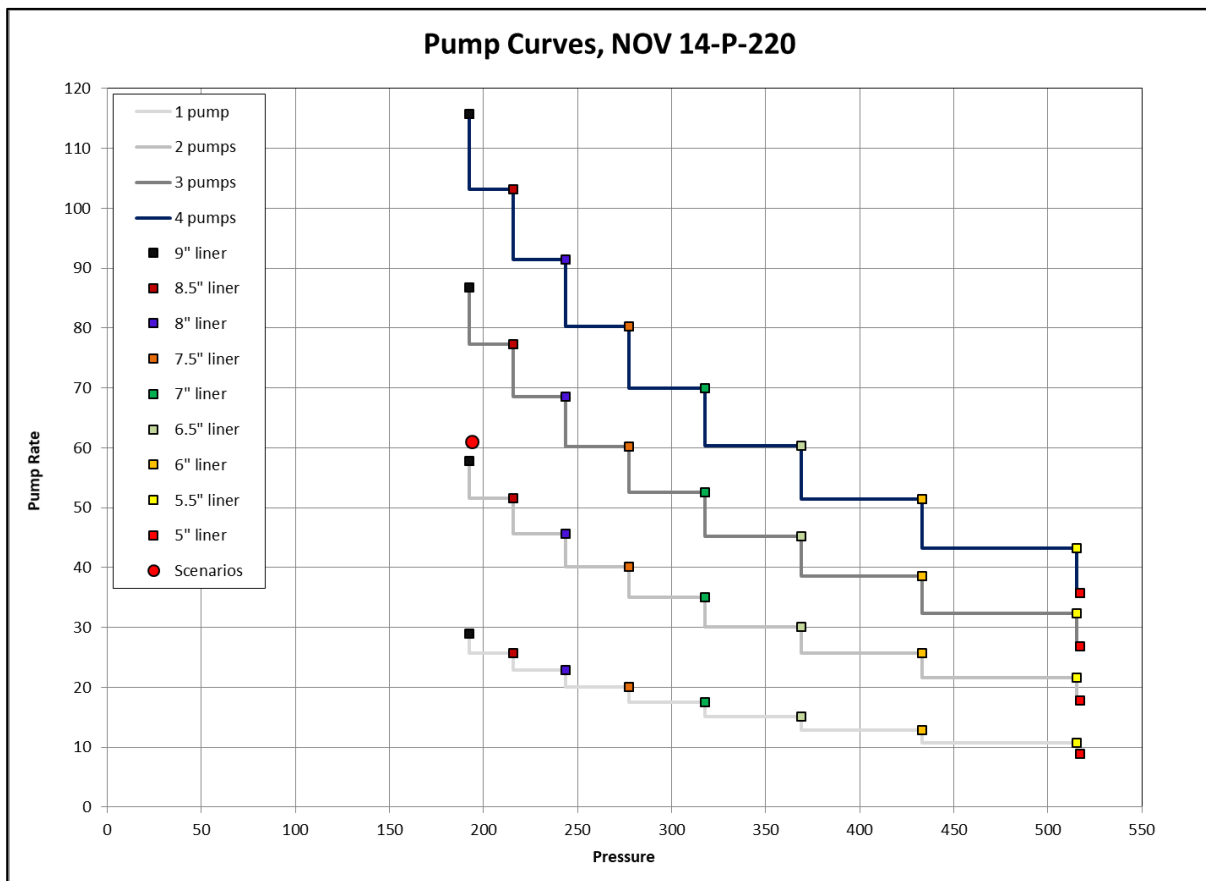


Figure A.3: Pump curves for the worst case kill scenario

A.6 Software



The OLGA-WELL-KILL software is a tailor-made application for well and well control simulations and has been used in a number of on-site incidents in addition to more than 1200 studies since it was first developed in 1989.

The model has been specifically adapted to calculation of pump rates and mud volumes for a variety of blowout situations. OLGA-WELL-KILL has been developed from the state-of-the-art three-phase flow simulator OLGA from Schlumberger. It can handle numerous well flow configurations - from a single vertical well to multiple horizontal wells with complex completions. Assistance with the model is available on-site in a blowout kill planning and control situation.

OLGA-WELL-KILL has been designed for planning and evaluation of kill scenarios and intervention options. The model can be used to analyze blowout flow, kill point, pumping schedule, casing design, kill fluid properties and volumes, temperature, pressure and other related parameters. The results may be presented versus time for a complete dynamic and volumetric response.

The development of OLGA started at Institute for Energy Technology (IFE) in 1980. A major research program, in cooperation with SINTEF and sponsored by a group of large oil companies, has resulted in an industry standard dynamic three-phase code used world-wide by most operators for multiphase flow design.

After experience from a North Sea blowout in 1989, IFE sponsored by Saga Petroleum, developed a multiphase dynamic flow simulator for well kill planning. The simulator, named OLGA-WELL-KILL, was based on the dynamic two-phase flow simulator OLGA and later further developed through an R&D program. An agreement with IFE and SINTEF and later SPT Group gave add energy the rights to offer this extremely powerful tool as a service to oil companies and operators world-wide.

Well kill applications for the model include:

- Dynamic kill simulations for relief well control operations
- Top kill simulations for underground blowouts from a rig or snubbing unit
- Bull heading analysis
- Momentum kill analysis
- Shallow gas analysis

Production applications include:

- Production and injection flow characterization
- Horizontal well flow analysis
- Water alternating gas injection analysis

OLGA-WELL-KILL features that are unique to well kill applications include:

- State-of-the-art multiphase flow technology
- Advanced controller system which is representative of real pumping operations
- High pressure pump models
- Oil and gas properties fully modeled
- Pressure and temperature effects on mud properties
- Non-Newtonian flow
- Well path obstructions and leaks
- Critical flow conditions
- Various models can be used for the reservoir inflow
- User defined graphical presentation

The results from OLGA-WELL-KILL will typically provide:

- Fully dynamic simulations of the kill operation with pressures, blowout rates, pump rates, cumulative volumes, hydraulic horse power requirements and temperatures. Parameters can be displayed versus time at any point in the well(s).
- Calculation of necessary kill fluid rates, time and volumes to obtain dynamic and static kill.
- Sensitivity analysis of different kill fluids; water, brine or mud with different densities and viscosities.

Please visit www.addenergy.no for more details.



Reservoir fluid characterization and property generation was performed by PVTsim. This is the market leading fluid characterization and simulation software. See www.calsep.com for more info.

B. Overburden Leakage Resistance

B.1 Introduction

This appendix addresses the potential leaks to seabed in shallow sediments in the Barents Sea based on the geomechanical understanding of the problem using relevant rock mechanics models.

B.1.1 The effects of fluid type

During drilling operations, a drilling fluid is used. Particles such as barite are added to this with the objective of building a filter cake to reduce mud losses

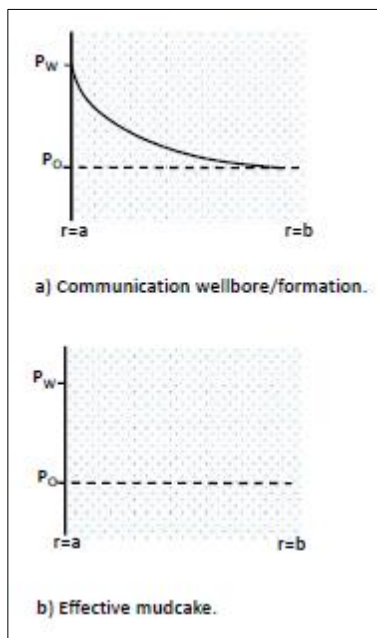


Figure B.1: a) penetrating fluid b) non-penetrating fluid (Aadnøy 2010)

Figure B.1 shows a wellbore wall and the rock outside. If a penetrating fluid is used (Fig.B.1 a), this fluid will build up the pore pressure inside the rock and change the effective stresses. This is a typical behavior seen when using clear fluids such as acid or water. However, if a mud is used which is non-penetrating due to the presence of a filter cake (Fig.B.1 b), the pore pressure inside the rock remains the same. Due to this pore pressure effect, a non-penetrating situation leads to higher fracture pressure.

B.1.2 Drilling with mud

A drilling mud is typically designed with a thin filter cake with low filtrate losses. The main objective is to avoid mud losses and differential sticking. Another effect is that a barrier is placed on the wellbore wall minimizing pore pressure buildup as shown in Fig. B.1 b. With a number of assumptions and simplifications such as vertical well and

isotropic horizontal in-situ stresses and no tensile rock strength the simplest fracturing model for this non-penetrating situation can be formulated as (Aadnøy, 2010):

$$P_{wf} = 2\sigma_h - P_o \quad (1.1)$$

Here P_{wf} is the fracture pressure, σ_h is the horizontal in-situ stress and P_o is the pore pressure

This comes from the Kirsch equation which is the most important mechanical model for wellbore stability analysis. The number (2) which is multiplied with the horizontal in-situ stress is actually a geometric stress concentration factor for a circular hole.

All fluids with filtrate control such a drilling muds obey Eqn. 1.1.

B.1.3 Well stimulation with solid free fluids

During well stimulation operations one is using clear fluids such as water, acids, diesel oil and others. These have no filter cake. For this case Figure B.1 a applies, allowing the fluids to build up the pore pressure inside the rock.

Inspection of Figure B.1 a shows that the pore pressure is equal to the fracture pressure at the borehole wall. Inserting this condition into Eqn. 7.1 gives the following fracture equation for a penetrating case:

$$P_{wf} = \sigma_h \quad (1.2)$$

This equation is applicable to all operations using clear fluids such as well stimulations operations. It is also applicable if pure water with no filtrate control is used while drilling top holes.

B.1.4 Comparing solutions

The following data will be used to demonstrate the difference between the two models:

Horizontal stress:	1.5 sg
Pore pressure:	1.03 sg

For the non-penetrating case the fracture pressure becomes:

$$P_{wf} = 2 \times 1.5 - 1.03 = 1.97 \text{sg}$$

For the penetrating case:

$$P_{wf} = 1.5 \text{sg}$$

This example illustrates that the wellbore is significantly strengthened if a filtrate cake is present.

B.1.5 Summary

The following observations can be made:

- Drilling mud gives higher fracture pressure than solids free fluids.
- Leakage from the reservoir is penetrating and cannot be controlled by a barrier. This depends on rock stresses and rock properties.
- Due to the above it is important that losses are minimized in the drilling phase.

B.2 Rock Mechanics

B.2.1 Injection scenario

The possible fracture patterns during injection are illustrated in Figure B.2 (Aadnøy and Looyeh, 2010).

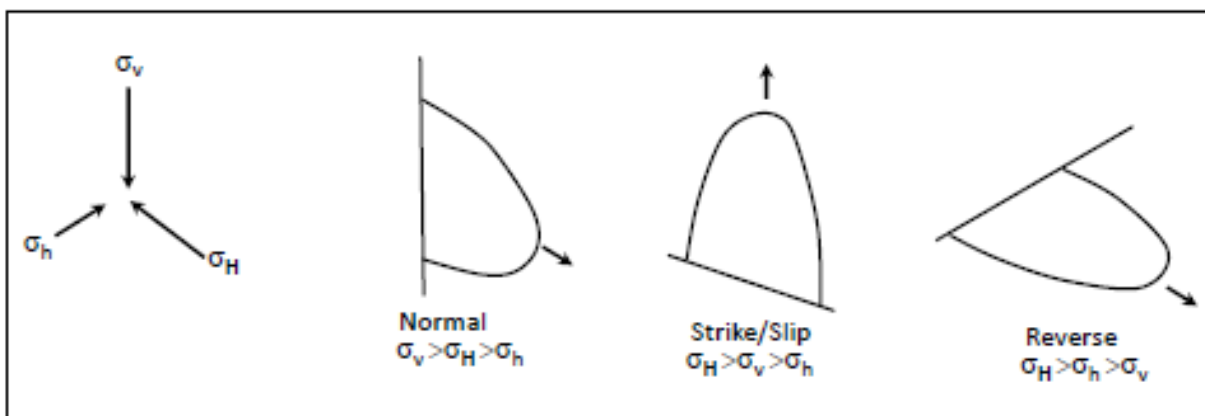


Figure B.2: Possible fracture patterns

In the North Sea, the shallower sediments are found in a relaxed depositional basin environment. With reference to Figure B.2, the expected fracture scenario here is a standing fracture that extends in the horizontal direction. If a large volume is injected, long fractures are created. The fracture will also attempt to grow upwards. This represents a potential risk for unintentional leaks to surface. In the following sections we will discuss the mechanisms that may arrest undesired upward fracture growth.

For deviated wells, the induced fractures will initiate along the borehole axis, but twist towards the in-situ stress state which controls fracture propagation outside the borehole region. The fracture propagates in a direction normal to the least in-situ stress but in the direction of the intermediate in-situ stress.

The oil industry assumes two opposite penny-shaped fractures (Figure B.2). However, Keck (2002) postulates that we in reality have multiple fractures caused by stress redistribution. These will have shorter extensions, and may also be favourable for reduced upward growth. It is believed that with low injection rates, two opposite fractures arise, whereas at high injection rates multiple fractures may form.

In the following section several fracture related issues will be discussed.

B.2.2 Prognosis for the model wells

Below are the resulting curves for the model wells, copied from Figure 5.4 in Section 5.

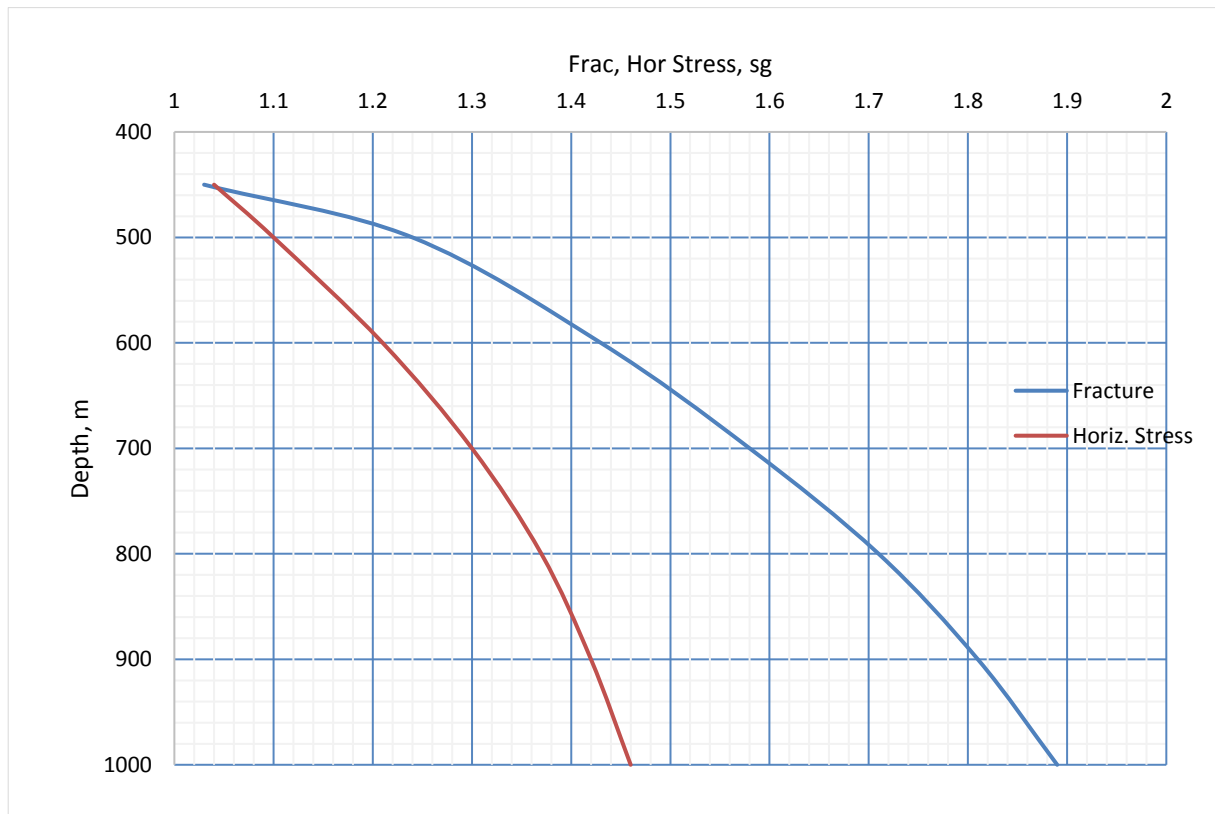


Figure B.3: Fracture curve and horizontal stress curve for the production and injection wells cases for a water depth of 450 mRKB

It is a well established principle that rock fractures propagate normal to the minimum principal stress. According to Figure B.1 the fracture should therefore propagate in the horizontal plane. In a normal fault stress regime upward growth would be preferred. A further discussion of other mechanisms follows.

B.3 Potential for leaks to surface

Leaks from a reservoir can occur during various times in a well's life such as:

- During drilling and production a leak can occur on both sides of a casing.
- During injection; or production pressure or stress variations may establish a leak to surface.
- The leaks may be near the wellbore but also away from the wellbore.

There are different failure mechanisms such as:

- Pure tensile failure with undisturbed geometry.
- Tensile or shear failure if there is deformation in the caprock.
- Different rock strengths depending on mud or oil (penetrating fluid).

In the following we will discuss a simple approach and also a more complex approach.

Problem statement

Below are some reported incidents which identify the potential for leaks to surface. These cases are examples from Davison et.al (2013):

- **Frade, Brazil** (Asher, 2012) - Leak to seabed of approximately 3,700 barrels of crude oil in November 2011. Whilst drilling the well, high formation pressures were encountered as a result of injection operations in the area. The BOPs were shut-in ensuring rig safety, but the pressures exceeded the formation strength causing an underground blowout. Upward fracture propagation led to leak of oil to the seabed.
- **Tordis, Norway** (Eidvin and Overland, 2008) - Produced water was injected into the Utsira Formation at a depth of 950 m TVDSS, below the Nordland Group shale caprock. A leak of oily produced water (estimated to be 1100 barrels) occurred on the sea floor 5.5 months after injection started, creating a crater 40 m wide and 7 m deep. The main cause of the expected tensile failure is due to higher than planned injection pressures and poor reservoir properties for the Utsira in this part of the basin.
- **Joslyn Creek, Canada** (ERCB,2010) - Steam release incident in the Joslyn Creek steam-assisted gravity drainage (SAGD) scheme, May 2006, which caused a surface disturbance of about 125 by 75 m. The most likely cause of this incident was deemed to be catastrophic shear failure of the Clearwater caprock. The operating bottomhole pressures were significantly higher than the approved maximum wellhead injection pressure.

Clemens et.al.(2017) give a comprehensive picture of the design process for such a well based on a Norwegian well with shallow penetration. Monitoring concepts which will reduce the risks for such projects include:

- Pressure-transient analysis to determine fracture half-length and height
- Wellhead-pressure monitoring
- Microseismic monitoring of fracture growth in the reservoir and in the caprock
- Tiltmeter measurements at surface or in offset wells
- Injection of tracers
- Distributed-temperature sensing

B.3.1 Simple analysis

Of the reported leaks, the common reason is injection of large volumes of fluids. The cure is to limit the injection volume. During drilling the leak would most likely be related to the well itself.

The Tordis example above is a relevant example, also caused by injecting larger volumes. In the North Sea above the Bottom Cretaceous Unconformity, we usually have a relaxed depositional basin environment. Here a *normal fault stress state* exists. With reference to Figure B.2, upward fracturing would be the preferred fracture propagation direction. From the previous analysis there are indications that the Barents area may have *reverse fault stress state*. In this case the preferred fracture direction is horizontal with low risk for surface leaks. The environmental consequences of a horizontal fracture trend in the Barents sea could be much less than in the North Sea.

The simplest model is to assume that a fracture initiates in the wellbore at the bottom of the well. Assuming no tensile stress due to rock fissures, the resistance for fracturing is simply:

$$P_{wf} = \sigma_h \quad (1.3)$$

The horizontal stress curve of Figure B.3 defines the limit for leaks upwards. The casings should be deep (TVD) set to maximize strength.

B.3.2 Complex analysis

Rock deformation plays an important role in cap rock failure. If the cap rock is deformed, cracks may arise. This is shown in Figure B.4 below.

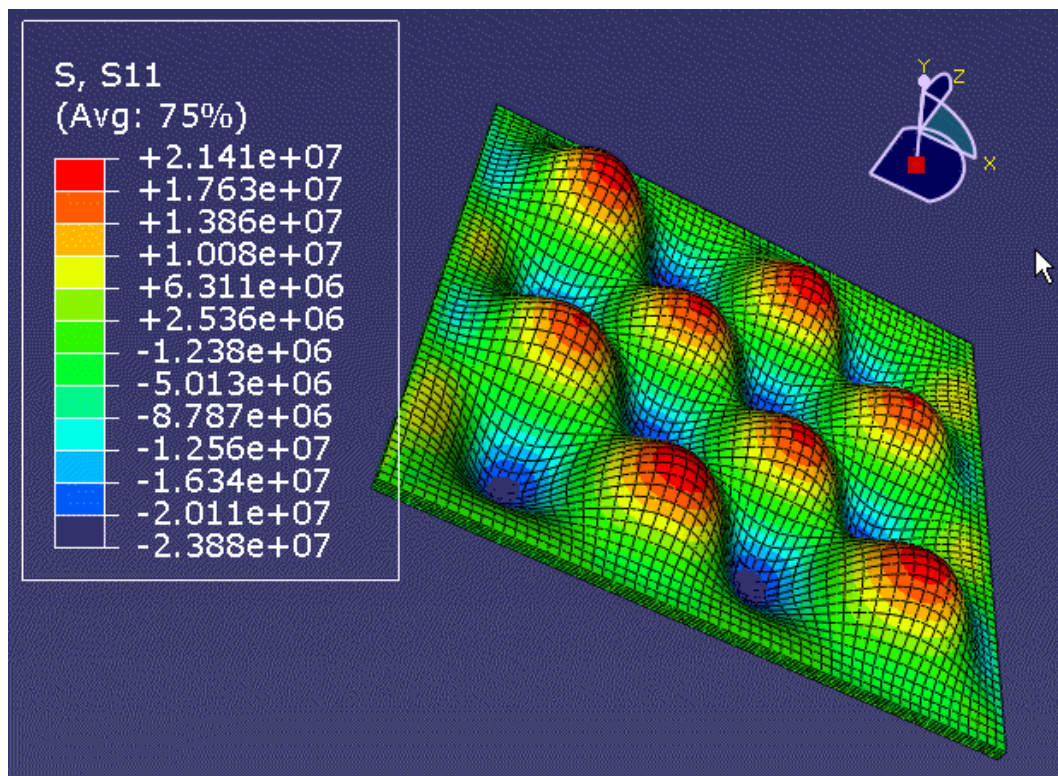


Figure B.4: Deformation caused by injection into several wells (Zhang, 2012)

Davison et. al. (2013) have derived a 3-step method for cap rock integrity analysis based on deformation of the rock above or below. The 3 steps are as follows:

1. **1D Empirical Data Analysis.** The key to the first step of the 3-step methodology is to evaluate the in-situ stress state, and most importantly, the minimum total principal stress (S_3) and its orientation. The pressure change during injection occurs in the reservoir unit. However, in terms of containment, the impermeable caprock is the key to understanding the risk of loss of containment. Given the relatively short lifecycle of the injection period (compared to geologic timescales) and the typically low permeability of the sealing caprock (which has held hydrocarbons for millions of years), we consider the caprock pore pressure to remain unchanged in our 1D assessment. With rocks being weak in tension and often exhibiting low tensile strengths, S_3 controls the tensile fracturing. This value needs to be determined for both the reservoir and caprock. Fortunately, well casing shoes are set in shales to obtain the best casing integrity. The subsequent leak-off test help to determine S_3 .

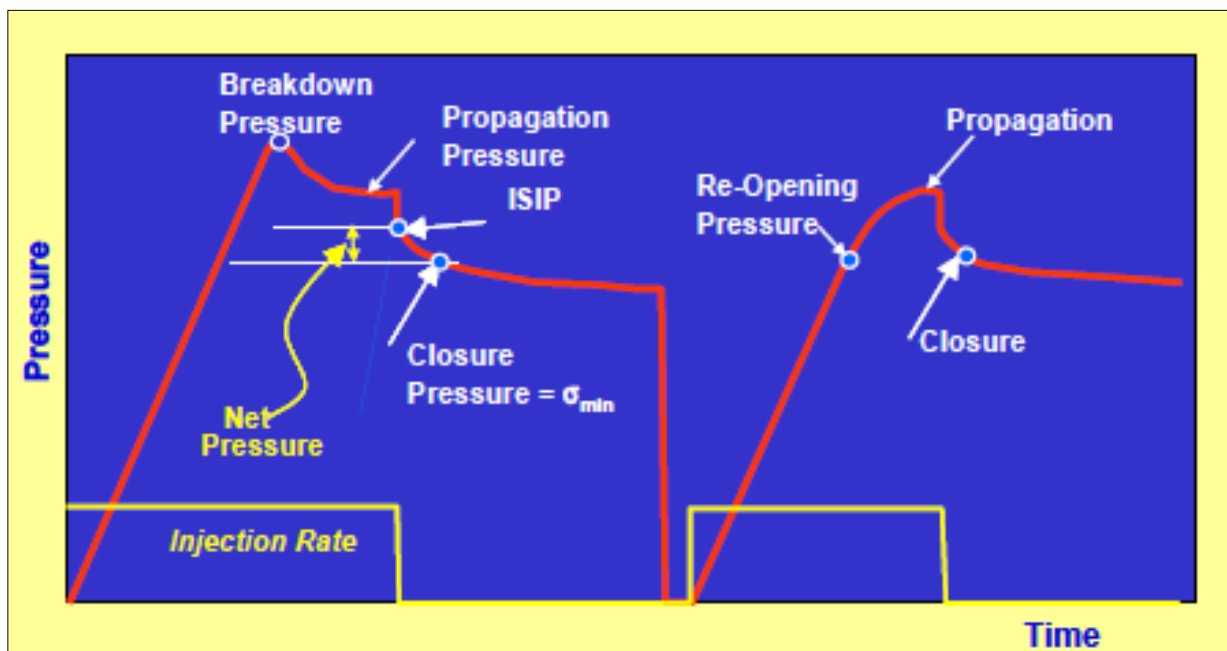


Figure B.5: Typical Pressure-Time curve for extended Leak-Off-Tests. From Ybray et.al. (2011).

2. **Analytical Modelling.** Tensile fracturing and shear failure of intact rock (also called “country rock”) and slippage along natural faults are evaluated in the second step of analytical geomechanical modelling. Both failure mechanisms may create permeable pathways through the reservoir seals, either during reservoir depletion or a subsequent injection stage. A depth-dependent in-situ stress model is used to evaluate both failure mechanisms under virgin conditions, after depletion and after subsequent injections. The stress path coefficients are used to simulate the change of total vertical and horizontal

stress components due to reservoir depletion and subsequent injection for waterflood operations.

3. **Numerical Modelling.** Numerical geomechanical models offer significant benefits to further refine analytical models. The key technical advantages include:

- Complex geological structures: using variable density meshes we can accurately reflect complex static reservoir architectures, incorporating numerous faults and variable relief of lithological bodies.
- Variable rock properties: we can incorporate 3D distributions and inelastic rock failure models.
- Variable pressure distributions: lateral and vertical pressure variations can be incorporated, as well as intra-reservoir pressure baffles adjacent to faults and lithological heterogeneity.
- Fault behavior: in the over-, side and under-burden.

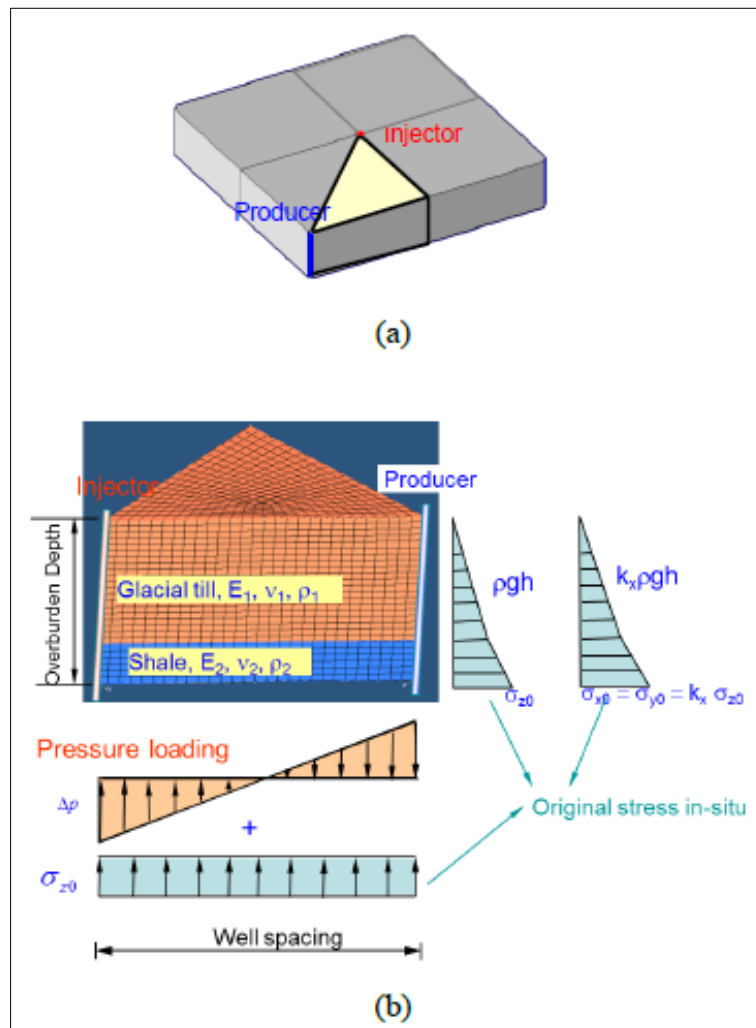


Figure B.6: Repetitive 5-spot pattern (a) and (b) Finite Element model with loading (Zhang et.al.2012)

Another analysis by Zhang et.al.(2012) found that softer formations above and below a stiffer shale cap rock can help in reducing bending stresses within the caprock, aiding in stability. These numerical modelling approaches are beyond the scope of this project.

Another reference is paper ARMA 12-669 presented at the 46th US Rock Mechanics/Geomechanics Symposium, Chicago, IL, 24-27 June 2012.

C. Clean Sea Payloads

Payload module	Task	Payload	Status
Standard	Environmental monitoring	Temperature, Conductivity (salinity), Pressure (depth), Turbidity (suspended solids), Fluorescence (chlorophyll), Fluorescence (colored dissolved organic matter), Dissolved Oxygen, Fluorescence (Polycyclic Aromatic Hydrocarbons), Dissolved CH ₄ , pH, Oxido-Reduction Potential (ORP), Digital Stills Camera with Flash Unit, LED lights, H ₂ S, CO ₂ , MEG, Nutrients	Operational
e-pod #1	Environmental monitoring	Automatic water sampler	Operational
e-pod #2	Asset inspection and hydrocarbon leakage detection	Hi-res Color video camera, Hi-res Stills camera, Laser profiler, Range laser, Lights, Acoustic leak detector, Dissolved CH ₄ sensor, Fluorescence (oil in water) sensors, CP probe, Pipe tracker	Operational
e-pod #3	In-situ analysis of trace pollutants	spectrophotometric analyzer for trace metals (Cr, Cu, Ni, Zn, Cd, Hg, Pb, Fe), TOC, COD, phenols, surfactants	Technol. demonstrator developed and tested
e-pod #4	Acoustic seabed surveys	Side-scan sonar, echo sounder	Operational
e-pod #5	Geochemical surveys	Mass Spectrometer, Gamma spectrometer, Water sampler	Technol. demonstrator developed and tested; field validation trials scheduled 2016
e-pod #6	<i>Scenario reconstruction</i>	<i>3D laser scanner, 3D imaging sonar</i>	<i>Study ongoing</i>
e-pod #7	Precision acoustic seabed surveys	Multibeam Echo Sounder, Side Scan Sonar, Sub Bottom Profiler, Echo Sounder, Sound Velocity Sensor	Under development; first operational use scheduled 2016
e-pod #8	<i>IMR</i>	<i>Manipulator (5 dof), Grabber, IMR tools</i>	<i>Study ongoing</i>

Potential extension is in italics (Gasparoni, F. et.al, 2016)

D. AUV Mounted Systems

The table below shows main specifications for the REMUS and HUGIN AUVs. Payload and navigation sensor and configurations listed are the most frequent used for Naval Applications. Other sensors are available for the different vehicles and can be configured for special applications.

	REMUS 100	REMUS 600	REMUS 6000	MUNIN	HUGIN
Imaging sonars					
Frequency	VHF, HF	VHF, HF	VHF, HF, MF	MF	MF
Type	DAS, PCS, SSS	SAS, FSSS, DAS, PCS	DAS, SSS	SSS, FLS	HISAS, SSS, FLS
Bathmetry	GS+	SAS, MBES	MBES	MBES, HISAS	MBES, HISAS
Optical imaging	Video	Video, ESC	ESC	ESC	ESC
Environmental	CTD, OBS	CTD, OBS	CTD, OBS	CTD, OBS, CH4,CO2, DO	CTD, OBS
Navigation	ADCP, GPS, PGPS, USBL, LBL, HiPAP	ADCP, GPS, PGPS, USBL, LBL, HiPAP	ADCP, GPS, PGPS, USBL, LBL, HiPAP	ADCP, USBL, UTP, HiPAP, TERRAINAV	ADCP, USBL, UTP(LBL), HiPAP, TERRAINAV
Navigation modes	DR, IN, LBL, Homing and docking	DR, IN, LBL, Homing and docking	DR, IN, LBL, Homing and docking	DR, IN, LBL, Homing and docking, Pipe tracking	DR, IN, LBL, Homing and docking, Pipe tracking
Communication modes	Acoustic,WiFi, Iridium	Acoustic, Wifi, RF Link, Iridium	Acoustic,WiFi, Iridium	Acoustic control and real time data,WiFi, Iridium, RF Link	Acoustic control and real time data,WiFi, Iridium, UHF radio link
Endurance (hours)	6 to 10	20 to 45	28	12 to 24	24 to 74
All sensors operational @ 2.1m/s					
Depth rating (m)	100	600	6000	600, 1500	3000, 4500, 6000
Physical					
Diameter (m)	0.19	0.32	0.67	0.34	0.75
Length (m)	1.6	3.2	3.94	2,6 - 3,5	5.4 - 7
Weight (kg)	37	272	863	300	1200 - 1900
Volume (m ³)					1.3 - 1.5

Abbreviations

- **CTD**: Conductivity Temperature Depth
- **OBS**: Optical Backscatter Sensor
- **ESC**: Electronic Still Camera
- **ADCP**: Acoustic Doppler Current Profiler
- **GPS**: Global Positioning System
- **P-GPS**: code GPS
- **USBL**: Ultra Short Base Line
- **LBL**: Long Base Line
- **HIPAP**
- **VHF**: Very High Frequency > 600 kHz
- **HF**: High Frequency: 300 - 600 kHz
- **MF**: Mid Frequency 50 - 300 kHz
- **TERRAINAV**: Terrain referenced navigation

Source:

<https://www.km.kongsberg.com/ks/web/nokbg0240.nsf/AllWeb/3CFE5477FE0913CC1257555004C606A?OpenDocument>

Resolution and coverage

The table below provides approximate values for resolution and area coverage rate for different imaging sonars. Along track resolution of synthetic aperture sensors is constant with range. For side scan sonar type of systems, along track resolution increases with range. In the table the quoted along track resolution matches the range for the area coverage rate.

Sonar system	Abbreviation	Frequency (kHz)	Along track resolution (cm)	Instantaneous area coverage rate (Sq-km/hour)
Synthetic aperture (interferometric)	HISAS 1030	50 - 120	2	2.6
Synthetic aperture sonar	Other types	MF	2	1.2
Dynamic focused sonar	DFS	850	15	0.5
Interferometric side scan sonar	ISSS	MF		
Conventional side scan sonar	SSS	MF, HF, VHF	20 - 30	0.25
Multibeam echo sounder	MBES	MF		

Mobile Early Leak Detection System

The Mobile Early Leak Detection System (MELDS) is a unique system for detection, localization and qualification of subsea oil and gas leakages at a very early stage. It combines three completely independent methods for direct and indirect detection of hydrocarbons and associated anomalies. Mounted on an ROV/AUV or towed behind a vessel, MELDS allows for a wide area coverage in a short time span and investigations at specific locations of interest.

Source:

<https://www.km.kongsberg.com/ks/web/nokbg0240.nsf/AllWeb/C1F7121D0FF78ADB,C1257DFF004DF51E?OpenDocument>